Examining Preexisting Immune Mediators that Augment Immune Responses to Drifted Influenza Exposure

Emily Gage

A dissertation

submitted in partial fulfillment of the

requirements for the degree of

Doctor of Philosophy

University of Washington

2018

Reading Committee:

Rhea Coler, Chair

Leonidas Stamatatos

Lisa Jackson

Peter Rabinowitz

Program Authorized to Offer

Pathobiology

University of Washington

Abstract

Examining Preexisting Immune Mediators that Augment Immune Responses to Drifted Influenza Exposure

Emily Gage

Chair of the Supervisory Committee:

Rhea Coler, PhD.

Department of Global Health

Influenza A annually infects 5-10% of the world's human population resulting in an estimated one million deaths, severely afflicting the elderly population in particular. Influenza causes annual epidemics and re-infects previously exposed individuals because of antigenic drift in the surface glycoprotein hemagglutinin (HA). Due to antigenic drift, the immune system is simultaneously exposed to both novel and conserved parts of the influenza virus via vaccination and/or infection throughout life. Additionally, over time humans experience a gradual deterioration of the immune system, termed immunosenescence. Preexisting immunity and immunosenescence has long been known to influence subsequent hemagglutination inhibitory

antibody (hAb) responses. However, the resulting immunological contributors that either dampen or enhance hAb responses are not fully understood.

Here, we address basic questions regarding what preexisting immune components effect subsequent responses and how we can enhance and optimize responses to influenza in the face of preexisting immunity and immunosenescence. Therefore, to begin to address what preexisting immune components augment responses, both detrimentally and constructively, we adapted and characterized two sequential infection and vaccination mouse models with strikingly different hAb outcomes. We found that this differential response was due to disparities in T cell reactivity between the two mouse models. With both mouse models established we then used depletion and transfer methodologies to isolate the impact of immunological memory components on subsequent responses. Increased hAb responses were memory $CD4^+$ T cell and B cell dependent, whereas dampening hAb responses were found to be due to a lack conservation between MHC Class II reactivity. We then characterized these different responses finding increased hAb responses corresponded to increased germinal center B and T follicular helper cells. We then reversed dampened hAb responses employing this knowledge by engineering conserved $CD4^+$ T cell reactivity. These results suggest conserved MHC Class II restricted epitopes within HA are critical for memory B cells to adapt to drifting influenza and could be leveraged to boost subsequent hAb responses. Last, we used an adjuvant paired with the seasonal vaccine to elicit enhanced hAb responses in an immunosenescent mouse model, characterizing and evaluating protective responses. Collectively, we demonstrate that cognate memory B and T cells synergize to update the B cell repertoire to drifting influenza exposure while lack of cognate T cell help leads to a less protective response and inclusion of adjuvant in seasonal vaccination elicits enhanced hAb responses in an immunosenescent mouse model.

TABLE OF CONTENTS

LIST OF FIGURES

Acknowledgments

The work described herein would not have been possible without the support of my friends, coworkers, family and mentors. I would like to thank my advisor, Rhea Coler for guidance, latitude, and encouragement throughout my project. I would also like to thank my committee members and scientists at the Infectious Disease Research Institute (IDRI) for their scientific guidance and support.

I would like to thank my family for their constant love and support in pursuing higher education. Last, I would like to thank my life partner Dave, for always inspiring me a little higher in science, life and in the mountains. The soundness and deepness of our love and rapport has softened the failures and intensified the joys of this process. I look forward to our next adventure, whether in science, a city park, our backyard, or the wilderness, always.

Chapter 1: Introduction

Influenza

Influenza A virus of the Orthomyxoviridae family is a zoonotic pathogen that continuously circulates through animal hosts, such as humans, birds, horses, dogs and pigs (1, 2). This enveloped virus has a segmented, negative-sense, single stranded RNA genome that traditionally encodes 11-12 proteins (1). Influenza A viruses are subtyped and named based on their hemagglutinin (HA) and neuraminidase (NA) surface glycoproteins that are incorporated in the viral envelope (3). At present there are virus strains from 18 HA subtypes and 9 NA subtypes circulating in birds, and two virus subtypes, Swine-origin H1N1 and H3N2, circulating in humans (2). Influenza A virus, via the surface HA glycoprotein, can bind host cells via sialic acid residues having 2,3 (avian) and/or 2,6 linkages (human) dependent upon the HA subtype and this step mediates viral entry (4, 5). Importantly, not all HA or NA subtypes can infect humans or birds and influenza strains have defined host-ranges due to variability and compatibility of entry receptor expression. Further, not all subtypes that can infect humans are transmissible from human to human (6).

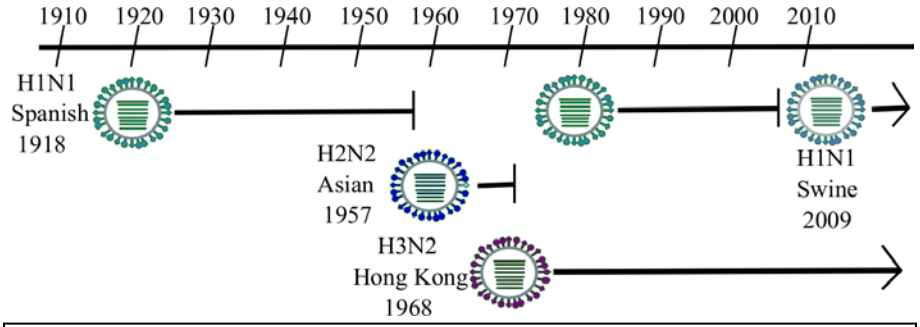

Figure 1.1 Historic timeline of human influenza epidemics with concurrently circulating group 1 (H1 and H2) and group 2 (H3) HA subtypes.

HA subtypes are defined in two major groups, Group 1 (H1, H2, H5 and Group 2 (H3, H7), which are defined in evolutionary terms by sequence similarity (7). Typically, there are two

concurrent influenza A viral subtypes circulating in the human population, one from a group 1 HA subtype (e.g. H1 and H2) and one from a group 2 HA subtype (e.g. H3) (**Figure 1.1)** (7). The ability of multiple strains to co-circulate in the human population is thought to be due to the disparity in HA between the 2 separate groups, suggesting that only one from each group can be in the human population at any given time because of too much cross-reactivity between strains in the same Group (7).

Globally, seasonal influenza epidemics are estimated to cause 3-5 million cases of severe illness, 250,000-500,000 directly attributable deaths, and 1 million deaths from fatal complications, making it a significant public health concern (8, 9). The economic burden from healthcare costs, reduced work productivity and other associated costs is extensive. The World Health Organization (WHO) estimates the annual cost of influenza in developed countries at 1-6 million US$ per 100,000 population; costs in lower income countries has yet to be ascertained.

Influenza Drift and Shift

Influenza epidemics in the northern hemisphere or the southern hemisphere occur during their respective winter months (10, 11). The seasonality of influenza virus is largely due to temperature-dependence of viral transmission, viral transmissibility and absolute humidity (11). Lower absolute humidity, found in winter is thought to stabilize virions and allow for smaller respiratory droplets to remain in the air longer and travel further. During these annual continual epidemics, evolution of human seasonal influenza typically undergoes antigenic drift characterized by point mutations in the HA and NA glycoproteins, necessitating a new yearly influenza vaccine (12-14). Immune pressure placed upon the influenza subtypes in current circulation cause the selection of drifted virus that can escape herd immunity, the immunity to the strain in the population, most notably by evading neutralizing antibody responses to HA that

prevent viral entry (15). The ability to drift is caused by the viral use of error-prone RNA-dependent RNA polymerase (RdRp) that produces mutations at a rate of 10^{-3}-10^{-4} substitutions per nucleotide in the viral genome leading to mutants and ultimately viral evolution (16). In this way there is interviral competition; viruses that are viable and contain mutations in HA portions targeted by neutralizing antibodies have increased ability to evade herd immunity and therefore are at an advantage (17).

Simultaneous infection of a single cell by two distinct influenza A viruses can cause reassortment of genes, due to the segmented nature of the viral genome, and result in the generation of a novel influenza strain (18). These larger changes in the HA subtype, typically caused by this reassortment of two strains results in antigenic shift and the emergence of novel strains that can cause devastating pandemics due to a lack of immunity, such as in 2009 when Swine H1N1 emerged displacing the current circulating H1N1 (19, 20).

Pathogenesis in Humans

Influenza infection typically presents with clinical signs such at fever, myalgia, malaise, headache and upper respiratory symptoms that include cough, sore throat, and rhinitis (21). The spectrum and severity of clinical presentation varies by an individual's current health status, age, vaccination status, and is dependent on strain of virus. The incubation period is short, averaging two days, followed by the abrupt onset of symptoms that typically last no longer than a week. A small percentage of patients develop complications from influenza infection, which may include pneumonia, bronchitis, and sinusitis, and rarely encephalitis, transverse myelitis, Reye syndrome, myocarditis and pericarditis. These complications frequently cause more than 80% of flu-related fatalities among the elderly, discussed in detail below (1).

In response to influenza infection, the innate immune system produces a pro-inflammatory and antiviral response in the form of cytokines and chemokines, driving the rapid onset of symptoms. Chemokines and cytokines play a major role in the pathogenesis of viral infections. Highly virulent strains of influenza viruses, such as avian H5N1 influenza, cause aberrant and excessive cytokine production, in addition to replicating lower in the respiratory tract, resulting in higher levels of morbidity and mortality for humans and other mammals (22-24). Increased levels of specific inflammatory cytokines, including tumor necrosis factor (TNF) α, interleukin (IL-) 1, IL-6, IL-8, IL-12, interferon (IFN) γ, and IFN-α have been linked to disease progression and death in seasonal outbreaks of influenza (24). Retrospective studies of patients severely infected with pandemic H1N1 have identified a strong correlation with high sera levels of IL-6 and IL-1. The underlying mechanism of how, or why, aberrant cytokine responses correlate with more severe outcomes of influenza infection largely remains unknown.

Influenza Vaccines

By far the most important public health countermeasure for preventing the spread and mitigating the impact of influenza infection is the yearly production, distribution, and administration of an influenza vaccine (12, 13, 15). Currently, the predominant influenza vaccine produced for worldwide distribution is the trivalent influenza vaccine (TIV), and comes in several different formulations: the split (chemically disrupted) or subunit (purified surface glycoprotein) vaccine. The trivalent vaccine contains 3 distinct HA subtypes, including the 2 circulating strains from influenza A. The TIV vaccine undergoes yearly reformulations due to the ability of influenza virus to undergo antigenic drift and, occasionally, antigenic shift that can cause the emergence of novel influenza strains. Consequently, six months prior to next season's distribution of vaccine, influenza specialists from around the world meet at the WHO and, based

upon data presented from surveillance systems that monitor circulating strains, come to consensus as to which three influenza strains will be used as the reference sequences for vaccine production. Compared to other vaccines, the TIV is not highly efficacious, but even in the adult population it reduces the risk of infection by ~59%, when the reference strains are correctly antigenically matched to circulating strains (25). However, even in low efficacious vaccine years, the TIV mediates some protection from more severe symptoms and shortens duration of illness (26).

Vaccine response is typically assessed by levels of hemagglutination inhibitory antibodies (hAbs), a surrogate marker for neutralizing antibodies (nAbs), to non-conserved areas of HA which prevent viral attachment and entry (13, 27-30). Additionally, healthy adults who receive the trivalent inactivated vaccine (TIV) seroconvert (4 fold or more increase in hAb titer) an estimated 50-80% of the time based on immunogenicity studies (31-34). High seroconversion is correlated with protection but the mechanism(s) of how preexisting immunity affects vaccine immunogenicity is not fully understood (32, 35). The major mechanisms thought to lead to vaccine ineffectiveness, aside from strain mismatch, are currently unknown but likely due to a failure to promote a robust immune response to the circulating strain and also, may be related to the egg-adaptation, which is how most of the vaccine stock viruses are grown, that introduces some mutations in the HA of the vaccine strain (36-38). Two additional prominent hypotheses for ineffective vaccine-induced immune responses are immunosenescence, a well-known source of vaccine ineffectiveness in the elderly, and preexisting immune responses that hinder subsequent responses (39-43).

Preexisting Immunity Shapes Responses

Humans, over their lifetimes, have a complex immunological interaction with influenza due to repeatedly being exposed, by infection of vaccination, to constantly evolving influenza strains (44). The influence of influenza immunological memory on future responses to antigenically distinct but within HA subtype influenza has been recognized since the 1960s, when Sir Thomas Francis Jr. coined the term "original antigenic sin" (OAS), after observing that an individual's antibody responses to influenza are preferentially cross-reactive to previously circulating strains of that subtype, compared to responses that exclusively target newer viral strains (45-47). OAS refers to the phenomenon that immunological memory responses predominate at the expense of *de novo* responses following secondary viral exposure to related but not heterologous subtype influenza strains. More recently, this phenomenon has been expanded and retitled 'antigenic seniority' to account for numerous sequential exposures, where the chronological order in which the immune system interacts with influenza programs a hierarchical response, resulting in the highest titers to strains circulating when individuals are 5-10 years old, diminishing thereafter to antigenically related drifted strains (44, 48).

In agreement with this, Fonville et al. enrolled 69 individuals and, using a longitudinal study design over the course of 43 years, measured antibody levels to a panel of circulating strains and observed that the highest titers are to strains that circulated during childhood with a "back boost" in individuals' history. For example, an individual born in 1970, who may have been exposed to the HK/68 H3N2 strain early in life, and who then later was infected with the antigenically related 2009 H3N2 strain had a boosted antibody response to the earlier HK/68 (H3N2) strain compared with an individual born in the early 2000s whose antibodies only displayed specificity to the infecting 2009 strain (49, 50). Consistent with these results, a 20-year longitudinal study using sera from the Framingham Heart study documented that antibody titers

to previously encountered strains increased over time. For example the geometric mean titer increased from 104.8 to 735.2 to HK/68 from 1990 to 2008 in humans born between 1917 and 1962, this was also seen with USSR/77 (H1N1), suggesting a hierarchal nature where periodic boosting of previous titers upon subsequent exposures to subtype-related drifted strains occur (51). Collectively, these results suggest a model wherein antibody responses to previously encountered strains are periodically boosted by exposures to subtype-related drifted strains resulting in the greatest titers against strains encountered earlier in life and may not provide the most optimal response to current circulating strains.

De novo and Preexisting Antibodies

Antibodies and specifically, neutralizing antibodies (nAbs) to influenza are crucial for preventing infection and induction of these antibodies is the major goal of vaccination against influenza (13). Neutralizing antibodies canonically, prevent viral attachment and entry, fully inhibiting the viral life cycle, but antibodies can further, limit cell-to-cell spread of the virus and ultimately reduce the severity and duration of illness. However, while nAbs are the major correlate of protection for influenza they target the very HA epitopes that are constantly undergoing antigenic drift and therefore are usually strain-specific and ineffective against further drifted strains, limiting their ability over time to provide protection. Measuring nAbs for influenza strains is classically determined by the hemagglutinin inhibition assay (HAI), with a seroconversion of inhibition of 40 Log2 titer considered adequately responsive in vaccine trials (52, 53). While nAbs are undoubtedly the best correlate of protection for influenza, other HA and NA reactive antibodies contribute to protection through various effector methods, but can also lead to enhanced or suppressed subsequent antibody responses.

Antigen-specific antibodies passively administered with cognate antigen can either upregulate or downregulate subsequent antibody responses to that antigen depending on their Fc-receptor or complement interaction (54, 55). The upregulation of antibody responses is caused by enhanced targeting of antigen delivery to B cells and $CD4^+$ T cells. Whereas the downregulation of antibody responses can be caused by two distinct mechanisms that are not mutually exclusive: 1. reducing antigen availability via sequestration and clearance by antibody effector function engagement, and/or 2. binding the epitopes that remain conserved between drifted viruses, causing epitope masking and thereby sterically hindering access to antigen (54-59). Due to the combination of new and previous epitopes in drifting HA, and additionally, known antibody responses to conserved regions of HA, preexisting antibodies that cross-react with subsequent drifted HA's have the potential suppress subsequent novel antibody responses.

Recently, antibodies specific to the conserved, HA2 region (stem) of HA or other conserved regions of the head (HA1 region) have been shown to initiate effector functions via engagement of their respective Fc receptor (54, 56, 58, 60). Fc engagement by different Fc receptors can initiate multiple different effector function pathways, such as antibody dependent cell-mediated cytotoxicity (ADCC), opsonization and phagocytosis and complement dependent cytotoxicity (CDC) in which the HA antigen can be quickly cleared, providing complete protection against lethal challenge in the mouse preclinical model, if at a significantly high level (60). These findings, that broadly cross-reactive HA antibodies have capabilities of providing protection against multiple different influenza strains, including avian influenza (H5), has refocused efforts to rationally design a universal influenza vaccine driving conserved stem antibodies to a more abundant level in the human population (28, 29, 54, 55). It further suggests that preexisting cross-reactive antibodies, typically found in low levels in the human population,

have the capability to reduce antigen load, particularly in a case when antigen is limited, such as vaccination.

Recent experimental evidence of epitope masking has been found by passively administering antigen-specific IgG together with antigen in effector function receptor knockout mice (FcγR -/-) (60). While researchers observed that wild-type mice did have reduced antigen load post immunization with the antigen-IgG combination when compared to FcγR -/- mice, this did not correlate with antibody suppression suggesting that clearance was not responsible for epitope masking. They further went on to demonstrate that antigen-IgG in FcγR -/- mice suppressed the very epitopes that were bound by IgG and further, saw suppression of germinal center B cells, long-lived plasma cell and memory B cell responses. This experimental evidence of preexisting antibody suppression of *de novo* responses through either mechanism, along with the knowledge that memory B cells are more apt to respond, suggest that in limiting antigen circumstances, *de novo* responses could be suppressed or uninitiated.

B cells

In addition to serological evidence of OAS, recent technological advances in high-throughput sequencing of B cell repertoires have confirmed that responses to the trivalent influenza vaccine (TIV) and infection are recall responses in humans that are preferentially made up of memory B cells with extensively mutated variable regions suggesting multiple rounds of somatic hypermutation (SHM), where B cell receptors undergo mutational editing, and affinity maturation, where through selection B cell populations become more higher affinity for antigen (34, 61-64). Broadly, memory B cells are thought to predominate over *de novo* B cell responses due to both intrinsic factors and extrinsic factors of the memory B cell that aren't mutually exclusive. The intrinsic model hypothesizes that memory B cell receptors (BCR) cytoplasmic

domain is larger and contains more conserved amino acid sequences, leading to a reduced need for stimulus to become activated (65-67). It is likely in addition to intrinsic factors, that memory B cells specific for HA will have a B cell receptor (BCR) that has greater affinity for related HA antigen than the naïve B cell population. The extrinsic model proposes that stimulation history changes transcription factors and cell programming, allowing for a more robust response of memory B cells (67). In addition to intrinsic and extrinsic factors, memory B cells are at a physical advantage to encounter antigen prior to naïve B cells, by remaining near follicular dendritic cells and contracted germinal centers (68). In this way, memory B cells can expand and differentiate quickly into a plasmablast, an antibody secreting cell, or enter the germinal center to undergo further affinity maturation. Ultimately, this allows memory B cells to quickly and more robustly respond to re-exposure to identical or similar antigens and this enhanced and quicker response provides the basis for vaccination protection.

Recall of memory B cell responses elicited by influenza vaccination can and does provide protective responses for influenza; however, there is disagreement on whether or not vaccine induced plasmablasts have higher affinity toward current vaccine antigen or historical strains (62-64). Further, there have been recent studies where memory responses were shown to interfere with more effective responses targeted towards recent variants (39, 63). For example, Linderman et al. found that middle-aged individuals during the 2013-2014 influenza season were disproportionally affected with pH1N1 because a single point mutation in the HA of the pH1N1 circulating virus changed from lysine to glutamine. That antigenic site within HA where the lysine was located had previously circulated in humans in H1N1 viruses from 1969-1980 and was highly targeted by middle-aged individuals sera, consequently the virus escaped in the 2013-2014 season by changing the lysine to glutamine, rendering this predominate response

ineffective. Younger individuals who had not been previously exposed to that antigenic site had a more diverse antibody response, thus were less affected by that particular viral escape mutant (39).

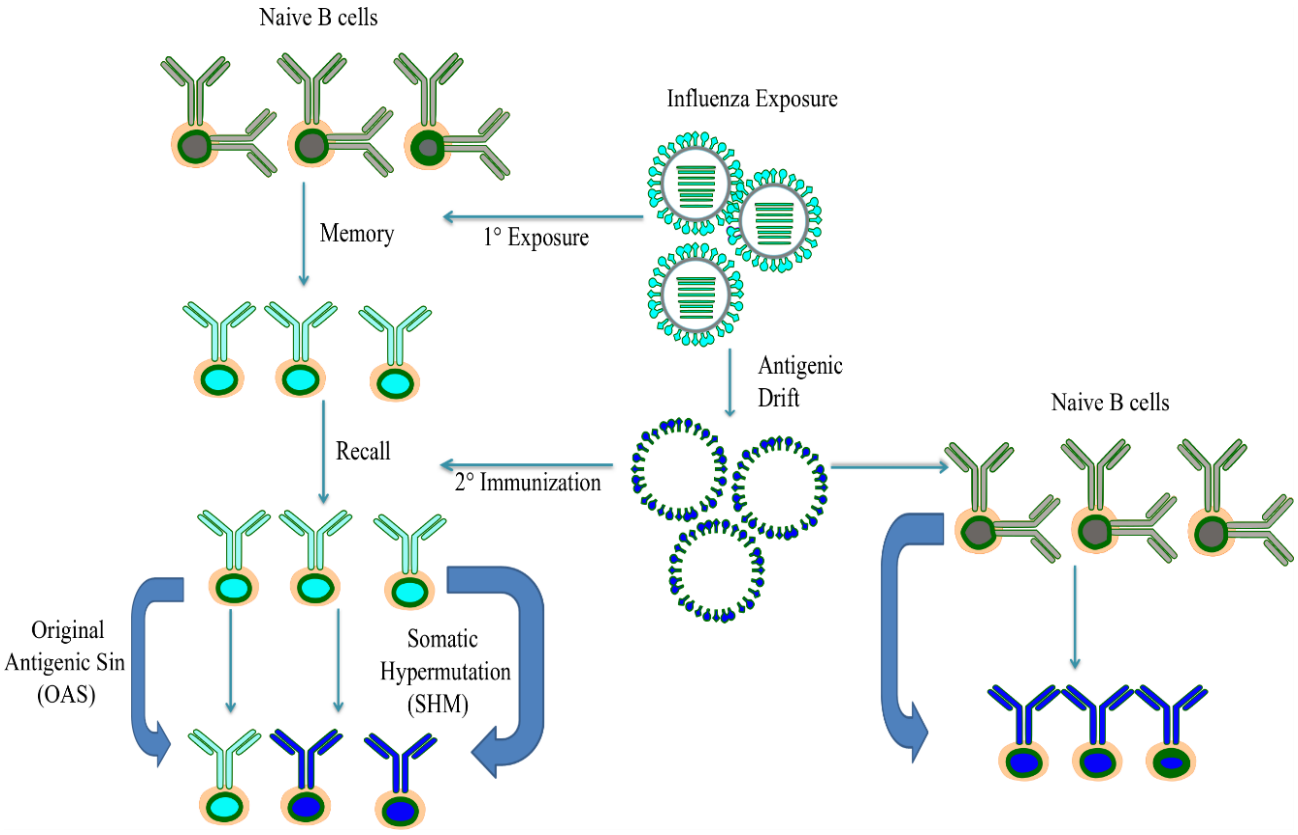

Figure 1.2 Hypothesized ontogeny of B cells upon re-exposure to drifted influenza.

These results were then further experimentally recapitulated by sequentially exposing ferrets to those influenza viruses. Interestingly, while memory B cells have been shown to quickly differentiate into plasmablasts upon antigenic re-stimulation (69), it wasn't until recently that vaccine induced class-switched memory B cells were found to be the main precursor cells that reenter germinal center responses when transferred to naïve hosts upon vaccination and rediversify their BCRs in a mouse model (70). This is in addition to IgM memory B cells, which have historically been thought of the main precursors to reenter germinal centers (71). Taken together with the serological evidence, these results suggest recall responses elicited by antigenically-related but distinct influenza strains prevail over *de novo* responses, and are potentially modified by SHM to bind current strains but do not lose the capacity to bind historical antigens (**Figure 1.2**).

$CD4^+$ T cells

In addition to memory B cells influencing future responses, memory $CD4^+$ T cells can also play diverse roles during heterologous influenza exposure and therefore can promote or suppress subsequent antibody responses in multiple ways. These roles include providing help to B cells and providing heterologous protection via direct cytotoxic function and/or IFN-γ production (72-74).

While more extensive research has been done on understanding the antibody repertoire to heterologous influenza, there has been a renewed interest in $CD4^+$ T cells with a focus on the T follicular helper cell (Tfh) subset interactions with B cells (49, 75). Recent studies using intravital imaging and experimental systems have shown that high-affinity B cell selection in the germinal center (GC) outcompete lower affinity B cells for antigen, but additionally, Tfh cells promote selection of GC B cells independently of the affinity of the BCR for antigen (27, 75).

This led to the postulation that higher BCR affinity is directly associated with greater antigen capture which leads to a higher density of peptide-MHC presentation on the surface of the B cell, enabling these B cells to interact with Tfh cells and enter the GC (76). In agreement with this model, a recent study by A.D. Gitlin et al. demonstrated that GC B cells receiving the greatest magnitude, as measured by contact time, of T cell help, divide and undergo SHM the greatest number of times, suggesting that antigen acquisition and T cell help are both crucial for continued GC B cell progression (76). Interestingly, using an influenza mouse model and peptide-priming regimen, S. Alam et al. demonstrated that memory $CD4^+$ T cells preferentially help B cells with the same intramolecular specificity and accelerate antibody responses to that protein, suggesting that influenza immunity is linked based on protein specificity (77). Furthermore, priming individuals with recombinant avian influenza H5 boosts and accelerates subsequent responses to a drifted H5, correlating with responsiveness to $CD4^+$ T cell epitopes (78-81). These results suggest that $CD4^+$ T cell memory can be manipulated by inclusion of $CD4^+$ T cell epitopes in booster vaccines to accelerate responses to emerging influenza pandemics. Importantly for influenza responses, it further suggests that conservation of internal proteins and epitopes could distract and focus the immune system by mobilizing ineffective antibody responses to internal proteins such as nucleoprotein (NP) and diminishing the immunological resources for additional responses to constantly changing antigens with changing $CD4^+$ T cell reactivity (82). Additionally, it collectively suggests that memory B cells reactive to HA may only be licensed to undergo further adaptation by SHM when MHC Class II restricted epitopes have remained unchanged.

In addition to helping B cells, memory $CD4^+$ T cells are capable of providing a low level of heterologous protection in the context of infection and live-attenuated influenza vaccination

while still limiting more specific antibody responses (83, 84). This sublethal protection in mice is associated with $CD4^+$ T cell cytotoxic functions and/or IFN-γ production (85-88). Cytotoxic $CD4^+$ T cells have been shown by Brown et al. to partially protect against 0.1 LD_{50} levels of virus in severe combined immunodeficiency (SCID) mice (85, 86). This protection was dependent upon expression of perforin, as transfer of the same number of perforin deficient $CD4^+$ T cells resulted in increased viral titer and complete loss of protection. In addition to mouse studies, a human influenza challenge study found a significant correlation between cytotoxic $CD4^+$ T cells specific for internal influenza proteins and reduced disease suggesting a role for cytotoxic $CD4^+$ T cells in protection in humans (89). In addition to perforin production, J.R. Teijaro et al. found that memory but not naïve $CD4^+$ T cells are capable of protecting RAG2-/- mice in the absence of other B and T cells from a lethal dose of both homologous and heterosubtypic infection. However, upon intranasal and intravenous administration of neutralizing IFN-γ antibody (XMG1.2), protection was lost (88). The mechanism by which IFN-γ elicits protection could be multipronged including activating macrophages (90), neutrophils (91) or regulating the antiviral response in the lung (66, 92-94).

Influenza Responses in the Elderly

Despite having approximately two exposures to influenza per decade over an individual's lifetime, the elderly (age 65 and older) are at increased risk for serious outcomes from influenza infection (8, 44). The elderly account for nearly 80% of influenza related deaths and are more likely to have more severe sequelae from infection, requiring hospitalizations (95). In addition to having the cumulative exposure to influenza, the elderly undergo an age-related immune decline termed immunosenescence (96). Immunosenescence is the quantitative and qualitative deterioration of the immune system, in both cellular and humoral compartments. This global

immune decline not only limits vaccine effectiveness to mitigate influenza caused disease, it also increases the likelihood of other opportunistic diseases to take hold following influenza infection, such as pneumonia. For that reason, numerous strategies to increase influenza vaccine effectiveness in the elderly have been undertaken. One method to increase effectiveness has been to simply increase the vaccine dose, thereby providing greater antigen loads that stimulate more antigen presentation via antigen presenting cells and thus eliciting greater antigen-specific antibody responses (97). Another method employed to increase vaccine effectiveness is to use innate immune stimulants, known as adjuvants, coupled to the vaccine (13). Most contemporary adjuvants contain a pathogen-associated molecular pattern (PAMP) to stimulate pattern recognition patterns (PRRs), such as toll-like receptors (TLRs) and are formulated in an oil-in-water emulsion, such as squalene to stimulate T cell responses (98, 99). TLR-agonists are usually derived from a major component of a pathogen. One TLR-agonist commonly used in approved adjuvant formulations to stimulate TLR4 is derived from lipopolysaccharide (LPS), and induces innate activation via IL-1ß and antigen presenting cells. This class of adjuvants, oil-in-water emulsions, have been shown to increase both HAI titer and $CD8^+$ and $CD4^+$ T cells responses in the elderly leading to higher vaccine effectiveness. An inactivated influenza vaccine containing the MF59 adjuvant has been approved for use in Europe and the United States (100). Additionally, broad TLR- agonist adjuvants are very effective at boosting strain specific antibody responses and increasing antibody reactivity breadth, making them attractive for stockpiling with an avian H5 influenza vaccine (81). Collectively, engaging the innate immune system with TLR-agonist adjuvants in the elderly is crucial to mitigating influenza caused disease and providing the vaccine effectiveness, however, the mechanisms by which these adjuvants provide greater protection remain unknown.

Summary

Preexisting immunity and immunosenescence to influenza has long been known to augment subsequent influenza vaccination responses. The primary goal of this dissertation was to define the cellular contributors of preexisting immunity that augment future responses and use this knowledge to enhance subsequent responses. This was accomplished by addressing the following 4 specific aims.

1. Develop and characterize preexisting influenza immunity mouse models.
2. Investigate the cellular and humoral contributors to immunological outcomes.
3. Characterize and utilize preexisting immunity to enhance subsequent responses.
4. Characterize and utilize an adjuvant in an immunosenescence mouse model of influenza to determine if a TLR-agonist adjuvant can enhance responses to influenza vaccination.

The work described herein critically examines how preexisting immunity to influenza influences subsequent responses. In chapter 2, we establish and characterize two separate mouse models in which upon secondary exposure to drifting influenza exposure has strikingly different immunological outcomes. In chapter 3, we investigate the cellular contributors to these different immunological outcomes by systematic removal and transfers of different memory immune components. We then leveraged this mechanistic knowledge of how preexisting immunity affects subsequent responses to enhance subsequent responses, in chapter 4. Lastly, we employ adjuvant in an immunosenescent mouse model of influenza to determine if our TLR-agonist adjuvant can enhance responses to influenza vaccination.

Chapter 2*:* Establishment of Preexisting Influenza Experienced Mouse Models

Introduction

A human longitudinal study exploring how preexisting immunity to influenza impacts future responses is challenging as it would necessitate identifying and confirming every exposure to influenza, infection and vaccination beginning at very young ages. Consequently, it would be helpful to develop an animal model to begin to understand the impact of sequential exposure on host immunity. To that end, JH Kim et al. in 2011 established a mouse model of OAS, sequentially infecting mice with two drifted influenza strains, A/PR/8/34 and A/FM/1/47, which contain 90.5% sequence identity between their respective HAs (101). This model demonstrated that prior infection with A/PR/8/34 decreased antibody responses to A/FM/1/47 and boosted humoral responses towards the initial strain, A/PR/8/34, the two phenotypic hallmarks of antigenic sin. Further, they demonstrated that this OAS phenotype is reversible by inclusion of adjuvant, using both CpG and squalene-based oil-in-water nanoemulsion, in the second or first exposure (102). They hypothesized that overcoming OAS was due to dendritic cell activation by adjuvant, shifting antigen presentation and priming to dendritic cells instead of memory B cells acting as antigen presenting cells. However, they went on, using the exact same influenza strains, to observe that pre-exposure to live virus paradoxically intensified efficacious responses to immunization to the intra-subtype drifted HA without adjuvant, suggesting that the original OAS model results could largely be due to a significant reduction in antigen load from cross-protective responses and possibly not the only basis for OAS as observed in humans (103).

In addition to this model, JL Nayak et al. used a heterosubtypic influenza mouse model, using strains X-31 (H3N2) and x139 (H1N1) with 100% conserved internal proteins but very disparate HA's (82). This study demonstrated that X-31 pre-exposure antagonized the HA

antibody response to x139 despite the large disparity in HA between the two strains. This result was reputed to be due to both B and T cell immune responses to conserved internal proteins and they further went on to prove that $CD4^+$ T cell help to B cells is cognate (77). While reminiscent of OAS, in that it recreates a reduction of HA humoral responses to the second exposure, this model did not demonstrate reinforcement of the initial B cell response to the HA of the first strain, which may have been due to their subtype difference. However, this study did find that humoral responses to conserved internal proteins, but not HA, did receive a humoral boost from the second exposure suggesting that conservation of internal proteins could preferentially focus responses there and skew away from shifting viral proteins, like HA and NA, and this could contribute to the OAS phenotype.

Last, in an effort to characterize OAS further, Hensley and colleagues established a mouse model utilizing A/PR/8/34 and A/PR/8/34S12a, an engineered strain with 13 mutations spanning the 4 antigenic sites of HA, making them antigenically distinct by HAI assay but highly conserved (59). They went on to characterize the binding footprints and neutralization efficiencies in a sequential infection model. Interestingly they concluded that OAS Abs target the same region as non-OAS Abs, are clonally-related to one another and that OAS antibodies are a protective element to subsequent challenge. Collectively, these results fit a model wherein priming with infection or adjuvanted vaccine exposure enables memory B cells to produce unchanged OAS Abs upon secondary exposure to a sufficient amount of drifted HA antigen, but these B cells can clonally expand and change to become non-OAS Abs, displaying both antigen specificities in the polyclonal response.

Despite establishment of these mouse models, the underlying mechanism/s or immunological contributors that allow memory to predominate have yet to be elucidated for

influenza. Therefore, we first set out to establish and characterize our own OAS model, to then use for investigations into the immunological contributors in Chapter 3. For our own OAS mouse model, we used two significantly drifted H1N1 viruses, A/CA/07/09 and A/PR/8/34, which have 81.4% amino acid identity in their respective HA's but little to no convergence on antibody neutralizing regions (**Figure 2.1**). We hypothesized that these viruses of the same HA subtype, although significantly more drifted than the previously discussed OAS mouse model, would demonstrate a diminished secondary HA response and a concurrent humoral boost to more conserved regions in HA of the primary strain.

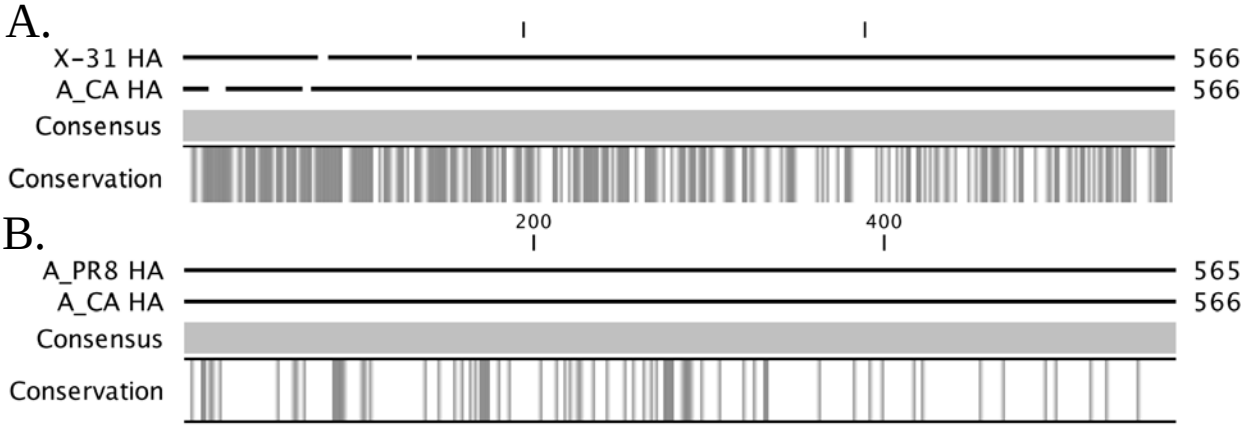

Figure 2.1 Amino acid comparison between HA's used in C57BL/6 mouse model. HA amino acid conservation shown in white and discrepancies shown in grey. Comparison between A/CA (H1N1) and X-31 (H3N2) in panel **(A)** and A/CA (H1N1) and A/PR8 (H1N1) in panel **(B)**. Graphics made by CLC sequencer (Qiagen).

Materials and Methods

Mice

Female C57BL/6, CB6F1 and B10.D2 mice, 6-8 weeks of age were purchased from Jackson laboratory. All animals were housed in the IDRI Vivarium (Seattle, WA) under specific pathogen-free conditions. All animal experiments and protocols were approved by IDRI's Institutional Animal Care and Use Committee (IACUC).

Immunization and influenza virus infection of mice

Mice were immunized by intramuscular (i.m.) injection with 1 µg recombinant HA (rHA) from A/PR/8/34 or A/CA/07/09 (Protein Sciences Corporation) or PBS.

Infection Studies

Mice were infected intranasally with 0.5 LD_{50} or 1000 LD_{50} dose of A/CA/07/09 (H1N1), A/PR/8/34 (H1N1), or A/X-31 (H3N2) in 25uL of phosphate-buffered saline (PBS). Mice were monitored for weight loss and other signs of virus induced morbidity daily, such as ruffled fur and lethargy, and sacrificed if weight loss exceeded 20% of initial body weight.

Enzyme Linked Immunosorbent Assays (ELISA)

Mouse sera were collected from individual mice and A/PR8 HA and A/CA HA reactive antibodies were determined by an enzyme-linked immunosorbent assay (ELISA) using rHA purchased from Protein Sciences Corporation as a coating antigen. Polysterene 96 well flat bottom immuno plates (NUNC) were coated overnight at 4°C with 0.1 µg rHA per well. Wells were washed three times with PBS- 0.5% Tween 20. Blocking buffer (1% bovine serum albumin (BSA) in PBS-Tween) was added to every well and incubated for 1 hr at RT. Wells were again washed and serial 2-fold sample dilutions were added to the plates in 0.5% BSA PBS and incubated at RT for 1 hr. Wells were again washed five times and incubated for 1 hr at RT with

100 µL/well horseradish peroxidase-conjugated goat anti-mouse secondary antibody specific for IgG (Southern Biotech) diluted in 1% BSA-PBS at a 1/4000 dilution. Subsequently, wells were washed five times and developed with 100 µL/well tetramethylbenzidine (TMB). Stop solution, H_2S0_4 (1N), was then added at 100 µL/well to stop the reaction. The optical density was read at 450nm (OD450) using a Biotek Synergy 2.

Hemagglutination Inhibition Assays

Hemagglutination Inhibition (HAI) activity specific to A/PR/8/34, A/CA/07/09 and A/X-31 was performed as previously described in using 1% Turkey Red Blood Cells (TRBCs) (104). Briefly, each serum sample was treated with receptor-destroying enzyme (RDE) overnight at 37°C followed by heat inactivation to remove nonspecific inhibitors. HAI titer was determined by the reciprocal of the highest dilution of sera that completely inhibited the agglutination of turkey RBCs following addition of 4 HAU (hemagglutination units) of virus, starting at a 1:10 dilution and serially diluting 2-fold down a 96 v-bottom plate.

T cell staining and stimulation

Antigen specific $CD4^+$ T cell responses were measured by peptide and rHA stimulation and flow cytometry. Briefly, splenocytes or cells isolated from lymph nodes were isolated and cultured ($2x10^6$ cells/well) for 8 hr with peptide (pools of 12 overlapping 15-mers that covered A/CA HA) or rHA (10 µg/well) in the presence of Brefeldin A (BD Biosciences). After stimulation, cells were permeabilized and stained with fluorochrome conjugated anti-mouse CD4 (clone RM4-5), CD8 (clone 53-6. 7), CD44 (clone IM7) and B220 (RA3-6B2) (BioLegend and eBioscience) antibodies in the presence of anti-CD16/32 (clone 93) for 15 minutes in the dark at RT. Cells were fixed and permeabilized with Cytofix/Cytoperm (BD Biosciences) for 30 minutes at RT in the dark. Cells were washed with Perm/Wash (BD Biosciences) and stained for

15 minutes with fluorochrome labeled antibodies to detect intracellular cytokines as follows: IFN-γ (clone XMG-1.2), IL-2 (JES6-5H4), TNF (MP6-XT22), IL-5 (clone: TRFK5) and IL-10 (clone: JES5-16E3) (BioLegend and eBioscience).

Results

Establishment of a C57BL/6 OAS Model

First, to establish our OAS mouse model we recapitulated the previous model by first exposing C57BL/6 mice to 0.5 LD_{50} (Lethal Dose 50%) A/CA, the prototype H1N1 virus from the 2009 pandemic, allowing the mice to undergo infection and recuperation for 28 days and then re-exposing mice to 0.5 LD_{50} of the drifted strain A/PR8 or shifted strain, X-31 (**Figure 2.2 A**). Mice were weighed daily post primary and secondary infection and sacrificed if they met weight loss criteria. The mice were bled at day 21 post-primary and secondary infection to measure both nAb titer by HAI assay and HA titer by enzyme-linked immunosorbent assay (ELISA). Mice given 0.5 LD_{50} A/CA lost significant weight but began to recover on day 10 post infection (**Figure 2.2 B**). To ensure that primary infection was adequate for seroconversion, A/CA HA reactivity was assessed by ELISA. All infected C57BL/6 mice demonstrated seroconversion to A/CA HA (**Figure 2.2 C**).

In our model, mice previously exposed to A/CA/7/09 (A/CA), display significantly decreased titers by HAI and ELISA to A/PR/8/34 (A/PR8) after secondary exposure (**Figure 2.3 B and E**). In addition to two closely related H1N1 viruses, we carried out sequential exposure with A/CA/07/09 and a virus from another circulating subtype, X-31 (H3N2), as a control (**Figure 2.3 C**). We observed significant back-boosting to A/CA HA by ELISA but not HAI upon secondary exposure to intra-subtype drifted virus (A/PR8) as compared to Ab levels on day 21 post primary exposure or secondary exposure to a shifted virus (X-31) (**Figure 2.3 A and D**). We observed insignificant reduction in neutralizing titer when using X-31 as the secondary exposure and no diminished titer to X-31 HA by ELISA (**Figure 2.3 C and F**).

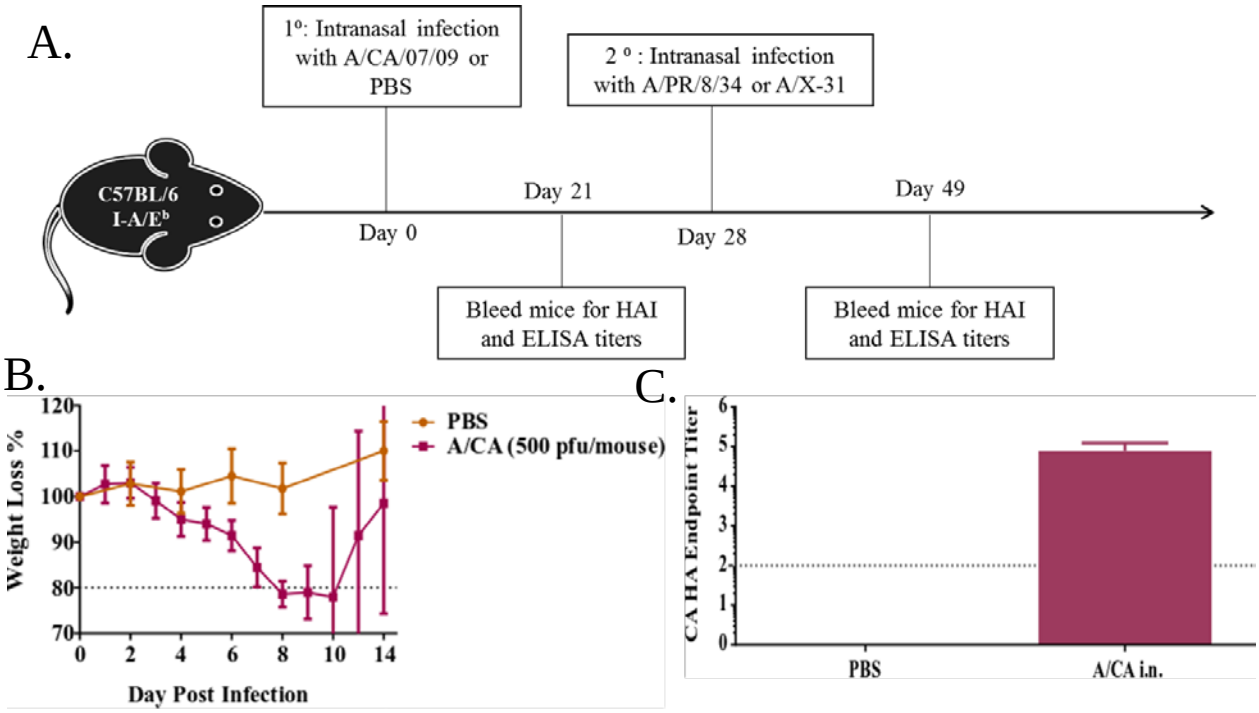

Figure 2.2 Experimental OAS mouse model development. Timeline of model in panel **(A)**. At day 0 mice (n=10) are given sublethal exposure to virus A (A/CA/7/09) or PBS. At day 28 post primary infection mice are again exposed sublethally to an antigenically related virus A/PR8 or to a shifted virus, X-31(A/Aichi/2/68). Weights are measured daily for up to 14 days post primary infection panel (**B**), error bars depict ± SD. Mice are bled at 21 days post primary infection to ensure seroconversion by ELISA ± SD (Log_{10}) in panel (**C**).

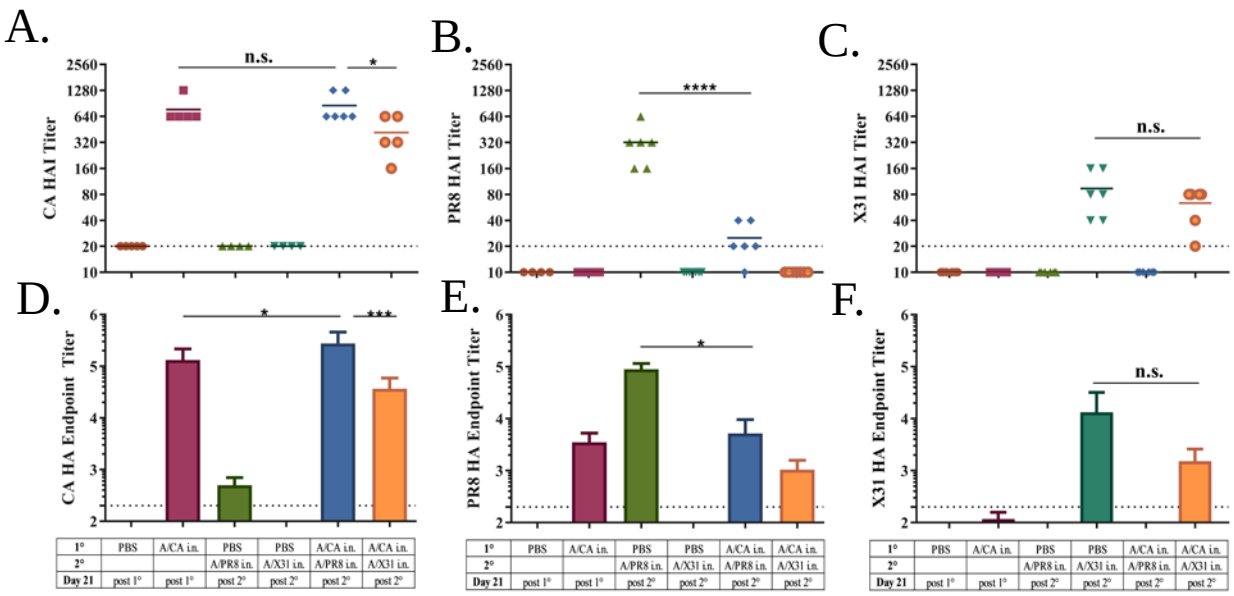

Figure 2.3 Pre-exposed C56BL/6 mice have dampened antibody responses to subsequent drifted influenza exposure. Serum Ab responses of individual mice (n=6 per group) to A/CA, A/PR8 and X-31 by HAI (Log_2) (panels **A**, **B** and **C** respectively) and endpoint titers ± SD (Log_{10}) (panel **D**, **E** and **F**, respectively) at day 21 post-primary infection (A/CA) and day 21 post-secondary infection with A/PR8 or X-31. Asterisks indicate significance between A/CA, A/PR8 or X-31 titers. (*p<0.05, ****p<0.0001, One-way ANOVA).

Establishment of CB6F1 mouse model

To further corroborate our OAS model, we sought to recapitulate the previous finding that pre-exposure can intensify secondary responses to drifted virus, if the secondary exposure is given as a sufficient standardized amount of antigen (1 µg). Deviating from the previous OAS model, we found that previously A/CA-infected C57BL/6 mice immunized with 1 µg PR8 HA, displayed no such enhancement of A/PR8 nAb titers, leading us to hypothesize this discrepancy was possibly due to mouse genetic background (103). To that end, we compared two mouse haplotypes, CB6F1 mice (I-A^b I-E^d I-E^d) and C57BL/6 (I-A^b), where both mouse strains were either A/CA infected, immunized or given PBS and then 28 days later infected or immunized with drifted A/PR8 (**Figure 2.4 A**). Strikingly, when both mouse models, previously infected with A/CA, were given standardized amounts of recombinant antigen, rHA A/PR8 (1 µg) by intramuscular (i.m.) immunization, CB6F1 mice demonstrated 32-fold increased antibody neutralizing responses to A/PR8 and HA reactivity by ELISA at day 21 post i.m. compared to C57BL/6 mice or PBS-treated CB6F1 mice (**Figure 2.4 B and C**). Additionally, upon immunization with drifted A/PR8 HA, C57BL/6 displayed the OAS phenotype of boosted A/CA HA reactivity whereas the CB6F1 mouse model did not (**Figure 2.4 D**). To further test if the increased neutralizing antibody titer to A/PR8 in CB6F1 previously infected mice resulted in protection differences, we then challenged with 1000 LD_{50} of A/PR8. Unsurprisingly, protection from weight loss and lethality directly associated with neutralizing A/PR8 titer, however C57BL/6 mice displaying significant non-neutralizing but cross-reactive antibodies by ELISA for A/PR8 HA were marginally protected from lethality but not weight loss (**Figure 2.5 A and B**).

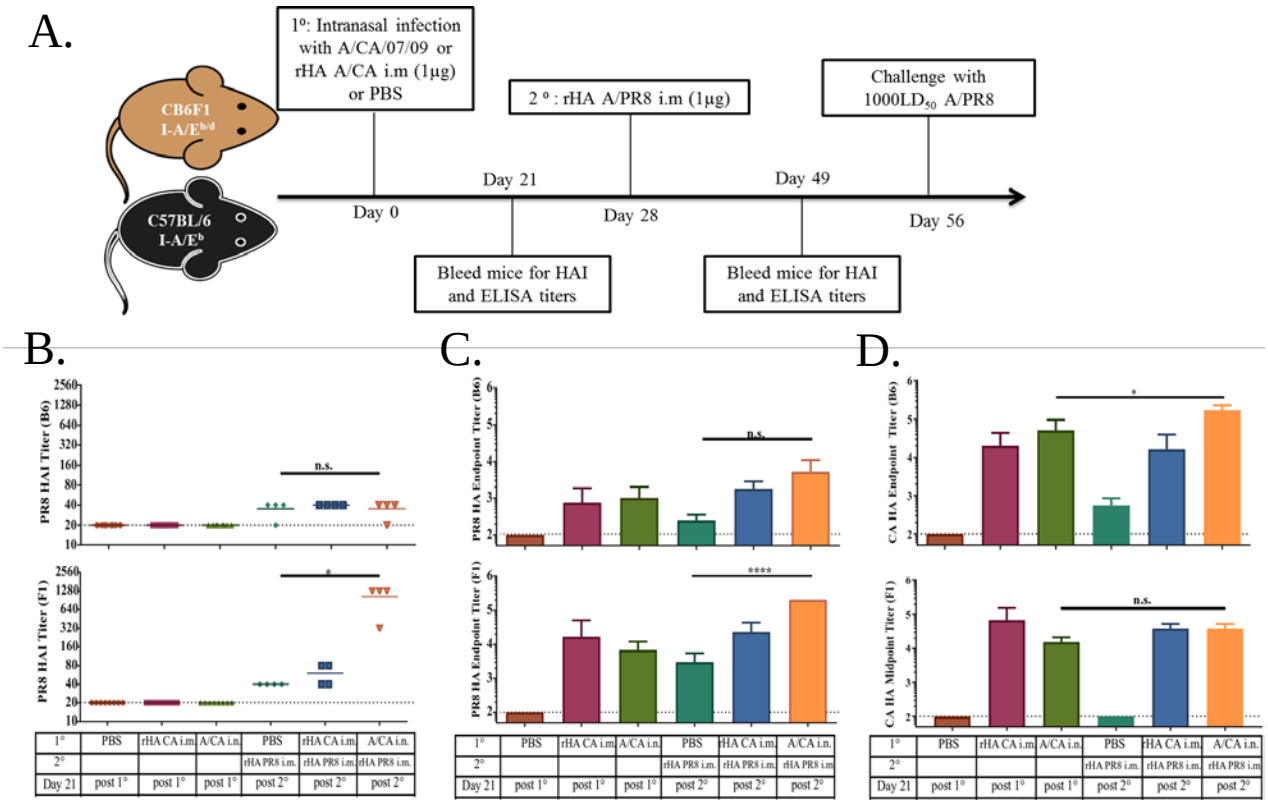

Figure 2.4 Pre-exposed CB6F1 but not C57BL/6 mice have increased antibody responses to drifted influenza vaccination. Model timeline in panel (**A)**: C57BL/6 (n=4 per group) and CB6F1 mice are intranasally exposed to A/CA (500 pfu/mouse) or PBS then 28 days later immunized with A/PR8 rHA (1 µg/mouse) or PBS. Mice are bled at 21 days post primary and secondary exposure to determine A/CA and A/PR8 HAI and endpoint titers. Mice are then challenged with 1000 LD_{50} A/PR8 to determine protection capability of the secondary response. A/PR8 HAI titer (Log_2) in panel (**B**) and A/PR8 endpoint titer ± SD (Log_{10}) in panel (**C**) and A/CA endpoint titer ± SD (Log_{10}) in panel (**D**) at day 21 post primary and secondary influenza exposure in C57BL/6 and CB6F1 mice. Error bars indicate ± SD (Log_{10}). (*p<0.05, ****p<0.0001, One-way ANOVA).

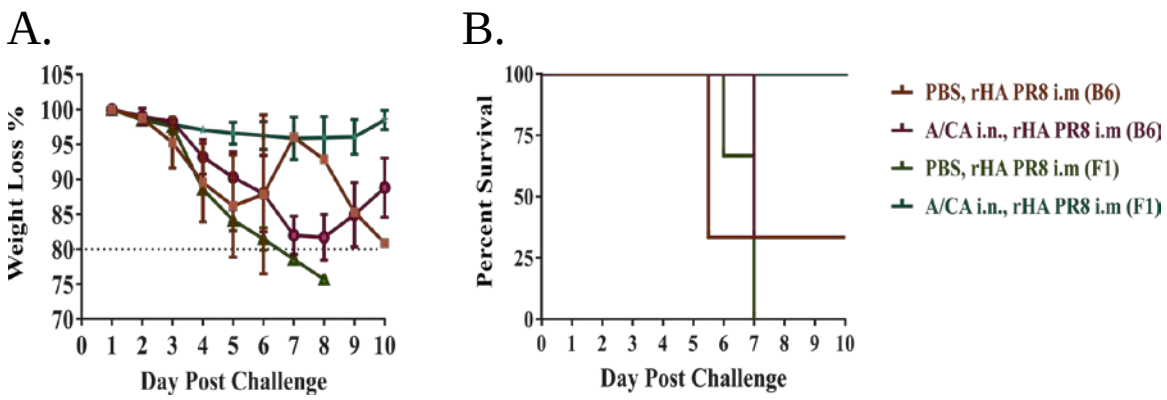

Figure 2.5 Neutralizing antibody titer correlates with protection against both weight loss and lethality to A/PR8. Weight loss in panel (**A**) and percent survival in panel (**B**) up to 10 days post 1000 LD_{50} A/PR8 challenge.

Since CB6F1 mice have an increased diversity of MHC class II genes compared to C57BL/6 mice, the differential secondary response to immunization with heterologous HA may be linked to MHC Class II reactive epitopes conserved across the drifted HAs. To test this hypothesis, we established $CD4^+$ T cell reactivity to A/CA peptide pools in both CB6F1 and C57BL/6 mice. Interestingly, A/CA exposed C57BL/6 mice display no significant $CD4^+$ T cell reactivity with A/CA peptide pools, suggesting the absence of MHC Class II reactive epitopes in C57BL/6 mice. Conversely, CB6F1 mice infected with either A/CA or A/PR8 demonstrated $CD4^+$ T cell reactivity to A/CA peptides as measured by IFN-γ production by flow cytometry (**Figure 2.6**).

To confirm that other genetic differences between the two mouse strains were not playing a significant role we utilized B10.D2 mice, which have C57BL/6 background but an I-A/$E^{d/d}$ haplotype, sharing an MHC Class II allele with CB6F1 mice. Similar to the CB6F1 mice, B10.D2 mice first exposed to A/CA and then immunized with rHA A/PR8 displayed an enhanced nAb response to A/PR8 as compared to previously uninfected mice and similar ELISA titer to A/PR8 HA (**Figure 2.7**). These results strongly suggest that the HA's of A/PR8 and A/CA share a common I-A^d or I-E^d restricted epitope, but no shared I-A^b epitopes.

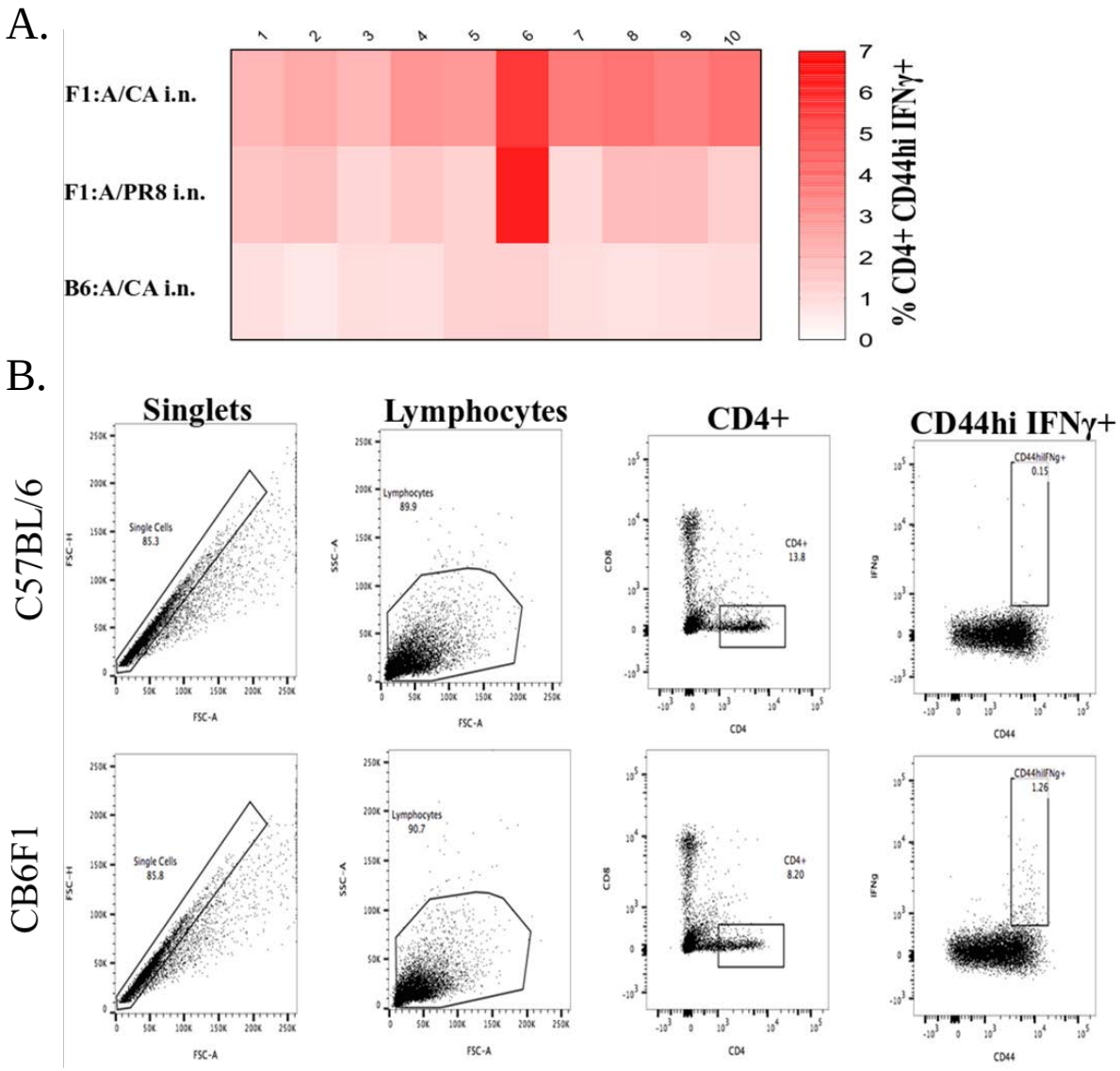

Figure 2.6 Enhanced neutralizing antibody responses correlated with CD4$^+$ T cell cross-reactivity. C57BL/6 or CB6F1 mice were intranasally infected with either A/PR8 or A/CA. Day 14 post infection spleens were harvested and stimulated with pooled peptides (1-10) of A/CA HA. Cells were then stained for analysis by flow cytometry and CD4$^+$CD44^{hi}IFNγ$^+$ cells frequency of parent percentage (FoP %) were quantified in panel (**A**). Representative flow plots and gating strategy are shown in panel (**B**).

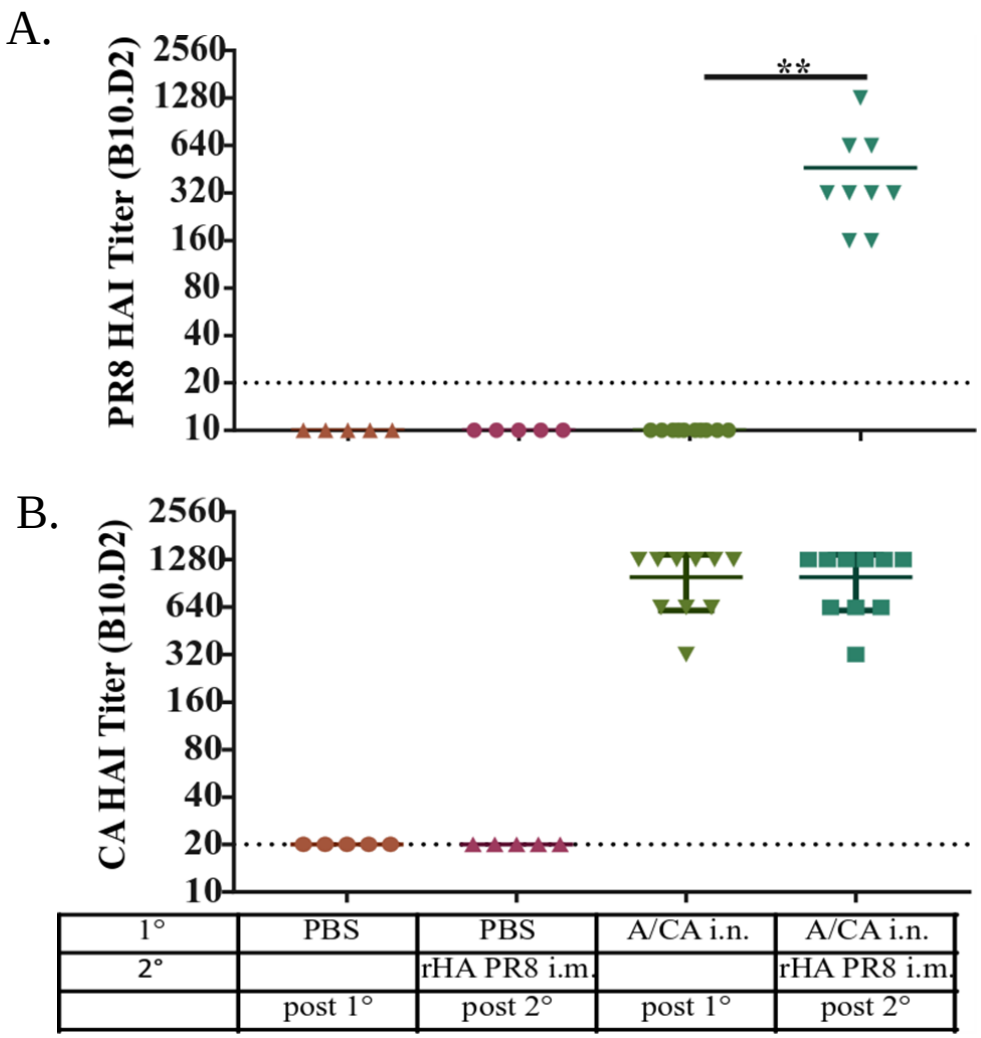

Figure 2.7 Pre-exposed B10.D2 mice display enhanced neutralizing antibody responses to drifted influenza immunization. B10.D2 mice (n=10 per group) were infected with A/CA or mock infected with PBS then 21 days later immunized with A/PR8 HA (1 µg). HAI titer (Log_2) to both A/PR8 in panel (**A**) and A/CA in panel (**B**) were evaluated in serum samples. (**p<0.01, One-way ANOVA).

Discussion

As a critical first step to investigating the mechanisms of OAS in the mouse model, we have successfully recapitulated OAS using more distantly related viruses than those previously described (101). However, fascinatingly, our OAS model demonstrated the OAS phenotype even when the mice given sufficient standardized HA antigen amounts via immunization after priming with live-related virus, in contrast to the previous model (103). This intimates that in addition to limiting the amounts of antigen upon intra-subtype exposure, there are additional immunological contributors to OAS, wherein you only see a 'back-boost' to the formative HA. Further these two mouse models, allow us to isolate the OAS phenomenon whereas other mouse models have shown mixed OAS and non-OAS Ab responses (59). While this mixed response of OAS and non-OAS Ab responses is likely to occur in humans a majority of the time, our OAS model affords us the opportunity to investigate the immunological contributors of only the OAS outcome, even with excess antigen and further contrast it to a model using the same strains with no OAS outcome. Further, previous mouse model results may be explained in part by antigen quenching to a greater extent, as opposed to memory B cell responses dominating over *de novo* responses. Indeed, OAS antibodies have been shown to be protective *in vivo*, diminishing morbidity, mortality and reducing antigen load (59, 105).

Intriguingly, when we compared the OAS C57BL/6 model to CB6F1 mice, we saw contrasting antibody phenotypes. Distinct MHC Class II haplotypes of these two mouse models indicated that this striking difference may be due to a lack of conserved $CD4^+$ T cell reactivity in the OAS mouse model. Consequently, we further epitope-mapped $CD4^+$ T cell reactivity to A/CA HA and found that CB6F1 mice displayed $CD4^+$ T cell reactivity to conserved HA epitopes across both priming and boosting intra-subtype virus HAs whereas C57BL/6 mice

displayed little reactivity to epitopes of HA. This further implicated MHC Class II reactivity in the OAS phenotype but to unequivocally rule out other genetic differences between the strains playing a role we utilized the B10.D2 model. These mice have a C57BL/6 background but share a CB6F1 MHC class II allele. This mouse model demonstrated the CB6F1 phenotype, enhanced responses, further implicating a lack of $CD4^+$ T cell reactivity playing a major role in OAS responses. Taken together with previous literature, these results here fit a model wherein priming with live influenza virus inhibits responses to subsequent live-exposure to intra-subtype virus by limiting antigen availability and providing only enough antigen to stimulate memory B cells eliciting an OAS phenotype. However, if immunized with sufficient standardized amounts of antigen, these responses are instead intensified and updated to be specific towards this new virus demonstrating a non-OAS phenotype. Importantly, our model further conveys that the intensification and non-OAS phenotype is likely due to conserved $CD4^+$ T cell reactivity between the two HAs, suggesting that drifting $CD4^+$ T cell epitopes in HA can inhibit potent nAb responses, as seen in our OAS model. These two mouse models with strikingly different antibody outcomes will serve as a powerful tool for defining the immunological contributors of OAS.

Chapter 3: Determining how Preexisting Cellular and Humoral Immunity Augment Secondary Responses to Drifted Influenza

Introduction

Broadly, two immunological memory compartments could influence subsequent responses detrimentally and constructively: cellular and/or humoral immunity. Memory cellular immunity includes $CD4^+$, $CD8^+$, and B cells; humoral immunity refers to cross-reactive antibodies. Previous research using removal and transfer methods for immunological memory has focused on assessing the role and potency of these immune components for protection against homologous virus and/or heterologous virus that have conserved elements. In this way, immunological memory can augment subsequent responses by diminishing antigen load and therefore dampening secondary responses, possibly contributing to antigenic sin in our OAS C57BL/6 mouse model (Chapter 2). For example, memory $CD4^+$ T cells with cytotoxic potential and $CD8^+$ T cells have been extensively studied to assess their contribution to protection against both homologous as well as heterologous strains of influenza that contain conserved proteins (57, 73, 74, 84, 86-88, 106, 107). While these memory cellular components, cytotoxic $CD4^+$ and $CD8^+$ cell responses, have been found to provide protection, they do not provide sterilizing protection, allowing viral replication, but considerably lowering viral loads. This diminishment of antigen production and viral replication by $CD4^+$ and $CD8^+$ T cells could decrease immune stimulation impeding *de novo* responses to drifted virus. Likewise, humoral immunity (preexisting antibodies), have the capacity to 'antigen-trap', decreasing antigenic load and hindering naïve responses as well (49). Lastly, memory B cells have advantages over naïve B cells, due to reduced activation thresholds, robust responsiveness, antigen affinity and

advantageous proximity to incoming antigens (65). Taken together, these immunological memory constituents contribute to an OAS model wherein memory $CD4^+$, $CD8^+$ T cells and cross-reactive antibodies diminish antigen load, with the remaining antigen only eliciting cross-reactive memory B cells, not undergoing adaptation due to a lack of cognate $CD4^+$ T cell help.

Immunological memory also has the ability to improve secondary antibody responses to drifted influenza antigen, as recapitulated in our CB6F1 mouse model (Chapter 2). Similar to the robust secondary response to vaccination, well established memory B and $CD4^+$ T cells respond quickly and strongly to homologous and related antigen exposure. Concomitant elicitation of these memory cell subsets can induce robust germinal center responses and increase neutralizing antibody production (42, 80, 81). This cellular interaction will be further explained and characterized in Chapter 4.

Preexisting immunity to influenza, as established by our mouse models and previous literature, demonstrates that immunological memory responses can ultimately be either beneficial or detrimental to subsequent responses to drifted virus. However, the cellular contributors of preexisting immunity that augment future responses to drifted virus have yet to be cogently and fully disassembled and reassembled to assess their respective impact. To that end, in Chapter 3, we used systematic removal and transfers of different memory immune components, to isolate their impact, both beneficial and detrimental, upon secondary responses to drifted influenza exposure using both the C57BL/6 and CB6F1 mouse model.

Materials and Methods

Mice

Female C57BL/6 and CB6F1 mice, 6-8 weeks of age were purchased from Jackson laboratory. All animals were housed in the IDRI Vivarium (Seattle, WA) under specific pathogen-free conditions. IDRI's Institutional Animal Care and Use Committee (IACUC) approved all animal experiments and protocols.

Immunization and influenza virus infection of mice

Mice were immunized by intramuscular (i.m.) injection with 1 µg recombinant HA (rHA) from A/PR/8/34 or A/CA/07/09 (Protein Sciences Corporation) or 5 nM of pooled conserved peptides, formulated with and without the adjuvant, SLA-SE (5 µg) or saline. Peptides used in this study included those listed in the table below.

Peptides
IGYHANNSTDTVDTV
STDTVDTVLEKNVTV
VLEKNVTVTHSVNLL
IDYEELREQLSSVSS
EQLSSVSSFERFEIF
RGLFGAIAGFIEGGW
WYGYHHQNEQGSGYA
IENLNKKVDDGFLDI
VDDGFLDIWTYNAEL
IWTYNAELLVLLENE
DSNVKNLYEKVRSQL
LKNNAKEIGNGCFEF
GVKLESTRIYQILAI
RIYQILAIYSTVASS
IYSTVASSLVLVVSL
LGAISFWMCSNGSLQ
MCSNGSLQCRICI

Table 1. Influenza HA peptides conserved between A/PR8 and A/CA HA used for immunization.

Mice were infected intranasally (i.n.) with 0.5 LD_{50} or 1000 LD_{50} dose of A/CA/07/09 and A/PR/8/34, in 25 µL of phosphate-buffered saline (PBS). Mice were monitored for weight loss and other signs of virus induced morbidity daily and sacrificed if weight loss exceeded 20% of initial body weight.

$CD4^+$, $CD8^+$ T cell and B cell depletion

InVivo Mab anti-mouse $CD4^+$ (clone GK1.5) and anti-mouse $CD8^+\alpha$ (clone 53 6.7) and isotype controls were purchased from BioXCell (West Lebanon, NH). Mice were intraperitoneally (i.p.) administered a dose of 250 µg per mouse twice day 27 and 28 post primary exposure depletion of $CD4^+$ and $CD8^+$ T cells. $CD4^+$ and $CD8^+$ T cell depletion was confirmed by flow cytometry with anti-$CD4^+$ T cell (clone RM4-5) and anti-$CD8^+$b (clone YTS156.7.7). Mouse Anti-CD20 antibody (clone 5D2, murine IgG2a) was graciously provided by Genentech. Mice were given two i.p. injections of 250 µg of CD20 antibody on consecutive days. Depletion was assessed by flow cytometry with an anti-B220 and anti-CD19 antibodies.

$CD4^+$ T cell adoptive transfer

C57BL/6 mice were sublethally infected with either A/PR/8/34 or A/CA/07/09 or given PBS as a control. At day 28 post infection, spleen, inguinal, axillary and brachial lymph nodes were processed into single cell suspension using a 100 µm nylon cell strainer (BD Falcon). $CD4^+$ T cells were isolated with the mouse $CD4^+$ T cell Isolation Kit (Miltenyi Biotec). Approximately, $6x10^7$ $CD4^+$ T cells/mouse in 200 µL of PBS were transferred into naïve C57BL/6 recipient mice by retro-orbital injection (r.o).

Enzyme Linked Immunosorbent Assays (ELISA)

Mouse sera were collected from individual mice and PR8 HA, CA HA and Nucleoprotein (NP) reactive antibodies were determined by an enzyme-linked immunosorbent assay (ELISA) using

rHA purchased from Protein Sciences Corporation as a coating antigen. Polysterene 96 well flat bottom immuno plates (NUNC) were coated overnight at 4°C with 0.1 µg rHA per well. Wells were washed three times with PBS- 0.5% Tween 20. Blocking buffer (1% bovine serum albumin (BSA) in PBS-Tween) was added to every well and incubated for 1 hr at RT. Wells were again washed and serial 2-fold sample dilutions were added to the plates in 0.5% BSA PBS and incubated at RT for 1 hr. Next, wells were washed five times and incubated for 1 hr at RT with 100 µL/well horseradish peroxidase-conjugated goat anti-mouse secondary antibody specific for IgG (Southern Biotech) diluted in 1% BSA-PBS at a 1/4000 dilution. Subsequently, wells were washed five times and developed with 100 µL/well tetramethylbenzidine (TMB). Stop solution, H_2S0_4 (1N), was then added at 100 µL/well to stop the reaction. The optical density was read at 450nm (OD450) using a Biotek Synergy 2.

Hemagglutination Inhibition Assays

Hemagglutination Inhibition (HAI) activity specific to A/PR/8/34 and A/CA/07/09 was performed as previously described in using 1% Turkey Red Blood Cells (TRBCs) (52). Briefly, each serum sample was treated with receptor-destroying enzyme (RDE) overnight at 37°C followed by heat inactivation to remove nonspecific inhibitors. HAI titer was determined using the reciprocal of the highest dilution of sera that completely inhibited the agglutination of turkey RBCs following addition of 4 HAU (hemagglutination units) of virus, starting at a 1:10 dilution and serially diluting 2-fold down a 96 v-bottom plate.

Antibody isolation and transfer

Serum was purified using a HiTrap Protein A antibody purification column (GE life sciences) and AKTA fast protein liquid chromatography. Briefly, serum was loaded onto the column in basic conditions in Glycine/NaOH (pH 9.0) then eluted using Glycine/HCL buffer (pH 2.5).

Fractions were immediately neutralized with TRIS/HCL buffer. Purified antibody was then dialyzed in PBS and run on an SDS-PAGE gel to confirm purification. Antibody was further quantified by ELISA for isotype and transferred into C57BL/6 mice twice with 200 µL by r.o. injection.

B cell Adoptive Transfer

C57BL/6 mice were sublethally infected with either A/PR/8/34 or A/CA/07/09 or given PBS as a control. At day 28 post infection, spleen, inguinal, axillary and brachial lymph nodes were processed into single cell suspension using a 100 µm nylon cell strainer (BD Falcon). B cells were isolated with the mouse B cell Isolation Kit II (Miltenyi Biotec). Approximately, $3x10^6$ B cells/mouse in 100 µL of PBS were transferred into naïve C57BL/6 recipient mice by r.o. injection.

Statistical Analysis

Statistical analysis performed using one-way or two-way ANOVA with Bonferroni correction for multiple comparisons, or Student's t-tests as indicated for each experiment. Graphs were generated and statistical analyses were performed using GraphPad Prism 5 (GraphPad Software, San Diego, CA). P value of <0.05 was considered statistically significant.

Results

$CD4^+$ T cell depletion limited neutralizing antibody responses and partially restored secondary responses in C57BL/6 mice.

We used the C57BL/6 model to determine if a lack of HA-specific $CD4^+$ T cell memory but established $CD4^+$ T cell memory to other conserved proteins dulled subsequent responses by focusing on internal conserved influenza proteins as suggested previously (82). First, we depleted $CD4^+$ T cells after contraction at day 27 and 28 post primary infection, confirmed depletion and then waited 36 days for reconstitution (day 65 post infection) of the naïve $CD4^+$ T cell compartment prior to secondary infection with A/PR8 (**Figure 3.1**). $CD4^+$ T cell depletion was found to be accomplished even in tissues, including lung, axial and brachial lymph nodes and spleen (**Figure 3.1**). Interestingly, $CD4^+$ T cell depletion partially relieved the suppression of nAb responses to A/PR8 in C57BL/6 mice implying that memory $CD4^+$ T cells to other conserved proteins in the virus may inhibit responses to drifted HA (**Figure 3.2**). Paradoxically, depletion of $CD4^+$ T cells did not prevent focusing on an internal conserved protein, nucleoprotein (NP), instead enhancing the antibody titers to NP (**Figure 3.2 Panel C**). This intimates that memory $CD4^+$ T cell depletion to internal components does not relieve OAS by rerouting focus back to HA but may rather suggest that by removing memory $CD4^+$ T cells, there is a loss of memory cross-protection, which therefore increases antigen production and thus increased seroconversion.

Additionally, to test if $CD4^+$ T cells alone were sufficient to transfer OAS or skew Ab responses towards conserved proteins, we transferred bulk $CD4^+$ T cell populations from previously A/CA infected C57BL/6 mice to naïve mice and subsequently infected them with

A/PR8. Transfer of $CD4^+$ T cells did not dampen nAbs in response to drifted influenza nor did it enhance the kinetics to a conserved viral protein, NP, as seen previously (**Figure 3.3**). This suggests that $CD4^+$ T cell depletion does not relieve OAS by rerouting resources to focus on internal conserved proteins but rather increases antigen availability possibly through loss of protection, as we depleted tissue-resident $CD4^+$ T cell subsets, leading to higher viral loads and therefore greater seroconversion, an area that will be discussed further in the discussion.

We employed the CB6F1 mouse model to establish the requirement of memory $CD4^+$ T cells for enhancement of antibody responses following heterologous boost. We infected CB6F1 mice, and depleted $CD4^+$ T cells post contraction on day 27 and 28 post primary infection, confirmed depletion and waited for reconstitution of the naïve $CD4^+$ T cell compartment prior to vaccinating with rHA A/PR8 similarly to the OAS model (**Figure 3.1**). Strikingly, $CD4^+$ T cell depletion diminished the neutralizing antibody response to heterologous immunization as compared to the isotype control treated group, demonstrating the requirement for homologous memory $CD4^+$ T cells in mounting a nAb immune response to a heterologous boost (**Figure 3.4 Panel A and B**). Further, $CD4^+$ T cell depletion recreated the OAS phenotype in CB6F1 mice, eliciting a 'back-boost' to A/CA by ELISA titers upon immunization with rHA PR8 (**Figure 3.4 Panel C**).

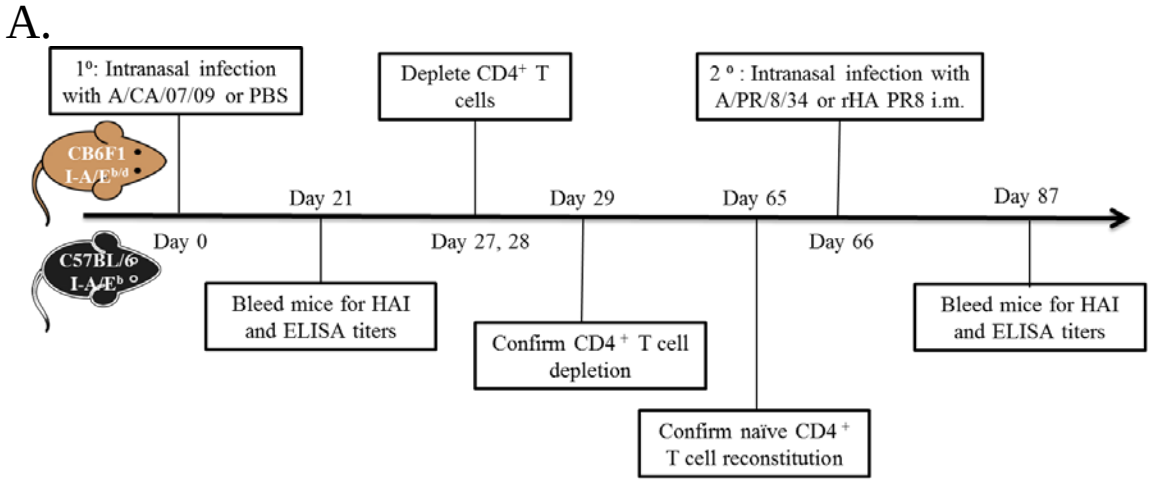

B.

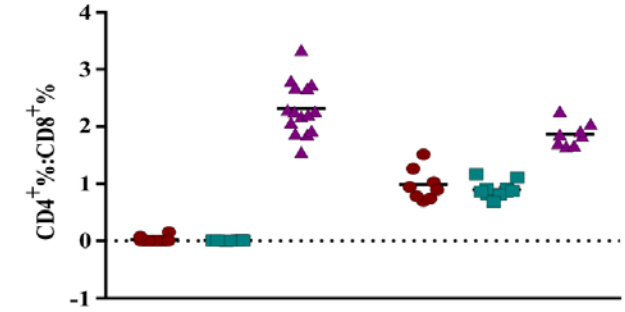

1°	PBS	A/CA i.n.	A/CA i.n.	PBS	A/CA i.n.	A/CA i.n.
Depletion	CD4	CD4	Isotype Ctrl	CD4	CD4	Isotype Ctrl
2°	PR8	PR8	PR8	PR8	PR8	PR8
Day	29	29	29	65	65	65

C.

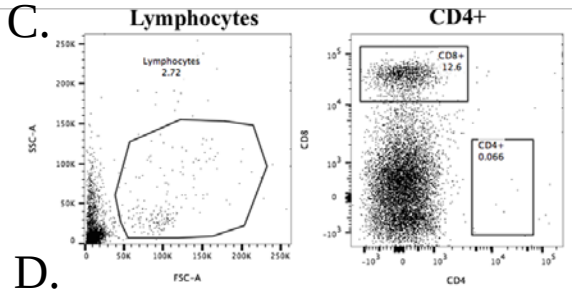

D.

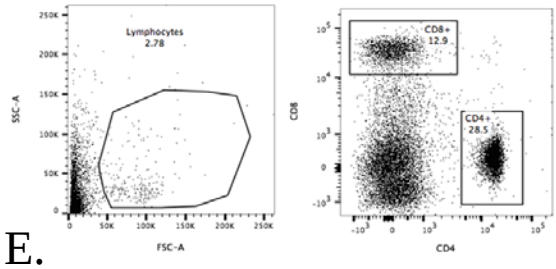

E.

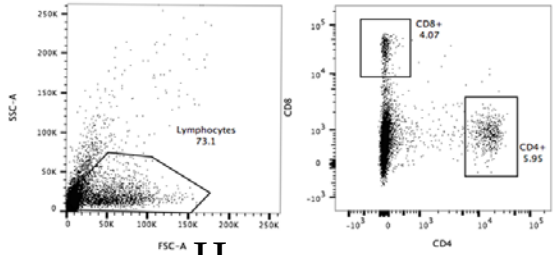

F.

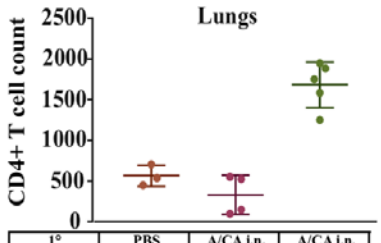

1°	PBS	A/CA i.n.	A/CA i.n.
Depletion	CD4	CD4	Isotype Ctrl
2°	PR8	PR8	PR8
Day	29	29	29

G.

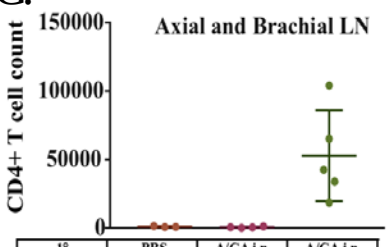

1°	PBS	A/CA i.n.	A/CA i.n.
Depletion	CD4	CD4	Isotype Ctrl
2°	PR8	PR8	PR8
Day	29	29	29

H.

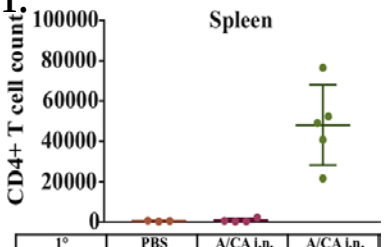

1°	PBS	A/CA i.n.	A/CA i.n.
Depletion	CD4	CD4	Isotype Ctrl
2°	PR8	PR8	PR8
Day	29	29	29

Figure 3.1 Depletion of memory $CD4^+$ T cells and reconstitution of naïve CD4+ T cells in blood and tissues of C57BL/6 and CB6F1 mice. Experimental outline in panel **(A):** C57BL/6 or CB6F1 mice were i.n. exposed to A/CA (500 pfu/mouse) or PBS and then depleted of $CD4^+$ T cells in between primary and secondary exposure using 500 µg Ab GK 1.5 given i.p., then allowed to reconstitute their naïve $CD4^+$ T cell population prior to secondary intranasal or intramuscular exposure to A/PR8 (5 pfu/mouse) or rHA PR8 (1 µg). $CD4^+$ T cells were quantified in blood in panel (**B**) post depletion with anti-$CD4^+$ Ab and isotype control and upon reconstitution using Flow Cytometry. Flow Cytometry plots to confirm $CD4^+$ T cell depletion with anti-$CD4^+$ Ab in panel (**C**) and isotype control in panel (**D**) and reconstitution in blood in panel (**E**)**.** Penetration of tissue $CD4^+$ T cell depletion + SD shown in lungs, axial and brachial lymph nodes and spleen in panel (**F**).

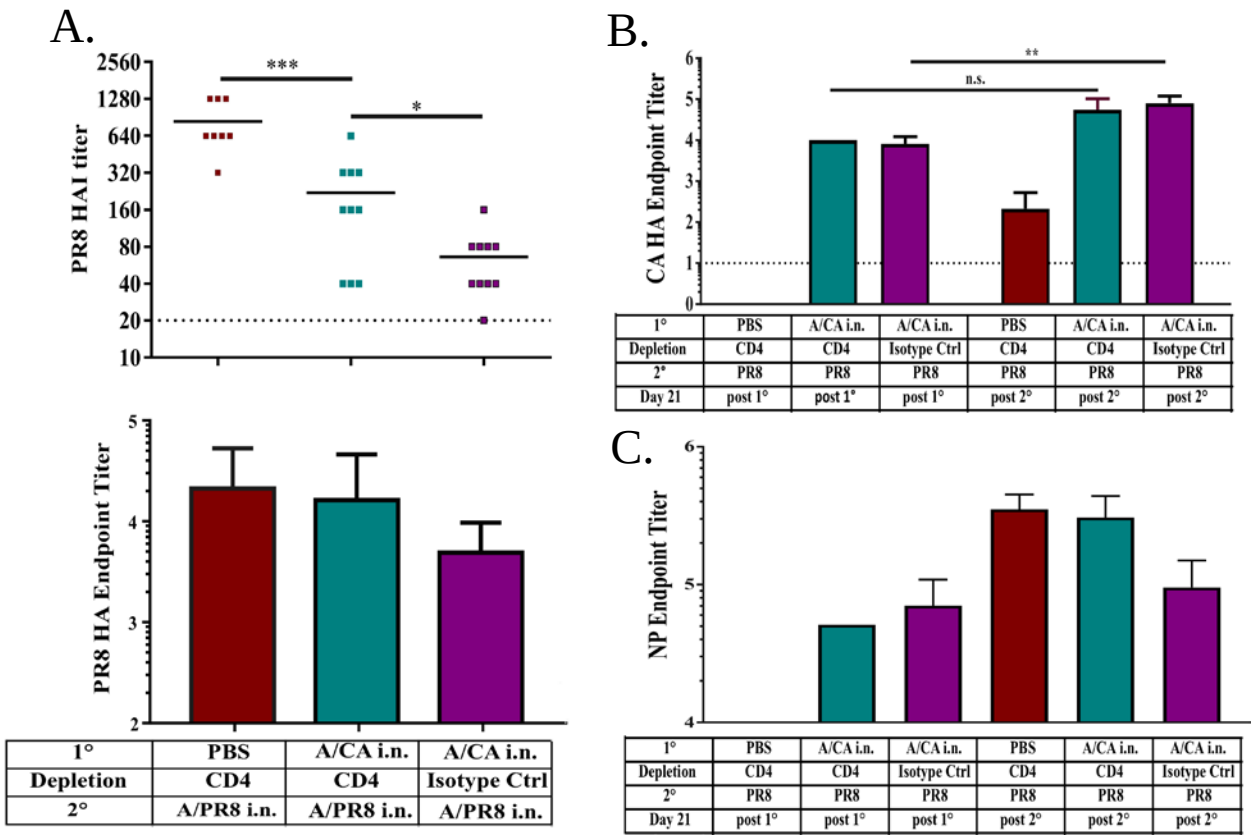

Figure 3.2 Memory CD4$^+$ T cell depletion reduces antigenic sin phenotype in C57BL/6 mice. PR8 HAI titer (Log_2) and PR8 HA endpoint titer ± SD (Log_{10}) at day 21 post-secondary influenza exposure in panel (**A**). CA HA endpoint titer ± SD (Log_{10}) post primary and secondary exposure in panel (**B**). Nucleoprotein endpoint titer ± SD (Log_{10}) day 21 post primary and secondary exposure in panel (**C**). (*p<0.05, **p<0.01***p<0.003, One-way ANOVA).

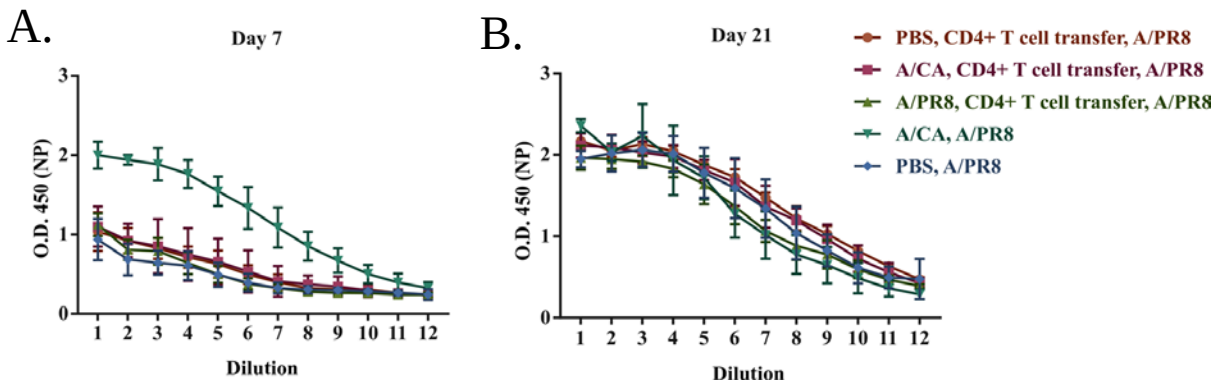

Figure 3.3 Transfer of $CD4^+$ T cells alone is insufficient to skew responses towards conserved internal viral proteins. C57BL/6 mice were sublethally infected with either A/PR/8/34 or A/CA/07/09 or PBS. At day 28 post infection, spleen, inguinal, axillary and brachial lymph nodes were processed and $6x10^7$ $CD4^+$ T cells/mouse were isolated and transferred in 200 µL to naïve mice by retro-orbital injection. Mice were then challenged with A/PR8 (5pfu/mouse) and bled at day 7 and 21. Nucleoprotein (NP) endpoint titer (Log_{10}) + SD post $CD4^+$ T cell transfer and day 7 post-secondary infection in panel (**A**) and day 21 in panel (**B**) with A/PR8. Two-fold dilutions were made starting at 1:300.

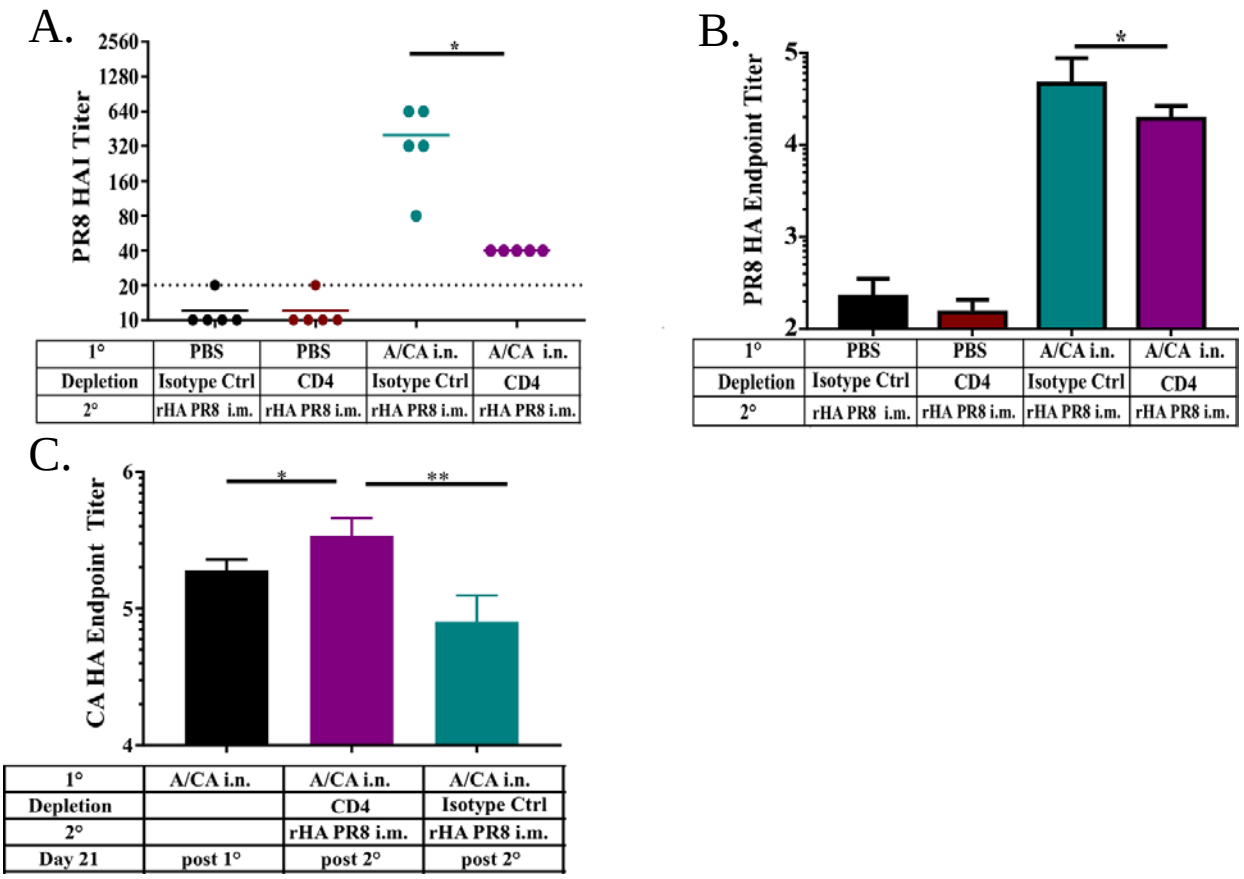

Figure 3.4 Increased neutralizing antibody response to vaccination in CB6F1 mice was dependent on memory CD4$^+$ T cells. CB6F1 mice (n=5 per group) were intranasally exposed to A/CA (500 pfu/mouse) or PBS and then depleted of CD4$^+$ T cells in between primary and secondary exposure using 500 µg Ab GK 1.5 given i.p., then allowed to reconstitute their naïve CD4$^+$ T cell population prior to secondary intramuscular exposure to rHA PR8 (1 µg/mouse)**.** Day twenty-one PR8 HAI titer (Log_2) in panel (**A**), **(B)** PR8 HA endpoint titer post rHA PR8 immunization and CA HA endpoint titer ± SD (Log_{10}) day 21 post prime and post rHA PR8 immunization in panel (**C**). (*p<0.05, ** p<0.01, One-way ANOVA).

Recombinant HA immunization with adjuvant can stimulate memory CD4$^+$ T cells for enhanced neutralizing antibody responses to subsequent immunization.

Adjuvants, including a fully synthetic lipid-A TLR4 agonist in a stable oil-in-water emulsion, SLA-SE, strongly increase memory CD4$^+$ T cell reactivity and induce T follicular helper cells (Tfh), the cells critical in aiding B cell responses (108). Therefore, we next determined if enhancement of neutralizing antibody responses to subsequent immunization was dependent upon infection for inducing CD4$^+$ T cells capable of aiding subsequent responses or if rHA protein in combination with adjuvant was capable of producing the immune memory necessary. Similar to previously published data, we found that primary exposure to rHA A/CA alone was unable to provide enhancement to secondary responses (**Figure 3.5**) (103). Conversely, adjuvanted rHA A/CA immunized mice did display enhanced neutralizing antibody responses to subsequent immunization (**Figure 3.5**). To assess further the role of CD4$^+$ T cells in this response, we again depleted CD4$^+$ T cells in between influenza exposures as outlined in **Figure 3.1**. The enhanced antibody response to secondary immunization was dependent on memory CD4$^+$ T cells (**Figure 3.5**). These results suggested primary exposure with infection or adjuvanted immunization affects subsequent responses based on CD4$^+$ T cell reactivity conservation.

Unlinked B and T cell responses using peptide immunization partially enhanced neutralizing antibody responses.

To determine if T cells alone enhanced neutralizing antibody responses to secondary heterologous immunization, we utilized a peptide immunization strategy wherein CB6F1 mice were immunized with peptides conserved between A/CA and A/PR8 HAs plus adjuvant (**Table 1**) (77). Interestingly, at day 21 post immunization CB6F1 mice previously immunized with

adjuvanted conserved peptides demonstrated enhanced neutralizing titer to A/PR8 but not of the same magnitude as previously infected or adjuvanted rHA immunization (**Figure 3.6**). This strategy resulted in T cell reactivity but not B cell reactivity, as we did not observe detectable Ab titers to A/CA upon immunization with adjuvanted peptides. This result suggested that $CD4^+$ T cells alone may not be able to alone enhance nAb titers to the same magnitude as adjuvanted recombinant whole protein or infection, however this may be caused by differences in the ability of adjuvanted peptide pools to elicit same quality of $CD4^+$ T cell responses.

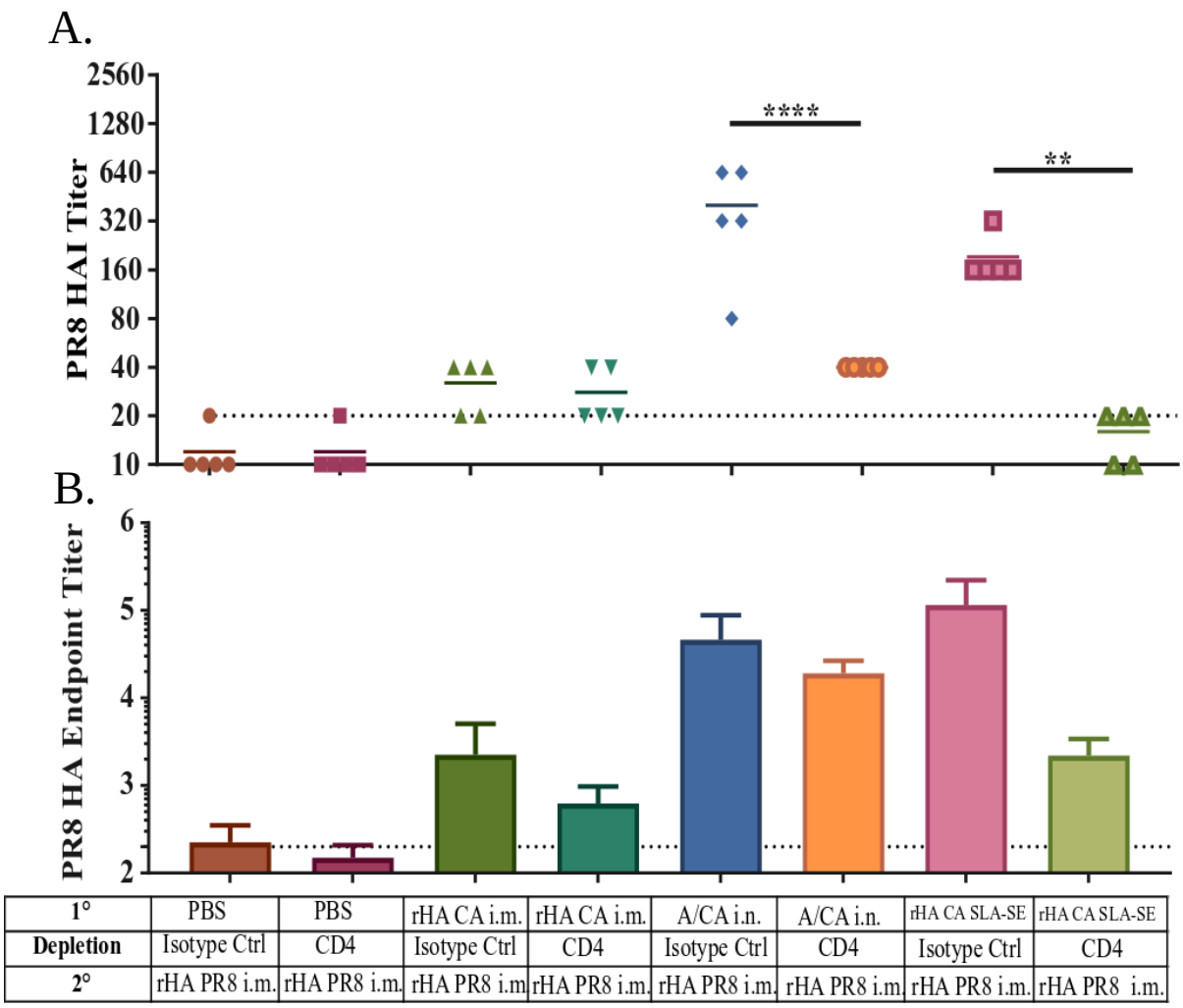

1°	PBS	PBS	rHA CA i.m.	rHA CA i.m.	A/CA i.n.	A/CA i.n.	rHA CA SLA-SE	rHA CA SLA-SE
Depletion	Isotype Ctrl	CD4	Isotype Ctrl	CD4	Isotype Ctrl	CD4	Isotype Ctrl	CD4
2°	rHA PR8 i.m.	rHA PR8 i.m.	rHA PR8 i.m	rHA PR8 i.m.	rHA PR8 i.m.	rHA PR8 i.m	rHA PR8 i.m.	rHA PR8 i.m.

Figure 3.5 Pre-exposure with adjuvanted A/CA HA protein enhanced neutralizing antibody responses to A/PR8 HA immunization and enhancement is $CD4^+$ T cell dependent. CB6F1 mice (n=5 per group) are intranasally exposed to A/CA (500 pfu/mouse) or PBS or rHA CA (1 µg/mouse) with and without adjuvant (SLA-SE) and then depleted of $CD4^+$ T cells in between primary and secondary exposure using 500 µg Ab GK 1.5 given i.p., then allowed to reconstitute their naïve $CD4^+$ T cell population prior to secondary intramuscular exposure to rHA PR8 (1 µg /mouse**).** A/PR8 HAI titer (Log_2) in panel (**A**) and endpoint titer ± SD (Log_{10}) in panel (**B**) at day 21 post-secondary rHA PR8 immunization in CB6F1 mice. (**p<0.01,****p<0.0001, One-way ANOVA).

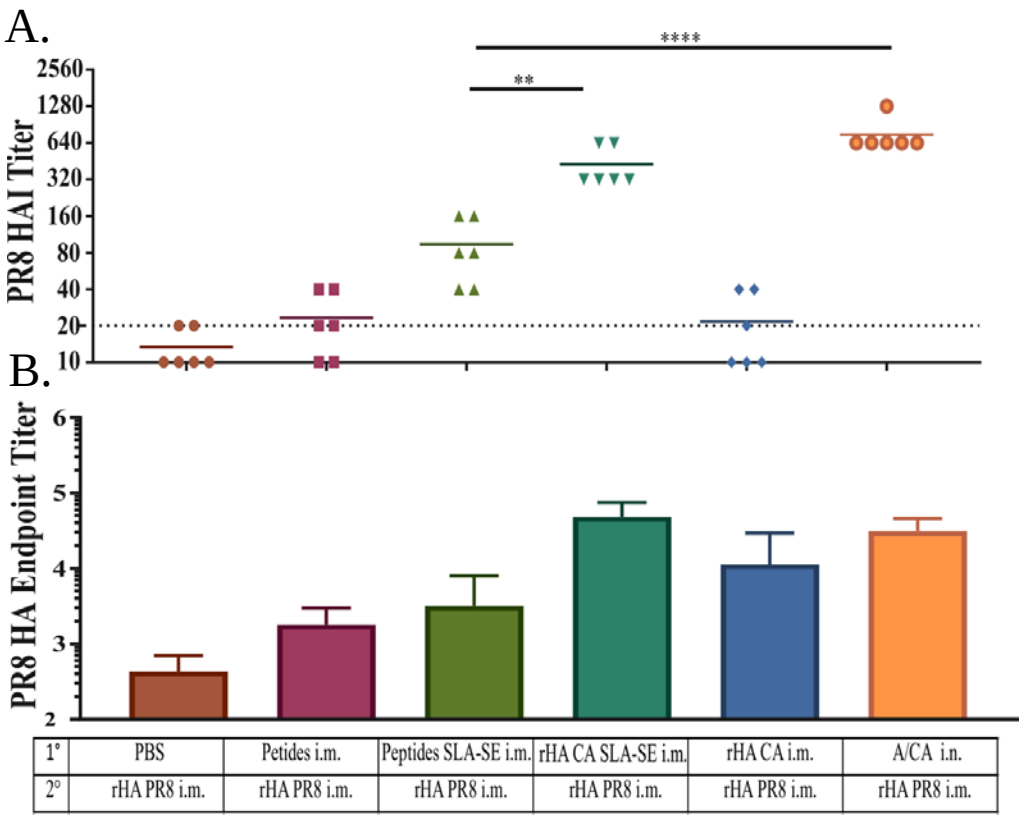

Figure 3.6 Memory CD4⁺ T cells are sufficient to enhance secondary responses to drifted rHA PR8 immunization but not to the same magnitude. Experimental model timeline: CB6F1 mice (n=6 per group) were intranasally exposed to A/CA (500 pfu/mouse) or PBS or rHA CA (1 µg/mouse) with and without adjuvant (SLA-SE) or A/CA peptides with and without adjuvant (SLA-SE) then secondarily i.m. exposed to rHA PR8 (1 µg/mouse)**.** A/PR8 HAI titer (Log_2) in panel (**A**) and endpoint titer ± SD (Log_{10}) in panel (**B**) at day 21 post-secondary rHA PR8 immunization in CB6F1 mice. (**p<0.01,****p<0.0001, One-way ANOVA).

Memory B cells are partially necessary for an increased magnitude of nAb response in CB6F1 mice and OAS in C57BL/6 mice.

To determine if B cells are necessary for enhanced nAb responses to secondary heterologous immunization in CB6F1 mice and OAS in C57BL/6 mice, we depleted B cells with anti-CD20 antibody, confirmed depletion and then rested animals to allow for reconstitution of the naïve B cell compartment before immunization with rHA immunization or A/PR8 intranasal infection (**Figure 3.7**). CB6F1 mice depleted of memory B cells demonstrated lower HAI and endpoint titers to A/PR8 compared to mock depleted mice (**Figure 3.10**). Taken together with the effects of memory $CD4^+$ T cell depletion, this suggested that both memory B cell and $CD4^+$ T cells are necessary for enhancement of subsequent immunization responses. To determine if B cells are necessary for the OAS phenotype, we similarly depleted B cells with anti-CD20 antibody, confirmed depletion and allowed for reconstitution of the naïve B cell compartment before subsequently infecting with A/PR8. While depletion of B cells did trend towards relieving the OAS phenotype both by A/PR8 HAI and by endpoint titer, it did not significantly raise titers, suggesting little contribution of relieving OAS (**Figure 3.8**). However, B cell depletion did abrogate the boost seen to the first exposure strain A/CA suggesting that memory B cells are indeed required for that component of antigenic sin. To determine if B cells are sufficient to confer the OAS phenotype alone, we transferred in B cells from previously A/CA exposed mice into naïve mice and then subsequently sublethally challenged with A/PR8. Recipient naïve mice receiving antigen experienced B cells demonstrated an increased reactivity to CA HA by ELISA, suggesting memory B cells alone are capable of the 'back-boost' (**Figure 3.9**).

A.

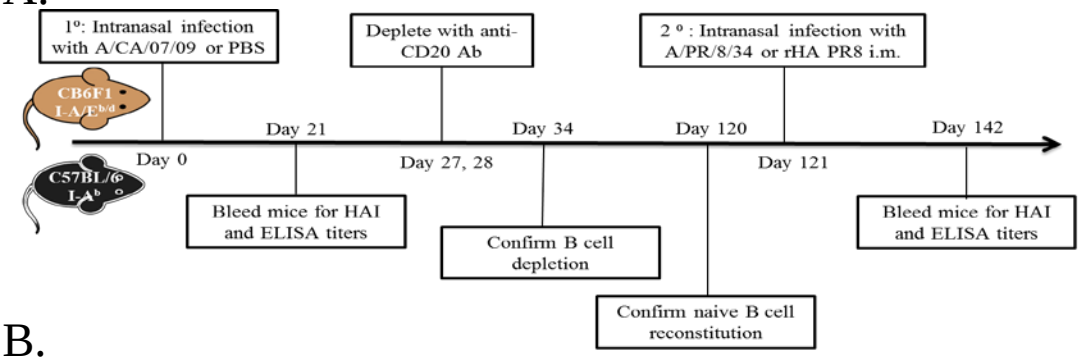

B.

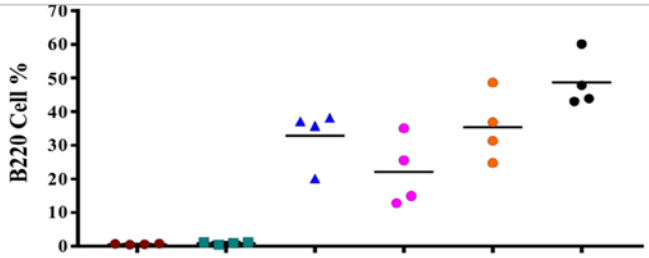

1°	PBS	A/CA i.n.	A/CA i.n.	PBS	A/CA i.n.	A/CA i.n.
Depletion	CD20	CD20	Isotype Ctrl	CD20	CD20	Isotype Ctrl
2°	PR8	PR8	PR8	PR8	PR8	PR8
Day	34	34	34	120	120	120

C.

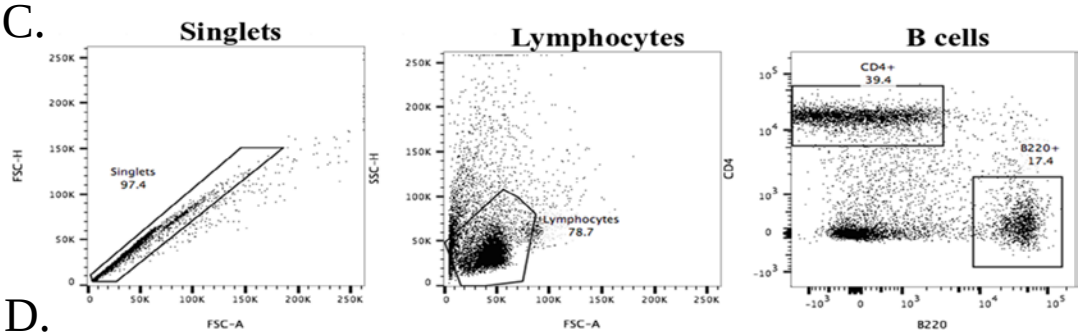

D.

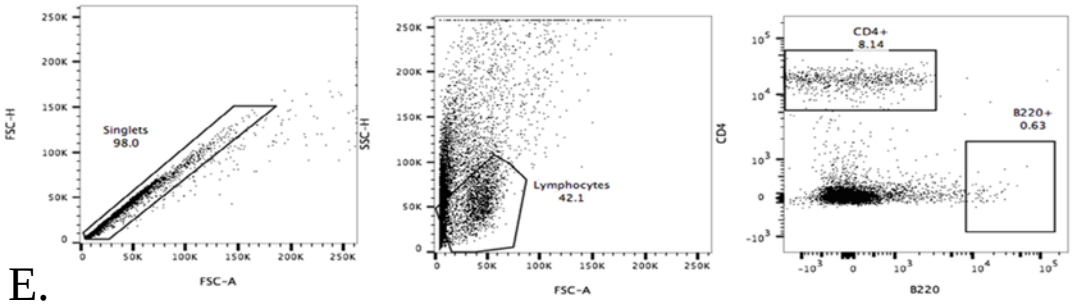

E.

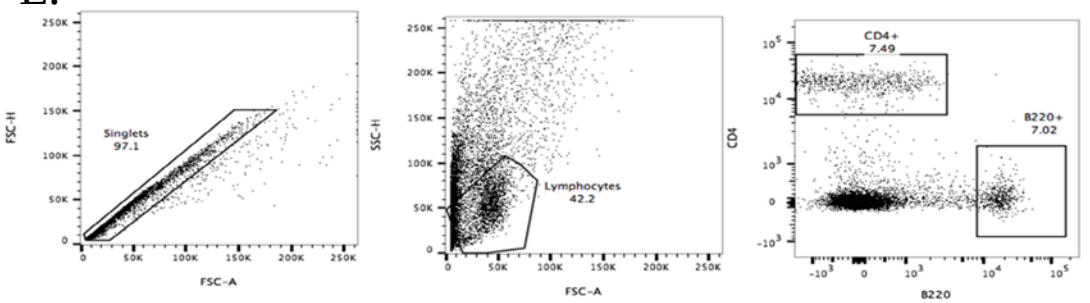

Figure 3.7 Experimental determination of memory B cell necessity in OAS C57BL/6 model and CB6F1 mouse model. Experimental model timeline: C57BL/6 or CB6F1 mice are intranasally exposed to A/CA (500 pfu/mouse) or PBS and then depleted of B cells in between primary and secondary exposure using 500 µg anti-CD20 antibody given i.p., then allowed to reconstitute their naïve B cell population prior to secondary intranasal or intramuscular exposure to A/PR8 HA (5 pfu/mouse or 1 µg/mouse) as shown in panel (**A**). B cells were quantified in blood post depletion and upon reconstitution using Flow Cytometry in panel (**B**). Flow Cytometry plots to confirm B cell depletion in panel (**D**), isotype control in panel (**C**) and reconstitution in blood in panel (**E**)**.**

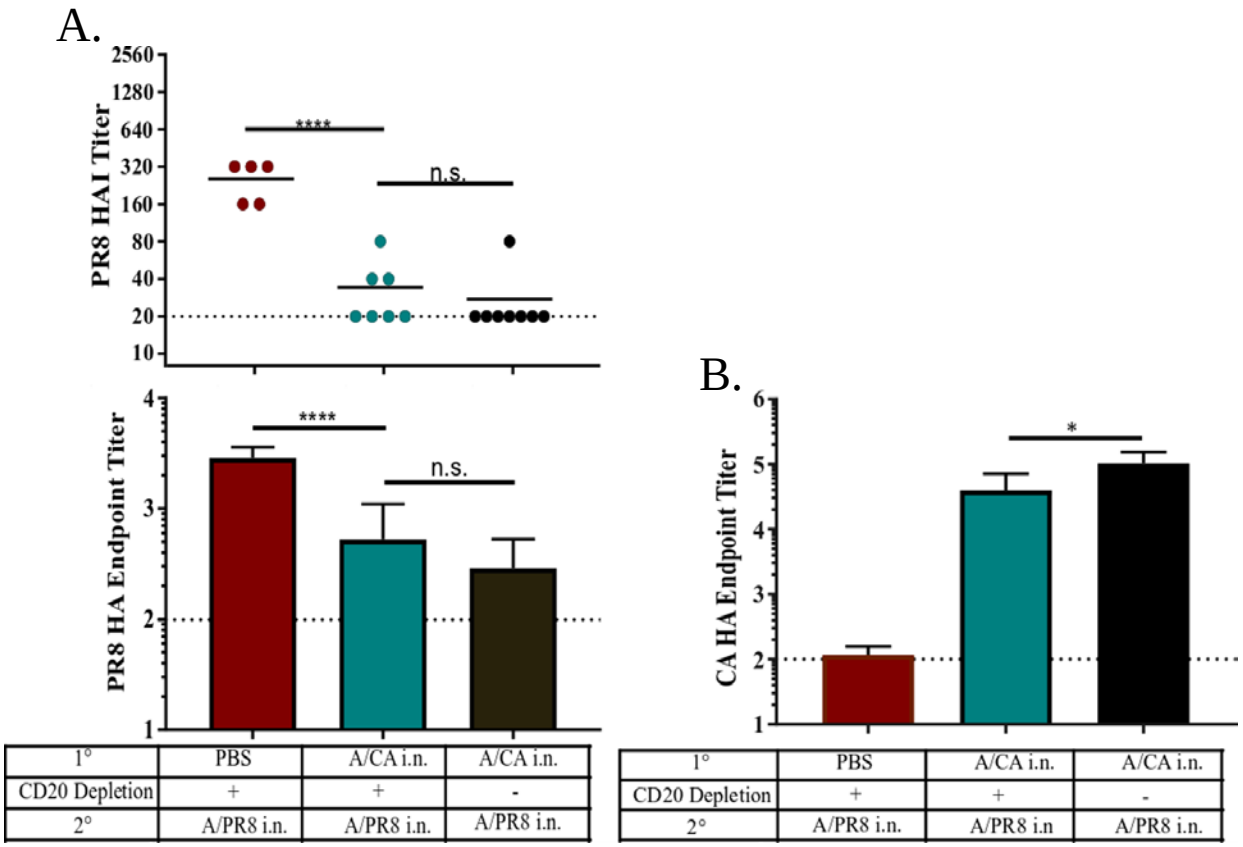

Figure 3.8 Memory B cell depletion does not significantly reduce antigenic sin. Day 21 A/PR8 HAI titer (Log_2) (upper) and endpoint titer (lower) ± SD (Log_{10}) post A/PR8 intranasal infection in C57BL/6 mice in panel (**A**). Day 21 rHA CA endpoint titer ± SD (Log_{10}) post A/PR8 infection in C57BL/6 mice in panel (**B**). (*p<0.05, ****p<0.0001, One-way ANOVA).

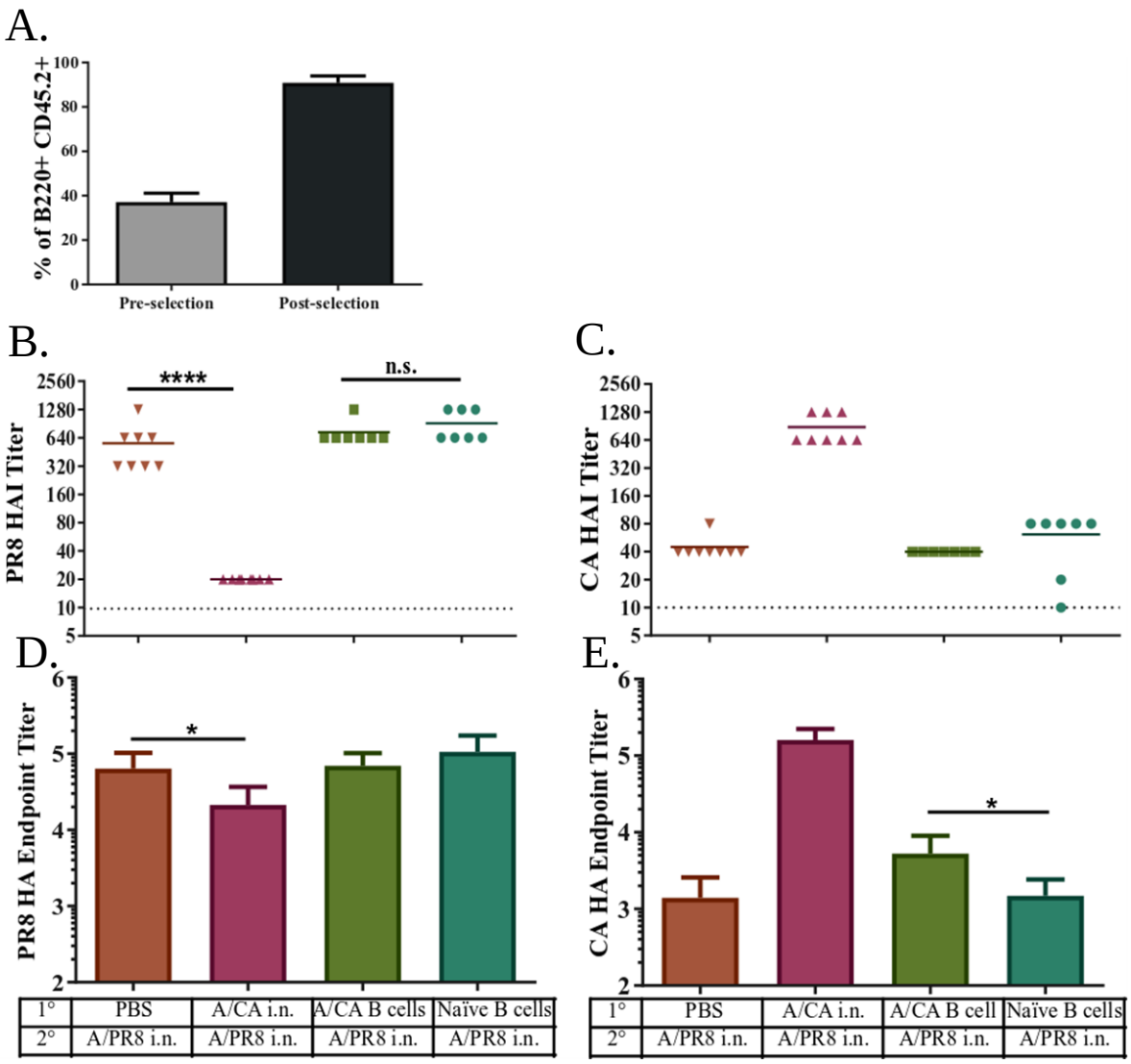

Figure 3.9 Memory B cells are insufficient to transfer antigenic sin phenotype. Mice received ~3 x10^6 B cells from CA infected mice or naïve mice using B cell enrichment as shown in panel (**A**). Serum Ab responses of individual mice (n=8 per group) to A/PR8 or A/CA by HAI (Log_2) (**panels B and C**, respectively) and endpoint (**panel D and E**, respectively) titers ± SD (Log_{10}) at day 21 post A/PR8 infection. (*p<0.05, ****p<0.0001, One-way ANOVA).

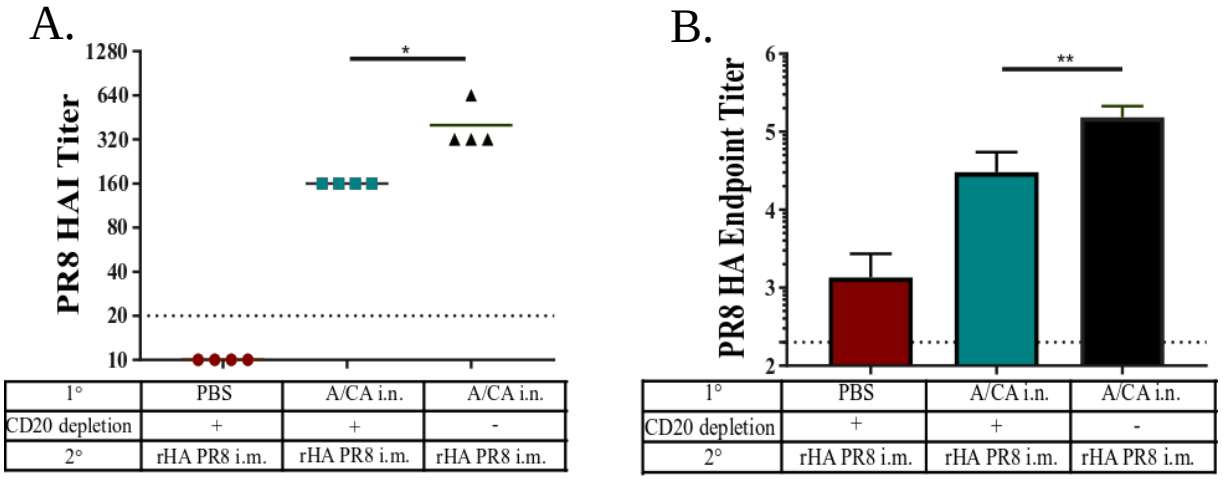

Figure 3.10 Increased neutralizing antibody response to vaccination in CB6F1 mice was dependent on memory B cells. Mice (n=4 per group) were depleted of B cells in between primary and secondary exposure using 500 µg anti-CD20 Ab given i.p., then allowed to reconstitute their naïve B cell population**.** Day 21 HAI titer (Log_2) in panel **(A)** and endpoint titer ± SD (Log_{10}) in panel **(B)** post A/PR8 HA immunization in CB6F1 mice. (*p<0.05, **p<0.01, One-way ANOVA).

A/CA HA antibodies did not transfer OAS phenotype in C57BL/6 mice.

In addition to memory B cells, it is possible that cross-reactive antibody could reduce responses to drifted exposure in our OAS model. To examine whether antibodies play a role in the establishment of OAS we purified convalescent serum from A/CA/7/09 infected mice using a protein A column and transferred this serum into naïve mice a day prior to infection with A/PR8 virus. Cross-reactive serum was primarily of IgG isotype 2c (**Figure 3.11 Panel E**). Transfer of serum did not confer OAS or trend towards reduced neutralizing antibody responses (**Figure 3.12**). This further suggests that preexisting antibody, in particular IgG, is not interfering with secondary responses. However, this does not fully rule out the contribution of antibodies due to possible differences in infection-induced antibody versus vaccination-induced. Mucosal IgA has been found to provide a low level of protection against variant virus (109). Further, in the influenza mouse model, IgA protection is based on Fc receptor mediated phagocytosis by macrophages (58).

$CD8^+$ T cells did not contribute to OAS phenotype in C57BL/6 mice.

Last, we also looked to determine if cross-reactive $CD8^+$ T cells could be stymieing secondary responses to drifted influenza in our OAS model. Similar to $CD4^+$ T cell depletion, we depleted $CD8^+$ T cells after contraction at day 27 and 28 post primary infection, confirmed depletion and then waited 36 days for reconstitution (day 65) of the naïve $CD8^+$ T cell compartment prior to secondary infection with A/PR8. Depletion was complete in blood and tissues; however, we did not observe any relief in OAS suggesting no role of cross-reactive $CD8^+$ T cells in dampening secondary responses (**Figure 3.13**).

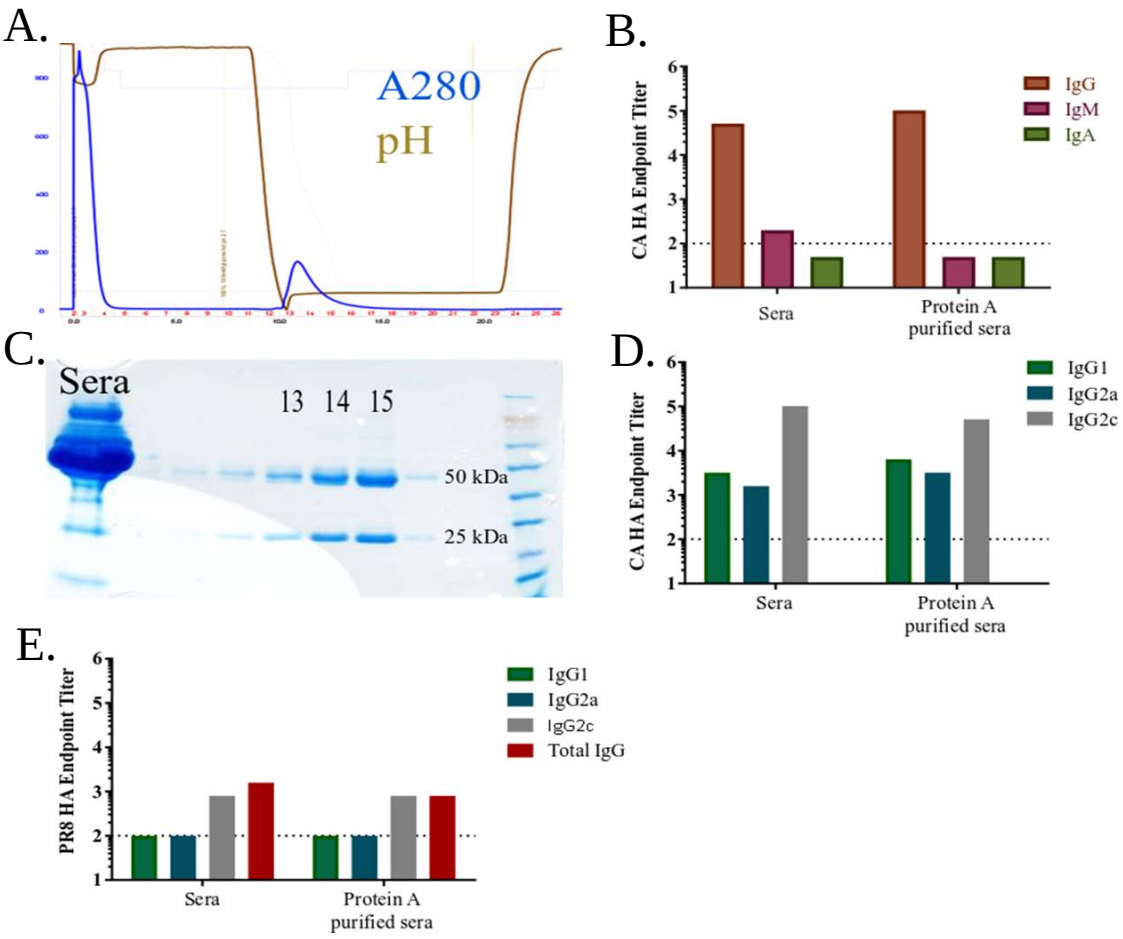

Figure 3.11 A/CA antibody purification, isotype profiling and cross-reactivity. Pooled serum was collected from previously A/CA infected mice (n=10). Graphical analysis of FPLC run for antibody purification with protein A column shown in panel (**A**). Brown line denotes pH over fractions and blue line denotes absorbance 280 (A280). CA HA endpoint titer (Log_{10}) of bulk sera before and after purification of antibody isotypes shown in panel (**B**). SDS-PAGE gel purification of fraction 13-15 confirming antibody size in panel (**C**). CA rHA endpoint titer (Log_{10}) of bulk sera before and after purification of antibody isotypes in panel (**D**). PR8 rHA ELISA cross-reactivity of sera from A/CA infected mice before and after protein A purification including isotypes in panel (**E**).

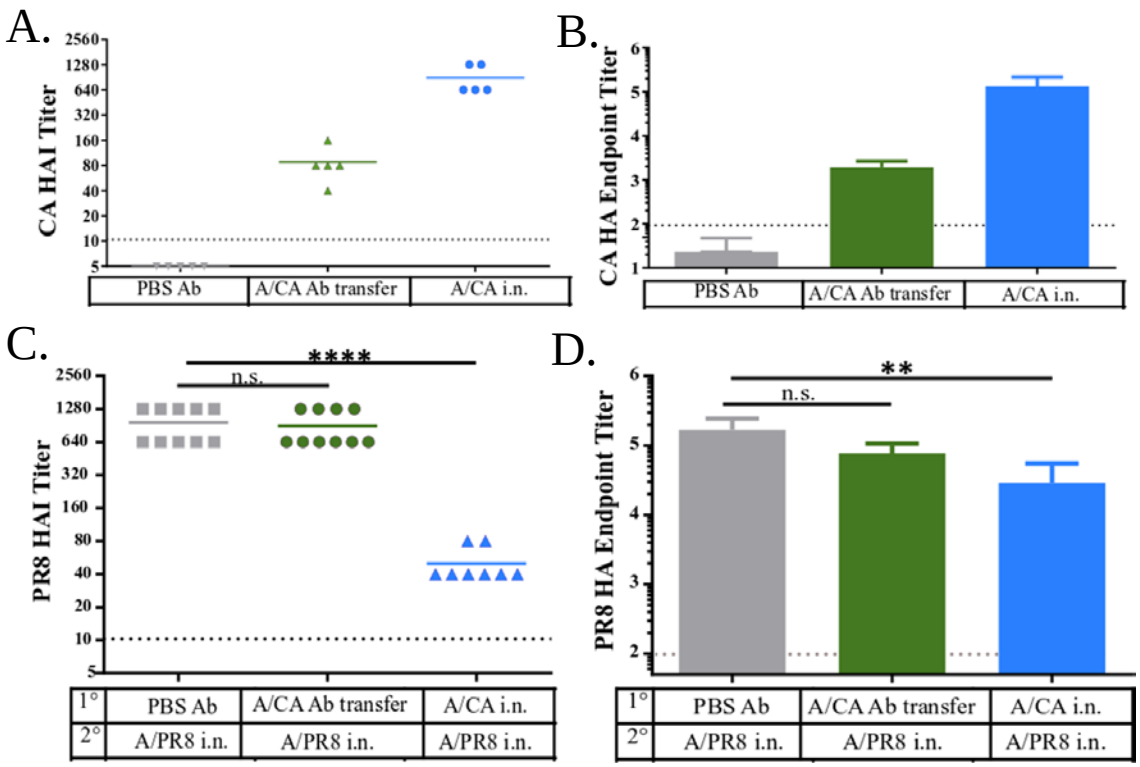

Figure 3.12 Transfer of A/CA serum does not transfer OAS phenotype in C57BL/6 mice. Serum Ab responses of individual mice to A/CA or A/PR8 by HAI (Log_2) (panel **A** and **C**, respectively) and endpoint titers ± SD (Log_{10}) (panel **B** and **D**, respectively) at day 21 post-PR8 infection. Groups of mice received either naïve antibody or CA antibody r.o. two days prior to A/PR8 infection. (**p<0.01, ****p<0.0001, One-way ANOVA).

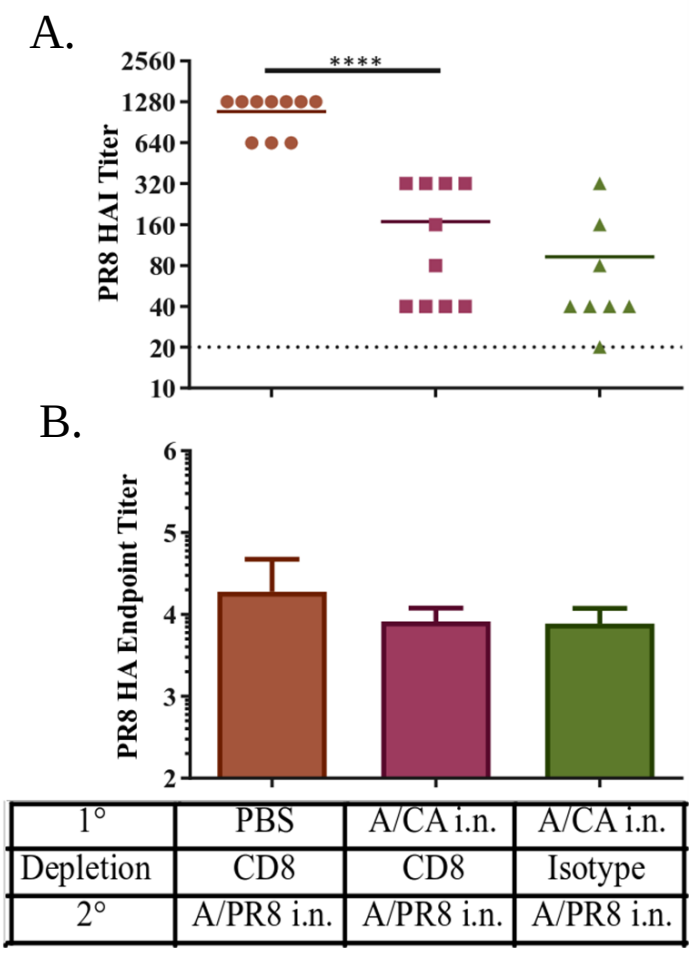

Figure 3.13 Memory CD8$^+$ T cell depletion does not reduce antigenic sin phenotype in C57BL/6 mice. PR8 HAI titer (Log_2) in panel (**A)** and PR8 HA endpoint titer ± SD (Log_{10}) in panel (**B**) at day 21 post-secondary influenza exposure. (****p<0.0001, One-way ANOVA).

Discussion

To better understand the immunological contributors that dictate responses to influenza, we have established mouse models in Chapter 2, wherein mice are infected or immunized and are then subsequently immunized or infected with drifted influenza HA protein, mimicking human influenza histories. Interestingly, we found that prior infection or adjuvanted immunization but not rHA immunization alone resulted in increased nAb responses upon heterologous immunization in CB6F1 mice but not in C57BL/6 mice that displayed an OAS phenotype, differing from previous OAS mouse models that recapitulated the CB6F1 mice when exposed to standardized antigen amounts (103). Distinct MHC Class II haplotypes allowed us to further epitope-map $CD4^+$ T cell reactivity to HA (Chapter 2). We found that CB6F1 mice displayed $CD4^+$ T cell reactivity to conserved HA epitopes across both priming and boosting heterologous virus HA's whereas C57BL/6 mice displayed no conserved reactivity to epitopes of HA. This finding suggests that if cognate memory T cells are not available, memory B cell reactivity to drifted influenza will respond with only an OAS phenotype, meaning no updating of BCR with SHM, a topic that will be further discussed and characterized in Chapter 4. Indeed, in C57BL/6 mice that previously displayed the OAS phenotype depletion of memory B cells or $CD4^+$ T cells increased nAbs to secondary exposure with drifted virus, but only partially relieved OAS.

Isolating the impact of each cellular compartment by cellular transfer experiments, the results suggest that memory B cells alone are responsible for the 'back-boost' effect to initial exposure but memory B cells alone do not quench secondary responses. Given that $CD4^+$ T cell depletion also relieved OAS, we hypothesized in alignment with previous literature that due to the lack of HA reactivity but conserved reactivity to internal proteins in the primary exposure

this may lead to an antibody focusing on internal proteins, however we found that not to be true. Rather, it seems likely that due to excellent tissue penetration of $CD4^+$ T cell depletion, we are seeing a reduction in protective cytotoxic $CD4^+$ T cells, increasing viral replication and therefore antigen production and dissemination (74, 83-87, 110). Further, this partial relief of OAS is likely explained by substantial cross-reactive antibodies to both HAs, which we cannot fully recapitulate by transfer experiments, providing protection from drifted influenza. This idea is in concurrence with recent literature, suggesting that non-neutralizing OAS antibodies contribute productively to protection and reduced antigen load, thus limiting *de novo* responses (59). Interestingly, $CD8^+$ depletion did little to relieve OAS, suggesting little importance of $CD8^+$ T cells in the protective response to drifted influenza, a topic of intense interest. Recently, it has been noted that retention of memory $CD8^+$ T cells in the lung in response to viruses is reduced (111). All together, these results align with the hypothesis that memory B cells pursue limited antigen upon secondary exposure, outcompeting naïve B cells for acquiring antigen, thus limiting *de novo* responses and through memory B cell depletion this effect is partially abrogated.

The $CD4^+$ T cell subset that has the potential to influence antibody responses by interacting with B cells has been identified as Tfh cells. Programming and activation of Tfh cells is dependent on antigen presentation by B cells (27, 76, 112, 113). Further, memory B cells rapidly reactivate cognate memory Tfh cells inducing accelerated antibody responses by the presenting memory B cell and directing reentry into GCs upon secondary immunization, a topic that will be covered more in Chapter 4 (70). However, it was unknown if memory B cells are necessary for the reactivation of memory Tfh cells upon heterologous immunization with HA or if naïve B cells could also be directed to provide an enhanced nAb response. We found using our CB6F1 mouse model, that memory B cells and $CD4^+$ T cells are necessary for the magnitude of

neutralizing responses observed and $CD4^+$ T cells are partially but incompletely sufficient. Further, we found that depletion of CD4 T cells recapitulates OAS in the CB6F1 mouse model, suggesting that concomitant cognate help between these two cell types is crucial for B cell adaptation. Additionally, in the context of protein immunization priming, adjuvants have been shown to elicit Tfh induction and robust memory $CD4^+$ T cells compared to protein immunization alone (98, 108, 109). Using our CB6F1 mouse model we found that adjuvant inclusion during protein immunization induced memory $CD4^+$ T cells capable of subsequently aiding heterologous neutralizing antibody responses, as we have found with infection-induced priming, demonstrating the ability to establish memory $CD4^+$ T cell help for subsequent responses.

These findings underscore the importance and complexity of immunological memory's impact on subsequent responses when B and T cell reactivity is changing, as is the case with drifted influenza. Therefore, it is crucial to understand the mechanism by which preexisting immune responses shape future responses in order to optimize and leverage vaccination design strategies. Further, this memory B and T cell interaction has potential implications in altering responses to viral infections that frequently have differing B cell and T cell reactivity and where antibody responses are critical for viral control, such as Dengue and HIV (114-116). Additionally, this knowledge could be leveraged to update preexisting immunity to be more potent against differing strains or alternatively, employed to prevent adaptation of memory B cells, retaining broader responses, a goal of many universal vaccine candidates.

Chapter 4: Characterizing and Reengaging Preexisting Immunity to Influenza Immunization

Introduction

Antibodies develop higher affinity for antigen through a multistep process known as affinity maturation, wherein B cells compete using their unique B cell receptor for antigen binding (117). This process of affinity maturation typically takes place in germinal centers in lymphoid tissues, primarily the spleen and draining lymph nodes of where the antigen is deposited or infection occurs, as shown in **Figure 4.1** (118). Germinal centers form upon antigenic stimulation and trigger B and T cells to migrate towards the T follicle border region (75, 119). At this location B cells then present antigen derived peptides via their major histocompatibility complex II (MHC II) to helper T cells (Tfh) and if recognized by the T cell receptor (TCR), are authorized to respond to antigen (120). This authorization can initiate several different outcomes based on initial B cell receptor (BCR) signaling and the nature of the engagement with T cells, as well as surrounding cytokine milieu. B cells can either directly differentiate into antibody secreting cells, known as plasmablasts, become nonproliferative and go into the memory B cell pool, or enter germinal centers to undergo somatic hypermutation (SHM) and editing of their BCR (69, 71, 121).

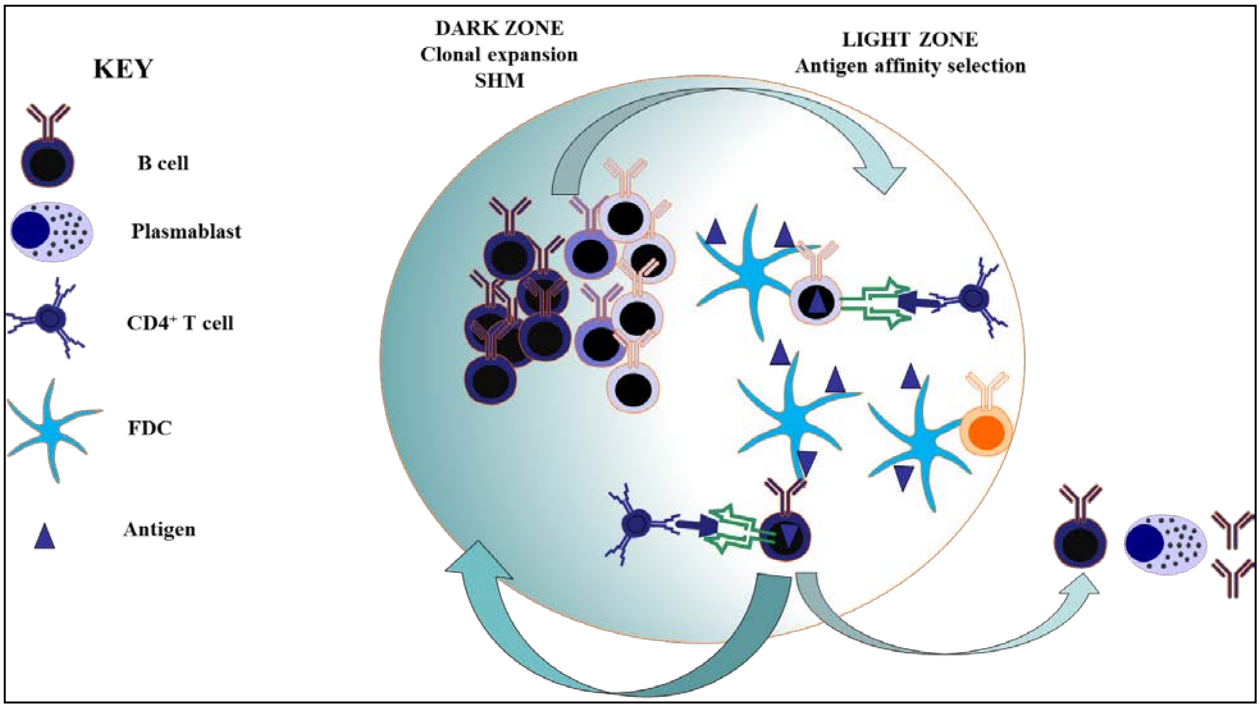

Figure 4.1. Overview of germinal center dynamics. Cycles of antigen affinity selection in the light zone followed by clonal expansion and somatic hypermutation (SHM) in the dark zone drives affinity maturation. Depending on B cell receptor signals and $CD4^+$ T cell engagement, B cells are directed to their respective fates.

Germinal centers typically materialize several days after exposure to antigen, where rapid clonal expansion of B cells creates a B cell follicle. These germinal center follicles are made up of two areas; the dark zone (DZ) and the light zone (LZ) (75). The DZ is where B cells proliferate and hypermutate, using the enzyme activation–induced cytidine deaminase (AID) and undergo class switch recombination (CSR) to switch Ig isotypes. The LZ is where antigen-affinity directed selection takes place. Upon entry into the DZ, B cells hypermutate and expand and then enter the LZ where they bind and compete for antigen to retrieve that is presented on immune complexes on follicular dendritic cells (FDCs)(122). B cells that successfully retrieve antigen then go on to present antigen to Tfh's and are either instructed to go through further iterative cycles affinity maturation or exit the germinal center to become memory or a plasmablast (27). This iterative process results in B cells and antibodies that are highly-affinity matured for the given antigen due to levels of antigen decreasing overtime and therefore

increasing competition. Currently, prompts to B cells that dictate their fate are largely unknown. However, it is known that high-affinity interaction in the LZ leads to plasmablast differentiation and survival whereas failure to bind antigen leads to cell death (121). Also, outcomes are not mutually exclusive; upon clonal expansion in the DZ, the same B cell specificity can have multiple different fates of differentiation by receiving different cues in the LZ (121).

Two theories exist on how affinity-based selection occurs in GCs that are not mutually exclusive. The first model suggests that strength of cell signaling through the BCR based on affinity for antigen directs selection but this has been recently disputed as BCR signaling may be inactive when in the LZ (e.g. the Ig with the greatest affinity will be most likely to retrieve antigen off of FDCs prompting their ability to reenter the DZ) (116, 123). The second model suggests that it isn't solely based on BCR stimulation but rather ability for the BCR-antigen interaction to trigger endocytosis thus allowing increased display of peptides on its own MHC Class II molecules promoting increased help from limited Tfh cells (120, 123). Experimental evidence for both BCR affinity and T cell help affecting GC cycling is present and therefore it is likely that both affect positive-selection of B cells.

Uniquely, for influenza it has been found that memory B cells re-enter germinal centers to become more specific to the drifted strain than the initial eliciting strain, an assertion based on how many rounds of mutations the B cell has undergone from germline sequence (27, 61). In that way drifting influenza and the B cell repertoire are constantly evolving to keep abreast of one another, analogous to the Red Queen hypothesis in evolutionary biology wherein adaptation and evolution is necessary to not only to gain reproductive advantage but to survive in the face of ever-evolving oppositional organisms (64). Indeed, recent experimental evidence has suggested that memory B cells, both Ig switched and unswitched (IgM), can re-enter germinal centers and

undergo further SHM to rediversify their BCRs (69-71, 124). This reentry into the germinal center was dependent on quality cognate memory T cell help (70). Nevertheless, in the face of drifting influenza occasionally the B cell repertoire doesn't update, instead having greater affinity for previous strains and displaying the OAS phenotype (27, 34, 62, 64). Collectively, these studies and evidence in Chapter 3, suggest that memory B cells that are reengaged by drifted influenza HA can reenter germinal centers to further undergo affinity maturation but without cognate memory T cells may not be signaled to revise and update their BCR.

Therefore in Chapter 4, we sought to characterize the germinal center response in our CB6F1 and OAS mouse models. We hypothesized that due to the deficiency of $CD4^+$ T cell reactivity that was conserved between drifted influenza HA's in our OAS model that secondary responses would lack germinal centers in contrast to our CB6F1 model. Further, we proposed that the OAS phenotype could subsequently be reversed by engineering in a conserved $CD4^+$ T cell epitope between the drifting HA's.

Material and Methods

Mice

Female C57BL/6 and CB6F1, 6-8 weeks of age were purchased from Jackson laboratory. All animals were housed in the IDRI Vivarium (Seattle, WA) under specific pathogen-free conditions. All animal experiments and protocols were approved by IDRI's Institutional Animal Care and Use Committee (IACUC).

Immunization and influenza virus infection of mice

Mice were immunized by intramuscular (i.m.) injection with 1 µg recombinant HA (rHA) from A/PR/8/34 or A/CA/07/09 or X31 (Protein Sciences Corporation), formulated with saline.

Mice were infected intranasally with 0.5 LD_{50} or 1000 LD_{50} dose of A/CA/07/09 and A/PR/8/34 in 25uL of phosphate-buffered saline (PBS). Mice were monitored for weight loss and other signs of virus induced morbidity daily and sacrificed if weight loss exceeded 20% of initial body weight.

CA/PR8Δ virus was made by replacing the RBS site of the HA PR8 vaccine plasmid with corresponding RBS CA site via Q5 mutagenesis. CA/PR8Δ virus was rescued using the vaccine plasmid system previously described (125-127).

Enzyme Linked Immunosorbent Assays (ELISA) Assays

Mouse sera were collected from individual mice and PR8 HA and CA HA reactive antibodies were determined by an enzyme-linked immunosorbent assay (ELISA) using rHA purchased from Protein Sciences Corporation as a coating antigen. Polysterene 96 well flat bottom immuno plates (NUNC) were coated overnight at 4°C with 0.1 µg rHA per well. Wells were washed three times with PBS- 0.5% Tween 20. Blocking buffer (1% bovine serum albumin (BSA) in PBS-Tween) was added to every well and incubated for 1 hr at RT. Wells were again washed and

serial 2-fold sample dilutions were added to the plates in 0.5% BSA PBS and incubated at RT for 1 hr. Wells then washed five times and incubated for 1 hr at RT with 100 µL/well horseradish peroxidase-conjugated goat anti-mouse secondary antibody specific for IgG (Southern Biotech) diluted in 1% BSA-PBS at a 1/4000 dilution. Subsequently, wells were washed five times and developed with 100 µL/well tetramethylbenzidine (TMB). Stop solution, H_2S0_4 (1N), was then added at 100 µL/well to stop the reaction. The optical density was read at 450nm (OD 450) using a Biotek Synergy 2.

Hemagglutination Inhibition Assays

Hemagglutinination Inhibition (HI) activity specific to A/PR/8/34, A/CA/07/09 and A/X31 was performed as previously described in using 1% Turkey Red Blood Cells (TRBCs) (104). Briefly, each serum sample was treated with receptor-destroying enzyme (RDE) overnight at 37°C followed by heat inactivation to remove nonspecific inhibitors. HI titer was determined by the reciprocal of the highest dilution of sera that completely inhibited the agglutination of turkey RBCs following addition of 4 HAU (hemagglutination units) of virus, starting at a 1:10 dilution and serially diluting 2-fold down a 96 v-bottom plate.

B cell and T cell staining

B cells were stained with (1:200) of fluorochrome conjugated anti-mouse CD138 (clone 281-2), GL7 (clone GL7), CD95 (clone Jo2), IgM (clone II/41), CD19 (clone 1D3 or 6D5), IgD (clone 11-26c.2a), CD38 (clone 90), AID (clone EK2-5G9) and 1:100 CD16/32 (clone 93) for 15 minutes in the dark at 4°C. Non B cell lineage cells were excluded by staining (1:200) and gating for Ly6G (clone 1A8), CD11b (clone M1/70), CD11c (clone N418), F4/80 (clone BM8), Ter119 (clone TER-119) and Thy1.2 (clone 53-2.1) hi populations, fixed and assessed by using a

BD Fortessa flow cytometer, analyzed using FACSDiva (BD Bioscience) and FlowJo software (TreeStar).

A/PR8-specific B cells were first purified out of lymph nodes using a B cell isolation kit II (Miltenyi), then staining with PR8-tetramer-PE (WLTEKEGSYP-biotin), CD138 (clone281-2), GL7 (clone GL7), CD95 (clone Jo2), CD19 (clone 1D3 or 6D5), and CD38. PE-avidin tetramer was sourced from prozyme (124, 128, 129).

T cells were stained with fluorochrome conjugated antibodies including anti-mouse CD4 (clone RM4-5), CD8 (clone 53-6. 7), CD44 (clone IM7), CD279 (PD-1, clone 29F.1A12), CD154 (CD40L, clone MR1) and B220 (RA3-6B2) (BioLegend and eBioscience) in the presence of anti-CD16/32 (clone 93) for 15 minutes in the dark at RT. Cells were fixed and permeabilized with Cytofix/Cytoperm (BD Biosciences) for 30 minutes at RT in the dark. Cells were washed with Perm/Wash (BD Biosciences) and stained for 15 minutes with fluorochrome labeled antibodies to detect intracellular cytokine IFN-γ (clone XMG-1.2) and tissue homing chemokine receptor CXCR5 (clone SPRCL5) (BioLegend and eBioscience).

Statistical Analysis

Statistical analysis was determined by one-way ANOVA with Bonferroni correction for multiple comparisons. Graphs and statistical analyses were performed using GraphPad Prism 5 (GraphPad Software, San Diego, CA). P value of <0.05 was considered statistically significant.

Results

Increased germinal center A/PR8-specific B and T follicular helper cells in previously exposed CB6F1 mice.

Next, we investigated the impact of previous influenza exposure on the draining lymph node following secondary exposure. We infected CB6F1 mice with A/CA, waited 28 days and subsequently immunized groups with rHA A/PR8 or rHA X-31, as a control, or PBS by i.m. immunization. At day 2 and 4 post rHA A/PR8 immunization, we examined the cellular composition of draining inguinal lymph nodes by flow cytometry. At day 4 post immunization with intra-subtype rHA A/PR8 but not shifted rHA X-31, we saw an increase in germinal center (GC) B cells ($B220^{+}GL7^{+}CD95^{+}CD38^{lo}$) and T follicular helper (Tfh) cells ($CD4^{+}CD154^{hi}CXCR5+PD\text{-}1^{+}$) in previously A/CA exposed mice but not unexposed mice (**Figure 4.2 B and 4.3 B).** Further, as shown in representative flow plots (**Figure 4.2 A**) the GC cells in the previously exposed group upregulated the SMH initiation enzyme, activation-induced cytidine deaminase (AID). To stain for A/PR8 specific B cells we attached a PE-avidin tetramer to a biotinylated immunodominant linear B cell epitope on A/PR8 HA that mapped to the receptor binding site (RBS) (128, 129). Using this staining tool, we were able to observe GC cells also became antigen-specific to A/PR8 (**Figure 4.4**). These results suggest in addition to our depletion studies in Chapter 3, that previous exposure deposits memory $CD4^{+}$ T cells and B cells that result in enhanced secondary responses capable of adapting to drifted HA.

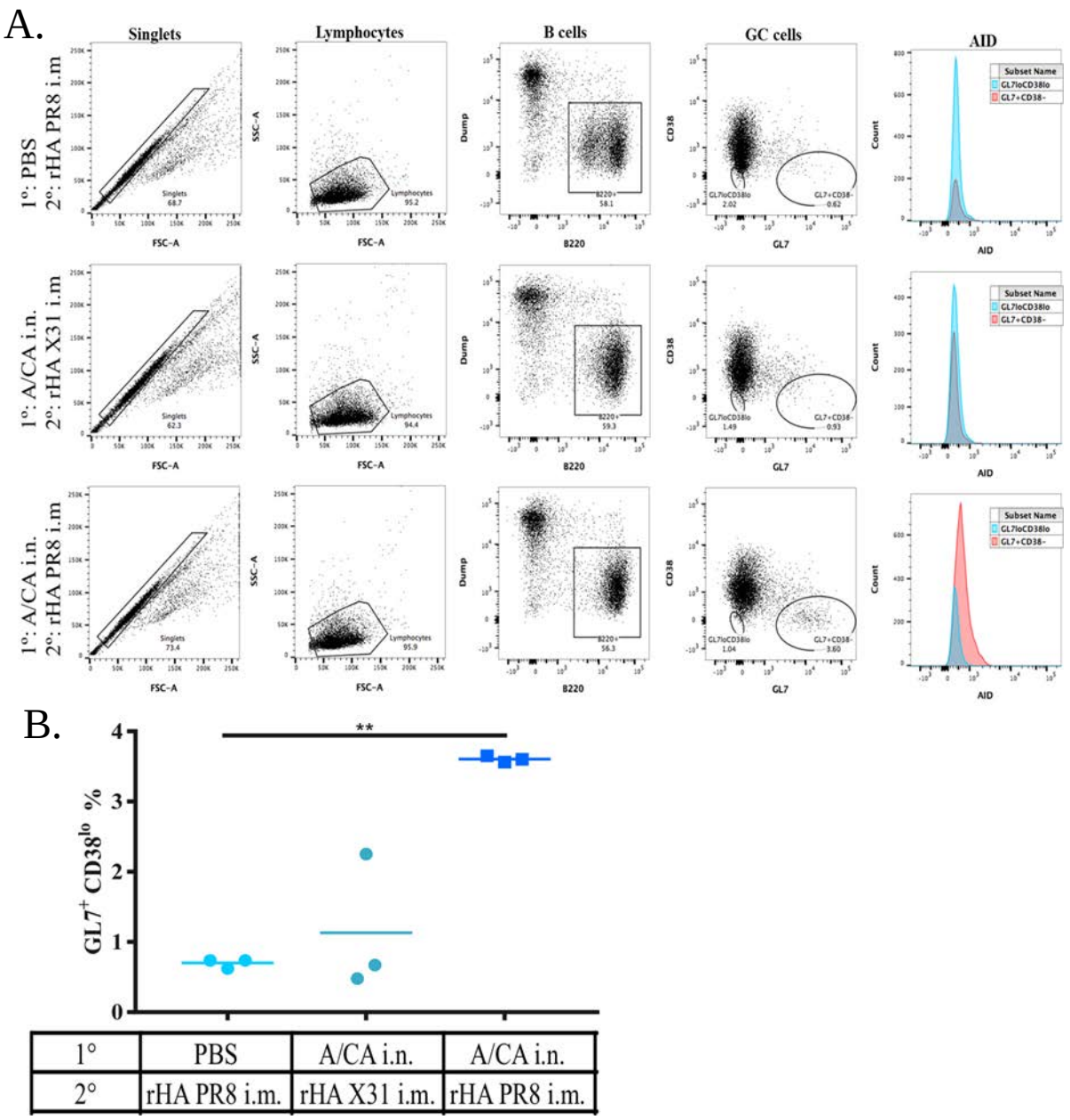

Figure 4.2 Increased Germinal Center B cells in response to drifted vaccination in previously exposed mice but not unexposed mice. Representative gating of draining LN (inguinal) tissue 4 days post vaccination with rHA A/PR8 or rHA X-31 (1 µg), in previously unexposed (upper) or A/CA exposed (lower panels) mice in panel (**A**). AID expression is in the red histogram from GC cells. Percentage of GC cells ($B220^{+}GL7^{+}CD38^{lo}AID^{+}$) in unexposed versus previously exposed CB6F1 mice vaccinated with rHA PR8 or rHA X-31 (1 µg) in panel (**B**). (**p<0.01, One-way ANOVA).

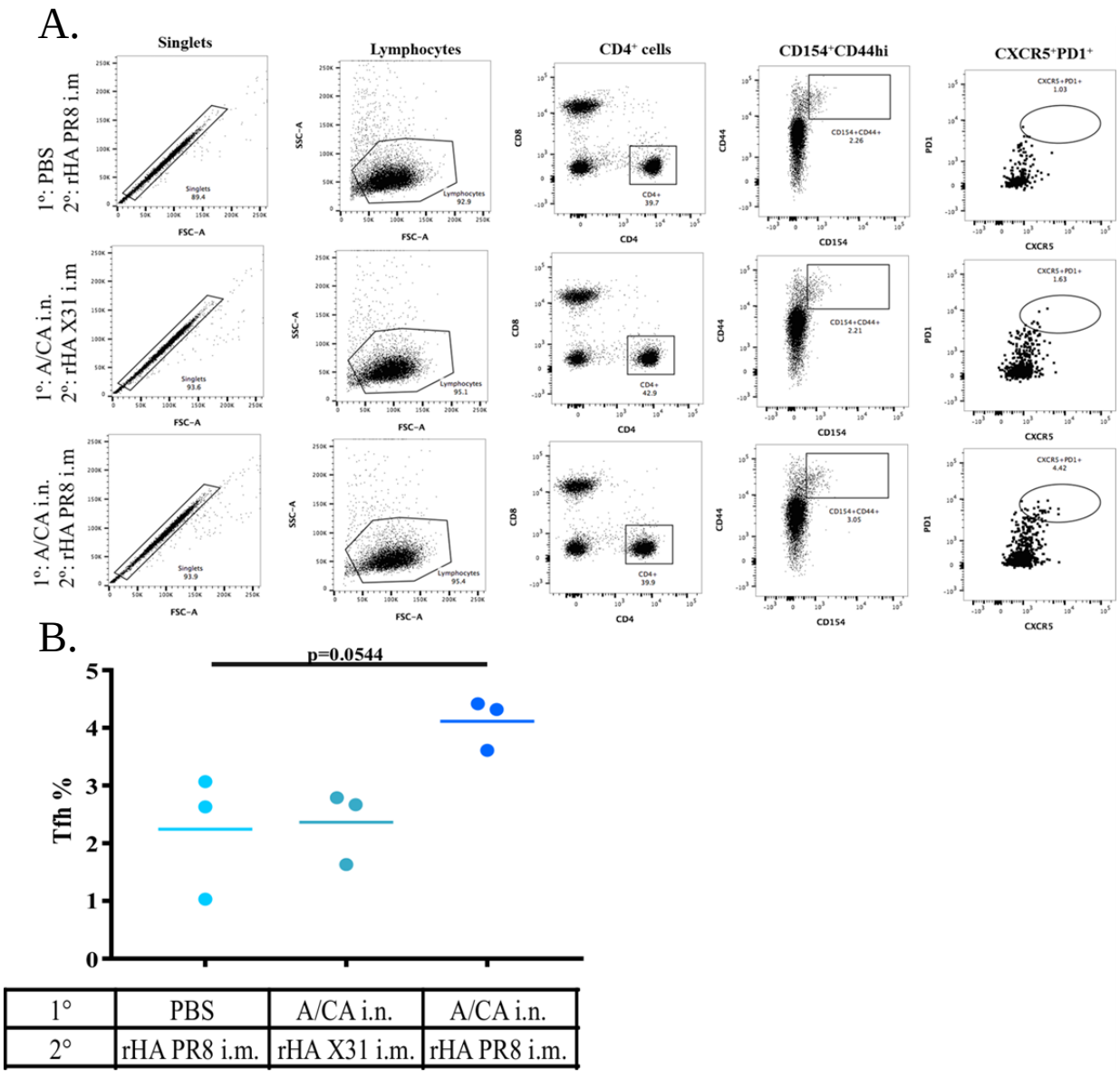

1°	PBS	A/CA i.n.	A/CA i.n.
2°	rHA PR8 i.m.	rHA X31 i.m.	rHA PR8 i.m.

Figure 4.3 Increased Germinal Center T follicular helper cells in response to drifted vaccination in previously exposed mice but not unexposed mice. Representative flow plots show increased Tfh cells ($CD4^+$ $CD154^+CD44^{hi}CXCR5^{hi}PD\text{-}1^{hi}$) in previously exposed CB6F1 mice vaccinated with PR8 rHA but not with rHA X-31 (1 µg) in panel (**A**). Percentage of Tfh cells in unexposed versus previously exposed CB6F1 mice vaccinated with rHA PR8 or rHA X-31 (1 µg) in panel (**B**). (p=0.0544, One-way ANOVA).

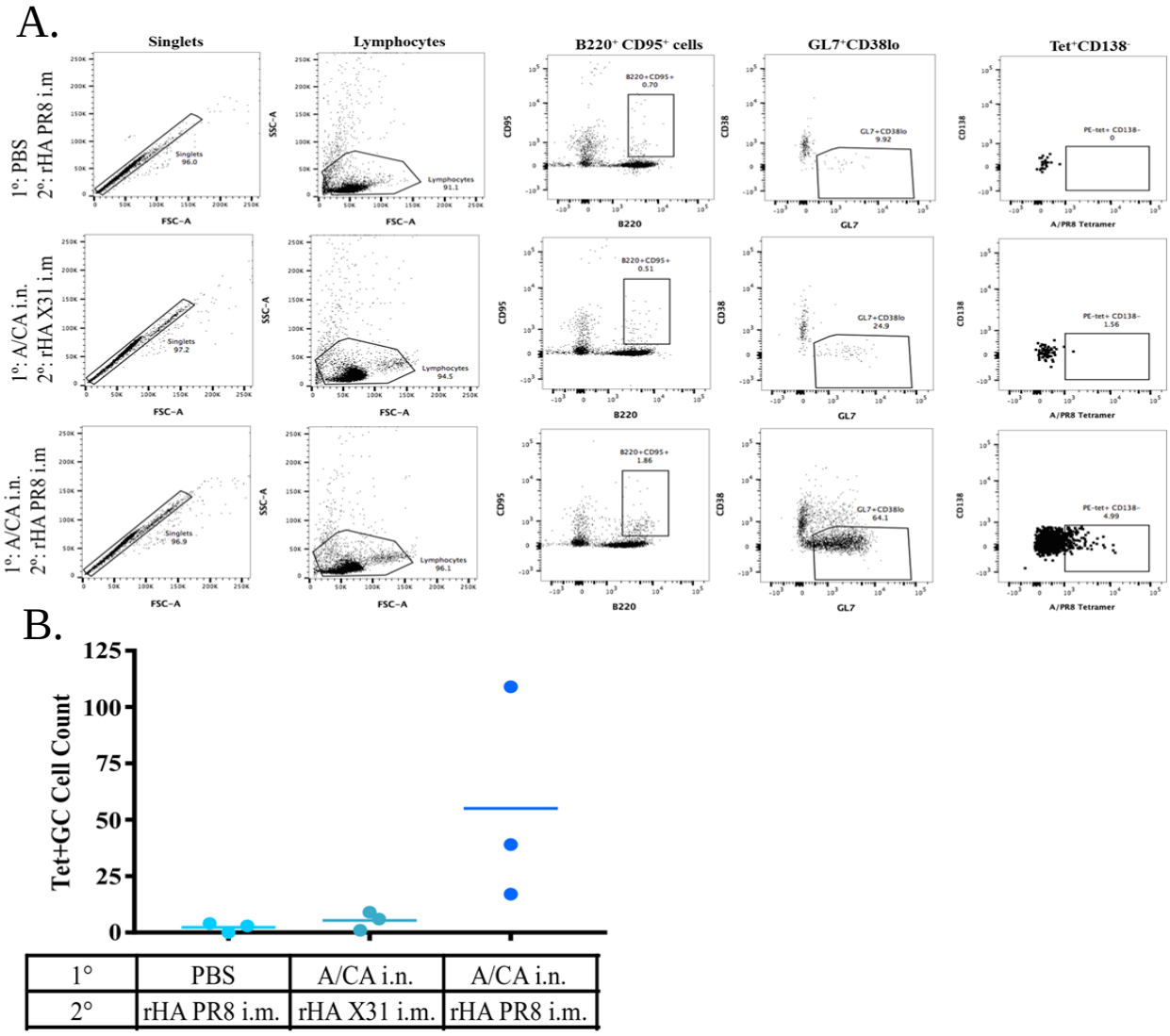

Figure 4.4 Increased Germinal Center A/PR8-specific B cells in response to drifted vaccination in previously exposed mice but not unexposed mice. Representative flow plots show increased A/PR8 HA specific GC B cells ($B220^{+}Tet^{+}GL7^{+}CD38^{lo}$) in previously exposed CB6F1 mice vaccinated with rHA A/PR8 but not rHA X-31 in panel (**A**). Percentage of A/PR8 HA specific GC B cells ($B220^{+}CD95^{+}GL7^{+}CD38^{lo}$ Tet^{+}) in unexposed and immunized with rHA PR8 (1 µg), previously A/CA exposed and immunized with rHA X-31 (1 µg) versus previously exposed CB6F1 mice immunized with rHA PR8 (1 µg) in panel (**B**).

Reversal of OAS phenotype in C57BL/6 mice with inclusion of CD4$^+$ T cell reactive epitopes in HA.

To investigate if conserved CD4$^+$ T cell epitopes, as observed in our CB6F1 mouse model, could reverse the OAS phenotype in our C57BL/6 mouse model we incorporated conserved MHC Class II epitopes within HA in both exposures. To do this, we replaced the A/PR8 HA plasmid receptor-binding site (RBS), a mapped immunodominant neutralizing epitope, with the corresponding A/CA HA RBS leaving the MHC Class II epitopes conserved and subsequently rescued virus (CA/PR8Δ), confirming the mutagenesis by sequencing (**Figure 4.5 A**). The CA/PR8Δ virus productively infected mice, seroconverting to both rHA PR8 and CA (**Figure 4.5 B**). Using our C57BL/6 OAS mouse model, we then exposed mice to PBS, A/CA or our engineered CA/PR8Δ virus, 28 days later we then immunized with A/PR8 i.m. (1μg) and evaluated the antibody responses. Mice exposed to the CA/PR8Δ virus displayed increased germinal centers, compared to controls or A/CA infected mice at 4 days post-secondary immunization (**Figure 4.6**). Likewise, mice had increased titers, both by HAI and ELISA to A/PR8 upon secondary immunization (**Figure 4.7 A**). Further, C57BL/6 mice pre-exposed to CA/PR8Δ and subsequently immunized with A/PR8 HA showed complete lethal and weight loss protection from challenge with 1000 LD_{50} (**Figure 4.7 B**).

A.

B.

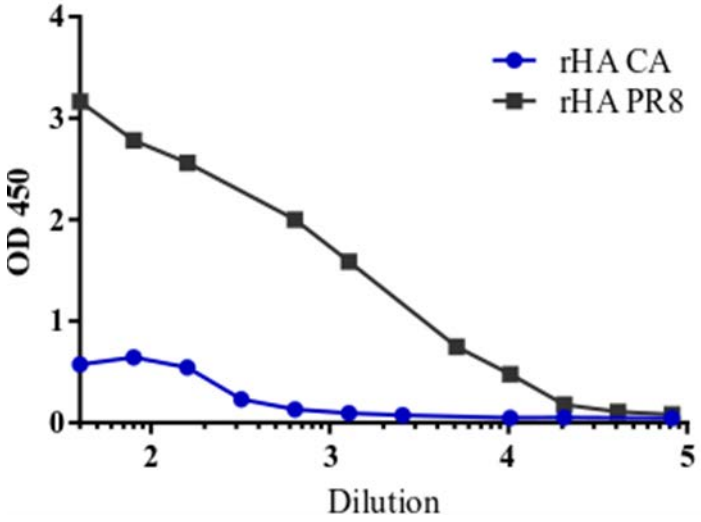

Figure 4.5 CA/PR8Δ Virus confirmation of sequence and seroconversion in C57BL/6 mice. Sequence results from modified virus with A/CA receptor binding site successfully inserted into A/PR8 HA plasmid in panel (**A**). C57BL/6 Infection with CA/PR8Δ infection elicits an A/PR8 and A/CA rHA ELISA response in panel (**B**).

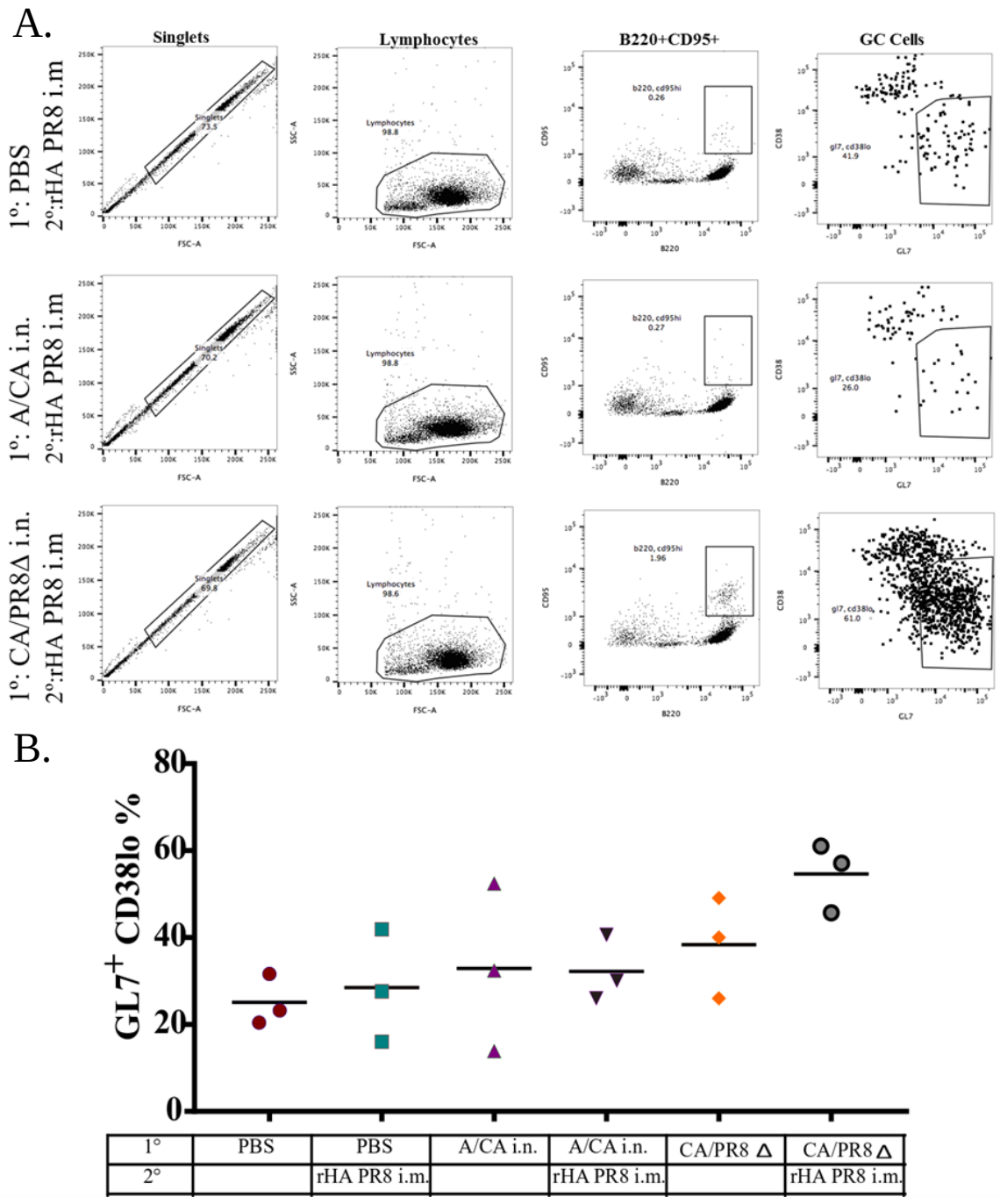

Figure 4.6 CA/PR8Δ exposed C57BL/6 mice have greater GC cell induction upon A/PR8 HA vaccination in draining LN (inguinal) at 4 days post immunization. Representative flow plots show increased GC B cells ($B220^{+}CD95^{+}GL7^{+}CD38^{lo}$) in previously exposed C57BL/6 mice vaccinated with rHA A/PR8 in panel (**A**). Percentage of GC cells in previously exposed C57BL/6 mice vaccinated with PR8 rHA (1 µg) in panel (**B**).

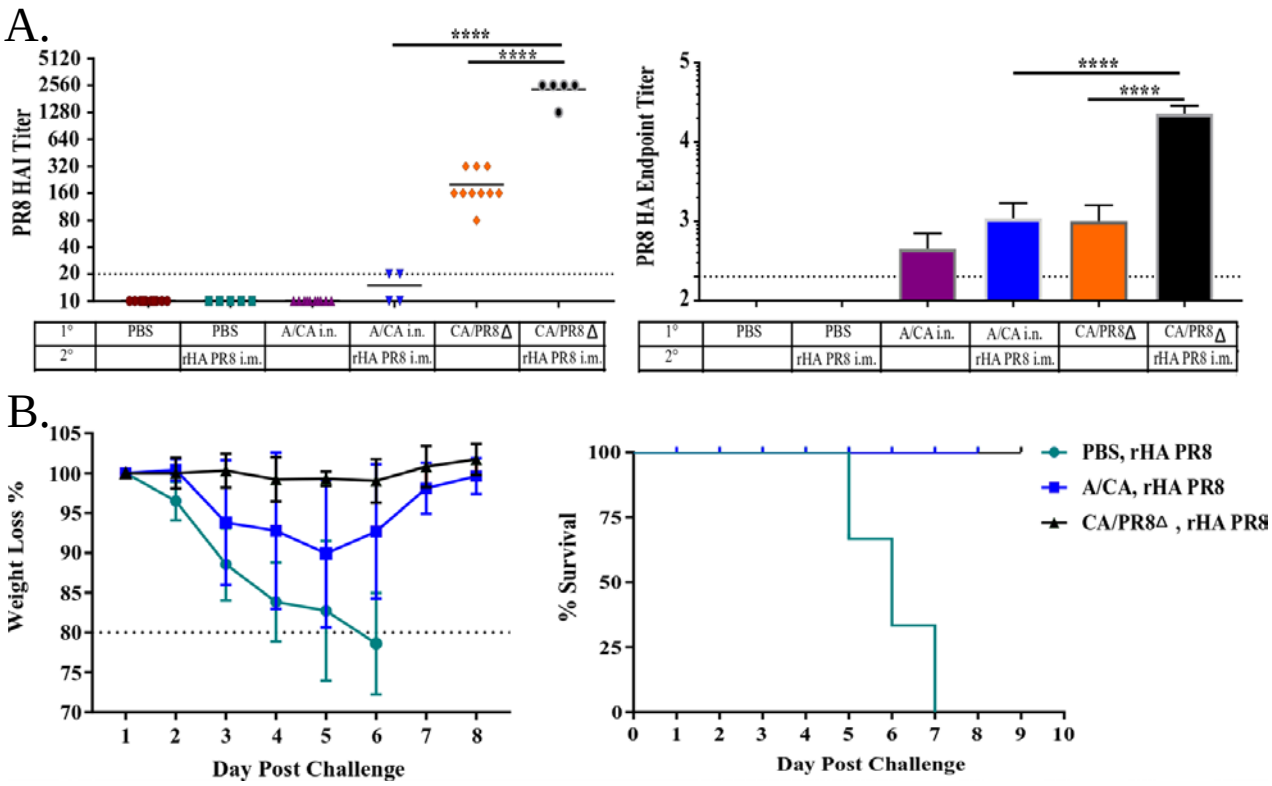

Figure 4.7 Including conserved CD4$^+$ T cell epitopes within HA antigen reverses OAS in C57BL/6 mice. A/PR8 HAI (Log_2) and HA endpoint titer ± SD (Log_{10}) of C57BL/6 mice post primary infection and subsequent immunization with A/PR8 HA (1µg) in panel (**A**). Challenge weight loss and survival from 1000 LD_{50} A/PR8 challenge in panel (**B**). (****p<0.0001, One-way ANOVA).

DISCUSSION

Germinal centers are indicative of B cell proliferation, differentiation and editing of their BCR to achieve greater affinity for antigen. To that end, we have found in our CB6F1 mouse model robust germinal center formation in the draining lymph node at day 4 post-immunization with drifted rHA but not shifted rHA. Further, these germinal center B cells expressed the somatic hypermutation enzyme, AID, suggesting that their BCR is undergoing editing to become higher affinity for drifted HA. Importantly, to overcome the hurdles of using HA antigen to identify antigen-specific B cells, we created a novel tool for determining antigen-specificity using receptor binding site peptide specific for A/PR8 HA that has previously been found to be immunodominant in epitope mapping studies. Using this new tool, we were able to show that germinal center B cells were becoming specific for this unique receptor binding site in A/PR8 HA.

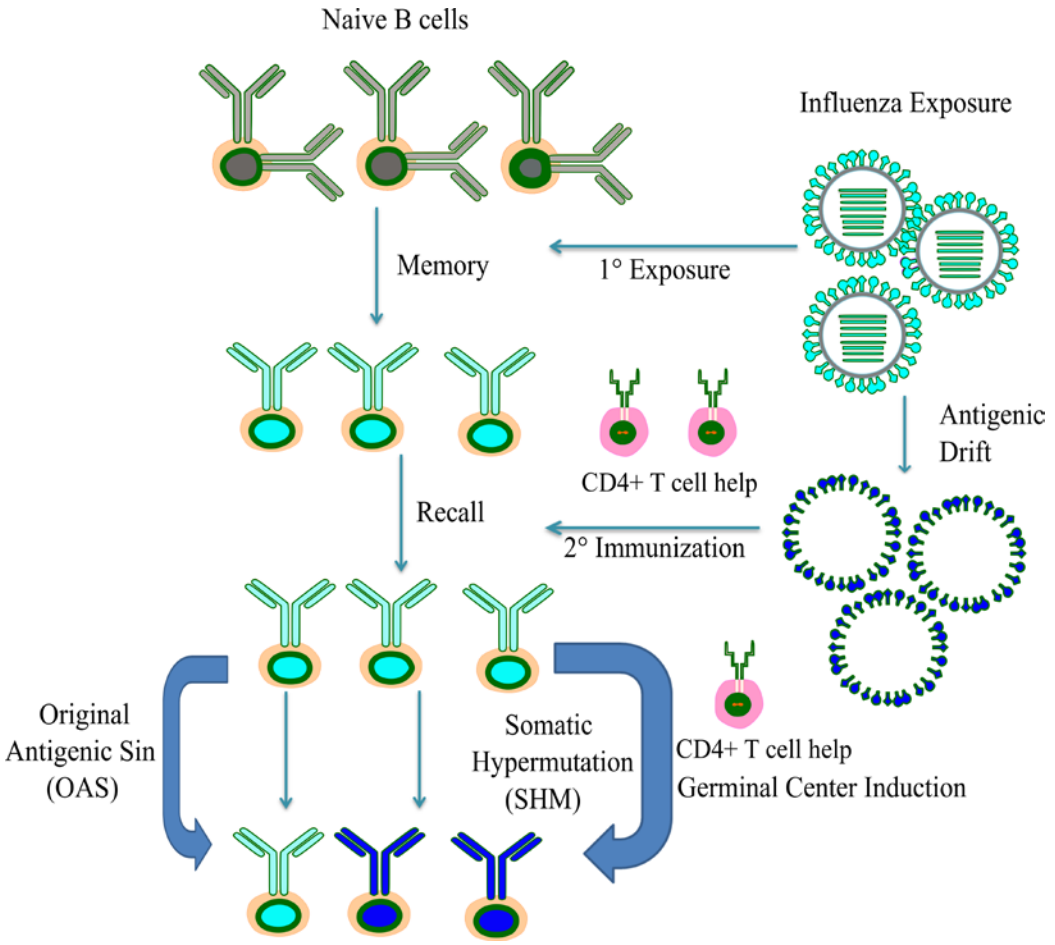

Figure 4.8 Re-engagement of both memory B and $CD4^+$ T cells are necessary for enhanced responses to drifted HA immunization and without cognate $CD4^+$ T cell help antigenic sin phenotype is observed.

In contrast to our CB6F1 mouse model, the OAS mouse model exhibits no germinal center formation upon immunization with drifted rHA. However, using the 8-plasmid genetic system of influenza we were able to incorporate the neutralizing site and therefore, neutralizing epitopes from A/CA into a A/PR8 HA plasmid backbone, leaving the MHC Class II epitopes unchanged. Using the CA/PR8Δ mixed virus, we were able to overcome the OAS antibody phenotype, leading to germinal center characterization and ultimately, protection from lethal challenge. This further supports the model that B and T cell synergism is crucial for adaptation

of B cells in the face of drifting neutralizing epitopes. It also strongly supports that for optimal engagement of B cells against drifting influenza, memory $CD4^+$ T cells reactivity must be considered and leveraged for enhanced responses. Collectively, Chapters 2-4 fit a model wherein if there is reengagement of both memory B and $CD4^+$ T cells, it results in intensified responses to drifted HA via germinal center induction, leading to greater protection (**Figure 4.8**).

Chapter 5: Improved Immune Responses in Young and Aged Mice with Adjuvanted Vaccines against H1N1 Influenza Infection

The following text is from the article:

Susan L. Baldwin[1#], Fan-Chi Hsu[1#], Neal Van Hoeven[1], **Emily Gage[1]**, Brian Granger[1], Jeffrey A. Guderian[1], Sasha E. Larsen[1], Erica C. Lorenzo[2], Laura Haynes[2], Steven G. Reed[1], and Rhea N. Coler[1, 3, 4]*

[1]Infectious Disease Research Institute, Seattle, WA, USA.

[2]Center on Aging and Department of Immunology, University of Connecticut School of Medicine, Farmington, CT, USA

[3]Department of Global Health, University of Washington, Seattle, WA, USA

[4]PAI Life Sciences, 1616 Eastlake Ave. E., Seattle, WA, USA

Figure numbers have been updated to conform to the dissertation. The text remains as published with minor editorial changes.

Introduction

Influenza and influenza-related complications are leading causes of death in elderly populations. Older people exhibit increased morbidity and mortality in response to influenza infection due to uncontrolled respiratory inflammation, severe pneumonia or multi-organ inflammation and failure (130). Although the annual influenza vaccine coverage rate has increased, the CDC estimates that individuals older than 65 years of age who have received influenza vaccines in consecutive years are still at high risk of influenza infection (131).

The process of immunological aging, also called immunosenescence, is associated with a progressive loss of functional physiological integrity including collectively increasing DNA damage and genome instability, stem cell exhaustion, cellular senescence, and altered intercellular communication, among other processes [reviewed in (132)]. Immunosenescence causes the attenuation of both innate and adaptive immune systems including reduced levels and function of TLRs in macrophages and plasmacytoid dendritic cells (133, 134), decreased output of naïve B cell numbers (135), severe reduction of thymopoiesis (136), and insufficient immune synapse generation (137). Furthermore, aged individuals also demonstrate a significant reduction in the quantity, but not quality of antigen-specific antibody responses, and this reduction in antibody quantity is concurrent with a decrease in antigen specific plasmablasts (138). Indeed, defective antigen presentation and reduced T cell and B cell repertoires in aged individuals results in poor cellular, humoral and vaccine-induced responses.

As vaccination is the most effective method to prevent infection, ways to improve influenza vaccines for use in the aging human population are continually being explored. These strategies include adjuvant use, intradermal delivery, increased dosage, and altering antigen selection that typically make up seasonal vaccines [reviewed in (139)]. The first seasonal

influenza vaccine containing an adjuvant (MF59), also known as Fluad™, was approved by the FDA in 2015 for use in people over the age of 65 years. Fluzone® High-Dose vaccine (an inactivated, split influenza virus vaccine containing 60 µg of HA for each component of the vaccine, rather than 15 µg) is also approved for use in people ≥65 years of age. Despite advancements in alternative vaccine options for the elderly population, they are still disproportionally affected, and continue to exhibit severe morbidity and mortality each year from seasonal influenza infections. Thus, a need still remains for better strategies, including additional adjuvant options, for the influenza vaccine to overcome the challenges of immunosenescence in the elderly.

The disparity of morbidity and mortality burden in elderly individuals is partly due to the incomplete understanding of how adjuvanted vaccines may circumvent immunosenescence in elderly people. Mechanistic details regarding how different adjuvants work in the elderly may reveal ways in which adjuvant formulations can be tailored and adapted for optimal responses that provide enhanced protection for this susceptible population. Administration of adjuvants, including squalene-based oil-in-water emulsions, and those including a TLR4 agonist, have been leveraged in vaccines in order to enhance immune responses in multiple studies (140-147). These adjuvants include MF59 (as described above), and AS04 (comprised of monophosphoryl lipid Aand Alum) included in FDA approved vaccines against hepatitis B virus (HBV) and human papillomavirus (HPV) (140). In preclinical studies, we have shown that glucopyranosyl lipid A (a synthetic TLR4 agonist) formulated in a stable oil-in-water emulsion (GLA-SE) expands immune responses to Fluzone® (141). GLA has also been included in several completed and ongoing human clinical studies for vaccines against *Leishmania* (NCT01751048), *Mycobacterium tuberculosis* (NCT02508376, NCT0246516, NCT01599897), HIV

(NCT01966900, NCT01922284), Schistosomiasis (NCT03041766), malaria (NCT02647489, NCT01540474), and avian influenza (NCT01991561, NCT01147068). In humans, GLA-SE combined with rH5 was considered safe and improved antibody titers compared to the recombinant protein alone (144). Furthermore, no defect has been identified in humans following stimulation with GLA-SE on antigen-presenting cells (APCs) from aged compared to young APCs (145) and enhances T cell responses from older adults following stimulation of peripheral blood mononuclear cells (PBMCs) with live influenza virus (148). Therefore, our approach in this study was to employ the use of different adjuvants combined with an influenza vaccine to overcome the challenge of immunosenescence in aged animals.

In this investigation, one of our main findings reveal that aged mice have dampened cytokine responses to *in vitro* stimulation of DCs and lung homogenates with a Th1 cytokine-inducing agonist. In addition, we show that aged mice require two immunizations with adjuvanted sH1N1 vaccines for robust *in vivo* protection against influenza whereas young mice are protected after a single immunization. Finally, we demonstrate that immunization in young mice with sH1N1 + GLA-SE results in enhanced alveolar macrophage (AM) homeostasis within the lung, increased TLR7 expression within the AMs, and faster clearance of virus after H1N1 challenge compared to mice immunized with sH1N1 + SE or vaccine alone. These results emphasize the age-related differences following immunization, the ability to improve responses to influenza infection in the elderly with two immunizations, and a mechanism of enhanced vaccine protection against influenza with a TLR4 agonist adjuvant.

Materials and Methods

Mouse Model

Young female C57BL/6 or CB6F1 mice were purchased from Charles River Laboratories (Wilmington, MA) or the Jackson Laboratories (Bar Harbor, ME) and were housed and maintained under specific pathogen free conditions at the Infectious Disease Research Institute. Experiments which included female C57BL/6 or CB6F1 mice aged 18-21 months were acquired with special request from the National Institute on Aging, from the aged rodent colony (National Institute of Health, Bethesda, MD). Mice were housed in a biosafety level 2 (BSL2) environment for the entirety of these studies (including H1N1 challenge studies) and all procedures were performed in accordance with the regulations and guidelines of the IDRI animal care and use committee.

Adjuvants and Immunization

Vaccines were formulated in saline, SE (2% final v/v oil concentration), an MF59-like adjuvant (2.5% final v/v oil concentration), or GLA-SE (5 μg of GLA in 2% SE). Mice were immunized intramuscularly (i.m.) one or two times three weeks apart. The split H1N1 vaccine, (sH1N1), (kindly provided by Novartis) and recombinant H1 (rH1) (A/California/4/2009; Protein Sciences Corp., Meriden, CT) was used at 0.01 μg or 0.1 μg, respectively, for the immunizations. Serum was collected 3 weeks after prime or boost immunizations. Spleens and bone marrow were harvested for immunogenicity studies either 1 week or 4 weeks following immunization(s) as described.

Endpoint antibody titers

Sera were analyzed for H1-specific IgG1 and IgG2c endpoint antibody titers by antibody capture ELISA. Polysorp ELISA plates (Nunc-immuno polysorp 96 well plates, VWR) were

coated with rH1 (A/H1N1/California/2009) (Protein Sciences Corp., Meriden, CT) at a concentration of 1 µg/ml in 0.1 M bicarbonate coating buffer at 100 µl per well for 4 hours at room temperature. Plates were then blocked with a 0.05% PBS-Tween solution plus 1% BSA, and incubated overnight at 4°C, followed by 5 washes in 0.1% PBS-Tween and one PBS wash. Serially diluted mouse sera were added and plates incubated at room temperature, on a shaker, for two hours. Plates were washed, dried, and secondary antibodies (IgG1-horseradish peroxidase (HRP) and IgG2c-HRP, Southern Biotechnologies, Birmingham, Al) were added at a 1:2000 dilution. Plates were incubated at room temperature for one hour, washed, and eBioscience™ TMB solution (Thermo Fisher Scientific) was added to the plates. The enzymatic reaction was stopped with 50 µl per well of 1N H_2S0_4. Plates were then read on a VERSAmax microplate reader (Molecular Devices) at 450 nm with a reference filter set at 570 nm. Endpoint titers were determined as the last dilution to render a response of greater than 0.1 mean optical density using Prism software (GraphPad Software, La Jolla, CA).

Hemagglutination inhibition (HAI) antibody responses

HAI assays were performed according to World Health Organization (WHO) guidelines. Briefly, sera was treated with receptor destroying enzyme (RDE, from *Vibrio Cholera*, Denka-Seiken, Tokyo, Japan) overnight and heated at 56°C for 30 minutes to deactivate the enzyme. HAI antibodies were then tested against the vaccine strain (A/H1N1/California/4/2009) with 0.5% turkey red blood cells (Thermo Fisher Scientific). The HI titer was defined as the reciprocal of the highest dilution of sera which completely inhibited the agglutination of the RBCs. All samples were run in duplicate, and pre-immune titers in all mice were ≤5.

Weight and Survival Measurement

Ten mice/group were immunized i.m. either once or twice, 3 weeks apart. About 3 weeks after the prime or boost immunization, mice were infected via the intranasal route with $100LD_{50}$ A/H1N1/California/4/2009. Survival and clinical signs (weights) were assessed daily, over 14 consecutive days. Animals exhibiting significant weight loss or that were under duress (ruffled fur, weighted breathing, or hunched backs) were sacrificed. All procedures with A/H1N1/California/4/2009 infected mice were performed under BSL2 conditions per IACUC procedures and guidelines.

In vitro stimulation of bone marrow-derived dendritic cells (BMDCs) and lung homogenates

Bone marrow was harvested from the femurs of vaccinated mice, and single cell suspensions were prepared at a concentration of 2×10^5 cells per ml in complete RPMI-1640 with 20 ng/ml recombinant mouse GM-CSF (rmGM-CSF; PeproTech). On day 3, additional rmGM-CSF was supplied. BMDCs were harvested on day 6 and were seeded at a concentration of 6.6×10^5 cells per well. Cells were stimulated with a range of 2 ng/ml to 20 μg/ml GLA-SE, 0.00008-0.8% SE or 10 ng/ml Lipid A 506 (a TLR4 agonist as positive control, Peptide Institute Inc., Osaka, Japan) in the presence of 20 ng/ml rmGM-CSF. A sterile single cell suspension was prepared from young and aged mouse lung by passing tissue through a 100 μM cell strainer (Thermo Fisher Scientific). Erythrocytes were lysed using ACK lysis buffer (Gibco by Life Technologies), while remaining leukocytes were enumerated and plated in triplicate wells at a seeding density of 5×10^5 cells per well. Lung homogenates were stimulated with the same conditions as BMDCs described above. Following an 18-hour stimulation, cell supernatants from BMDCs or lung homogenates were collected and cytokine levels in the supernatants were determined by using custom Luminex-based multiplex immunoassay kits (Procarta Cytokine

Assay Kit: Affymetrix, Santa Clara, CA). Cell supernatants were incubated with polystyrene beads coated with antibodies corresponding to the different cytokines including: TNF-α, IL-10, IL12p40 and IL-6, and developed according to the manufacturer's instructions. Bead size and fluorescence were measured on a Luminex 200 and data were analyzed using the Masterplex QT software (Miraibio).

Flow cytometry

The antigen-specific T cell memory response generated by vaccination was determined by flow cytometry following incubation of splenocytes with 10 μg/ml rH1 (Protein Sciences Corp., Meriden, CT). Cells were cultured at 1 x 10^6 cells per well in a 96-well plate (Corning Incorporated, Corning, NY) in RPMI-1640 supplemented with 10% heat-inactivated FCS and 50,000 Units penicillin/streptomycin (Invitrogen) for 18-20 hours in the presence of GolgiStop (BD Bioscience). Each sample was incubated with Fc receptor blocking (clone2.4G2) before incubation on ice for 30 minutes with the following antibodies: anti-CD4 (clone RM4-5), anti-CD8α (clone 53-6.7), and anti-CD44 (clone IM7). Expression of selected cytokines was determined by incubation with anti-IFN-γ (clone XMG1.2), anti-IL-2 (clone JES6-5H4), anti-CD154 (clone MRI), anti-TNF-α (clone MP6-XT22) and anti-IL-17A (clone TC11-18H10.1). For Tfh cell analysis, single-cell suspension of inguinal lymph nodes (149) were prepared and stained with following antibodies: anti-CD4 (clone RM4-5), anti-CXCR5 (clone L138D7), anti-PD-1 (clone 29F.1A12), anti-B220 (clone RA3-6B2), anti-CD44 (clone IM7) and anti-CD8 (clone 53-5.8), F4/80 (clone BM8), CD11b (clone M1/70) for dump gate. For GC B cell analysis, single-cell suspension of spleen or inguinal LNs were prepared and stained with following antibodies: anti-B220 (clone RA3-6B2), anti-GL7 (clone G7), anti-CD95 (clone SA367H8), anti-IgD (clone 11-26c.2a), anti-IgG1 (clone RMG1-1). For lung immune cell analysis, lungs were

chopped and digested with the presence of 70 μg/ml Liberase™ (Roche), 40 μg/ml DNase I (Roche), 10 mM Aminoguanidine (Sigma-Aldrich), and 5 mM KN-62 (Sigma-Aldrich). The homogenates were incubated for 30 min in a 37°C water bath. Single-cell suspensions were prepared by dispersing the tissues through a 70 μm nylon tissue strainer (BD Falcon). Cells were washed with 1X PBS and then stained with fixable viability dye (Tonbo Biosciences) before being stained with following antibodies: anti-CD11b (clone M1/70), anti-CD11c (clone N418), anti-CD45 (clone 30-F11), anti-NK1.1 (clone PK136), anti-Ly6G (clone 1A8), anti-TLR2 (clone T2.5), anti-TLR3 (clone 11F8), anti-TLR4 (clone SA15-21) and anti-TLR7 (clone A94B10). Antibodies were purchased from BD Biosciences, eBioscience, BioLegend or Tonbo Biosciences. Samples were analyzed with BD Fortessa or LSRII. Doublets and dead cells were excluded before analysis, and all the data were analyzed with FlowJo software (version 9; FlowJo, LLC).

Enumeration of long-lived antibody-secreting plasma cells (ASPC)

A bone marrow ELISPOT was used to determine the induction of vaccine-specific long-lived antibody-secreting plasma cells (ASPC) following immunization with sH1N1 vaccine with and without adjuvants. ELISPOTs were performed as previously described (147) with minor revisions. The developed plates were counted by an ELISPOT plate reader (C.T.L. Serie3A Analyzer, Cellular Technology Ltd., Cleveland, OH) and the data was analyzed using ImmunoSpot® software (Cellular Technology Ltd., Cleveland, OH).

Viral load measurement by real-time Q-PCR

RNA from whole-lung samples was extracted with Trizol® reagent following the manufacture instructions (Thermo Fisher Scientific). The mixture of $CHCl_3$ and Trizol was centrifuged at 11,500g for 15 min at 4°C. After centrifugation, the aqueous layer was transferred

and mixed with equal volume of 70% RNase-free ethanol. The RNA extracts were purified with RNA purification kit (Ambion®, Thermo Fisher Scientific). RNA was then reverse-transcribed with SuperScript® IV first-strand synthesis system (Invitrogen®, Thermo Fisher Scientific) into cDNA. Expression of H1 was measured using customized TaqMan probes (Applied Biosystem, Thermo Fisher Scientific) including forward primer: 5'-ATTGCCGGTTTCATTGAAGG-3'; reverse primer: 5'-ATGGCATTCTGTGTGCTCTT-3'; probe: 5'-(FAM) ATGAGCAGGGGTCAGGATATGCAGCCGACC (TAMRA)-3' to detect A/H1N1/California/4/2009 viral load (150). TaqMan probe for GAPDH was used as the internal control (Applied Biosystem, Thermo Fisher Scientific). Samples were analyzed using a Bio-Rad CFX384 real-time PCR detection system (Bio-Rad), and relative gene expression was calculated via the $2^{-\Delta\Delta CT}$ method.

Statistical Analysis

Statistical analysis of antibody responses (endpoint antibody and HAI titers) and flow cytometry data was performed using one-way ANOVA with the Tukey multiple comparison test unless noted in the figure legend. A two-way ANOVA with the Tukey multiple comparison test was performed on data represented in figure 5 (with the exception of 5A; which used one-way ANOVA and the Tukey multiple comparison test). Statistical analysis of BMDCs and lung homogenates represented in figure 4 were performed using two-way ANOVA and Sidak's post test. Statistical analysis of survival curves was performed using the Log-Rank/Mantel-Cox test. All statistical analyses were performed using GraphPad Prism version 7 for Windows (GraphPad Software, La Jolla California, USA). *p* values of <0.05 were considered significant.

Results

sH1N1 vaccine adjuvanted with GLA-SE enhances IgG2c:IgG1 ratios and high HAI titers in young CB6F1 mice

We were particularly interested in determining whether adjuvants could help overcome the immunosenescence observed in elderly populations. The induction of antigen-specific IgG1 antibodies is dependent on Th2-biased immune responses while class switching to IgG2c in mice is correlated with Th1-biased immune responses and has been well studied (149). We have previously reported that GLA-SE enhances antiviral protection through the induction of Th1-mediated immune responses (143) and therefore used this adjuvant formulation in this study. C57BL/6 mice were originally selected as the mouse strain for these studies, however our data showed no evidence of HA (A/H1N1/California/4/2009) CD4 T cell epitopes in C57BL/6 mice, whereas CB6F1 mice have a confirmed CD4 T cell epitope. This data provided the rationale for switching to the CB6F1 mouse strain for the remainder of the studies. As shown in Figure 5.1, the recombinant rH1 vaccine combined with adjuvants MF59-like, SE or GLA-SE in C57BL/6 mice induced both IgG1 and IgG2c responses post boost. An enhanced IgG2c:IgG1 bias was observed in C57BL/6 mice immunized with rH1+ GLA-SE (**Figure 5.1 B**). While HAI titers in young C57BL/6 mice given adjuvanted rH1 were all >1:40 after two immunizations, much lower HAI titers were observed in aged C57BL/6 mice, where only one out of three of the aged animals in the MF59 and GLA-SE adjuvanted groups tested had post-vaccination HAI titers of >1:40 (**Figure 5.1 C**).

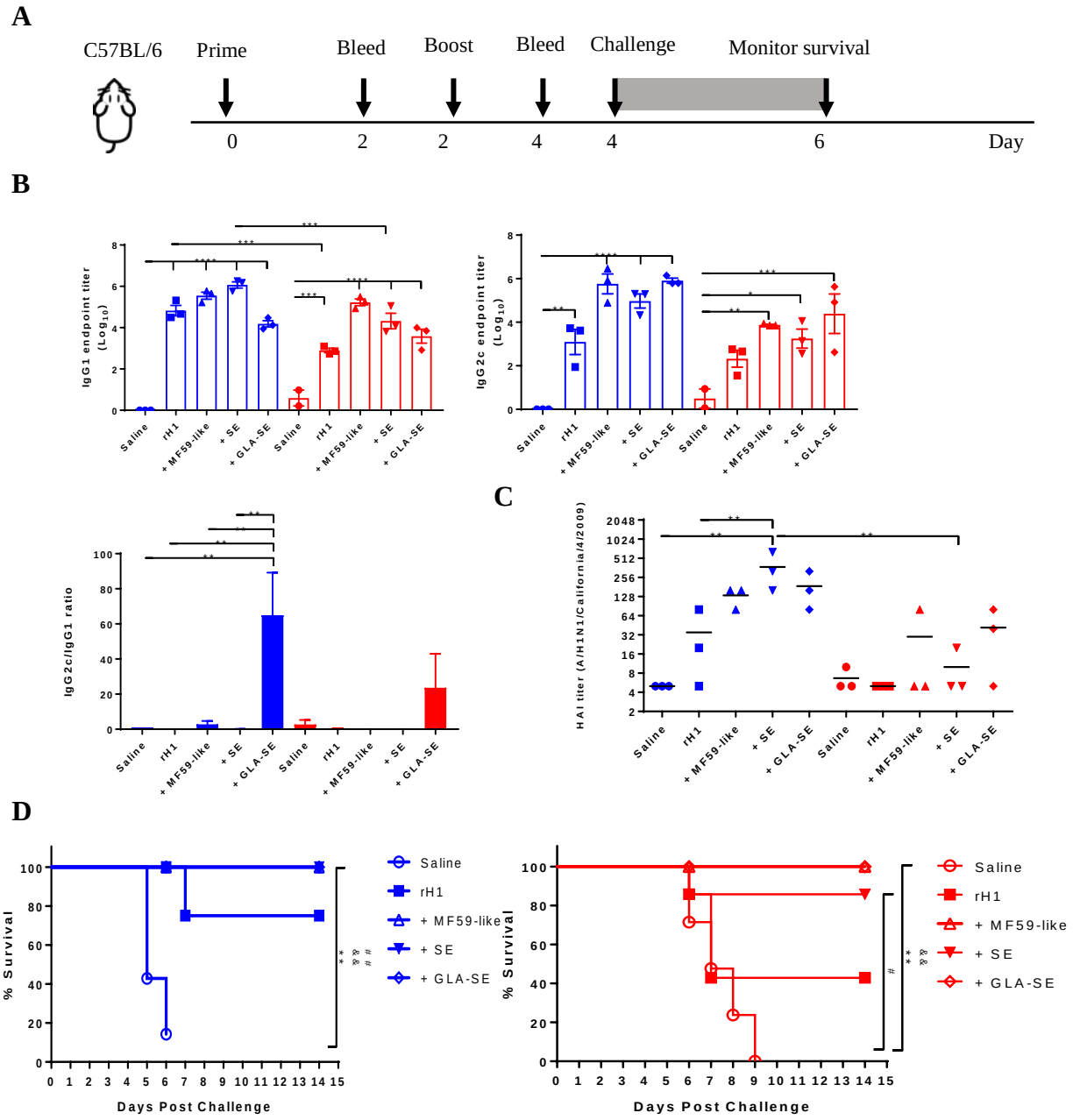

Figure 5.1 Adjuvanted rH1 vaccines enhance IgG2c:IgG1 ratios and protection in young and aged C57BL/6 mice following a boost. **(A)** Scheme of immunization procedure: C57BL/6 mice were immunized i.m. twice, three weeks apart, and antibody analysis was determined on sera collected four weeks following the boost. All mice were challenged with 100LD_{50} A/H1N1/California/4/2009 at day 49 and their physical condition was monitored over 14 days. Young mice (blue) and aged mice (red) are shown. **(B)** Sera collected from saline, rH1, rH1+MF59-like, rH1+SE and rH1+GLA-SE groups were analyzed for H1-specific IgG1 and

IgG2c endpoint titers. Results are represented as the mean endpoint titer ($\log_{10}$) ± SEM. *p* values are denoted as follows: * indicates <0.05; ** indicates <0.01; *** indicates < 0.001; **** indicates < 0.0001. **(C)** Sera harvested from mice after a boost (day 48) immunization were analyzed for HAI titers. An HAI titer of 5 represents responses below the assay detection limit. ** indicates *p* value <0.01. **(D)** Survival was monitored over the course of 14 days among all groups of young mice (left panel, blue) and aged mice (right panel, red). $^{\&\&}$ indicates *p* value <0.01 between saline vs. MF59-like groups; $^{\#\#}$ indicates *p* value <0.01 between saline vs. SE groups; ** indicates *p* value <0.01 between saline vs. GLA-SE groups.

We used the experimental design outlined in Figure 1A to assess the use of adjuvants in sH1N1 vaccine regimens and evaluate induced adaptive immune responses. Young (1 month old) or aged (18-21 month old) CB6F1 mice were immunized twice with the sH1N1 vaccine control (saline), or adjuvanted with MF59-like adjuvant, SE or GLA-SE. Three weeks following the boost immunization, H1-specific IgG1 and IgG2c antibodies were evaluated (**Figure 5.2 B**). We found that both young and aged mice receiving adjuvanted sH1N1 vaccines demonstrated measurable induction of IgG1 post boost over that of sH1N1 vaccine alone. However, the induction of IgG2c titers after two immunizations in aged mice were compromised even in adjuvanted groups, suggesting that the Th1-biased antibody response in aged mice, with the reduced dose of sH1N1 vaccine (shown to be effective in young mice), is not easily overcome by the action of adjuvants. Next, we tested whether adjuvanted sH1N1 vaccines could induce protective neutralizing antibodies in both young and aged mice. We observed that aged mice which received MF59-like, SE and GLA-SE adjuvanted vaccines could induce protective immune responses with two immunizations as compared to saline or sH1N1 vaccine alone, but not with one immunization (**Figure 5.2 C**). These data suggest that adjuvants similar to MF59-like, SE and GLA-SE could induce protective HAI titers in aged mice with a boost immunization, however a boost with the TLR4 agonist adjuvant (GLA-SE) was unable to generate a Th1-biased environment capable of inducing IgG2c responses in aged mice with the sH1N1 vaccine.

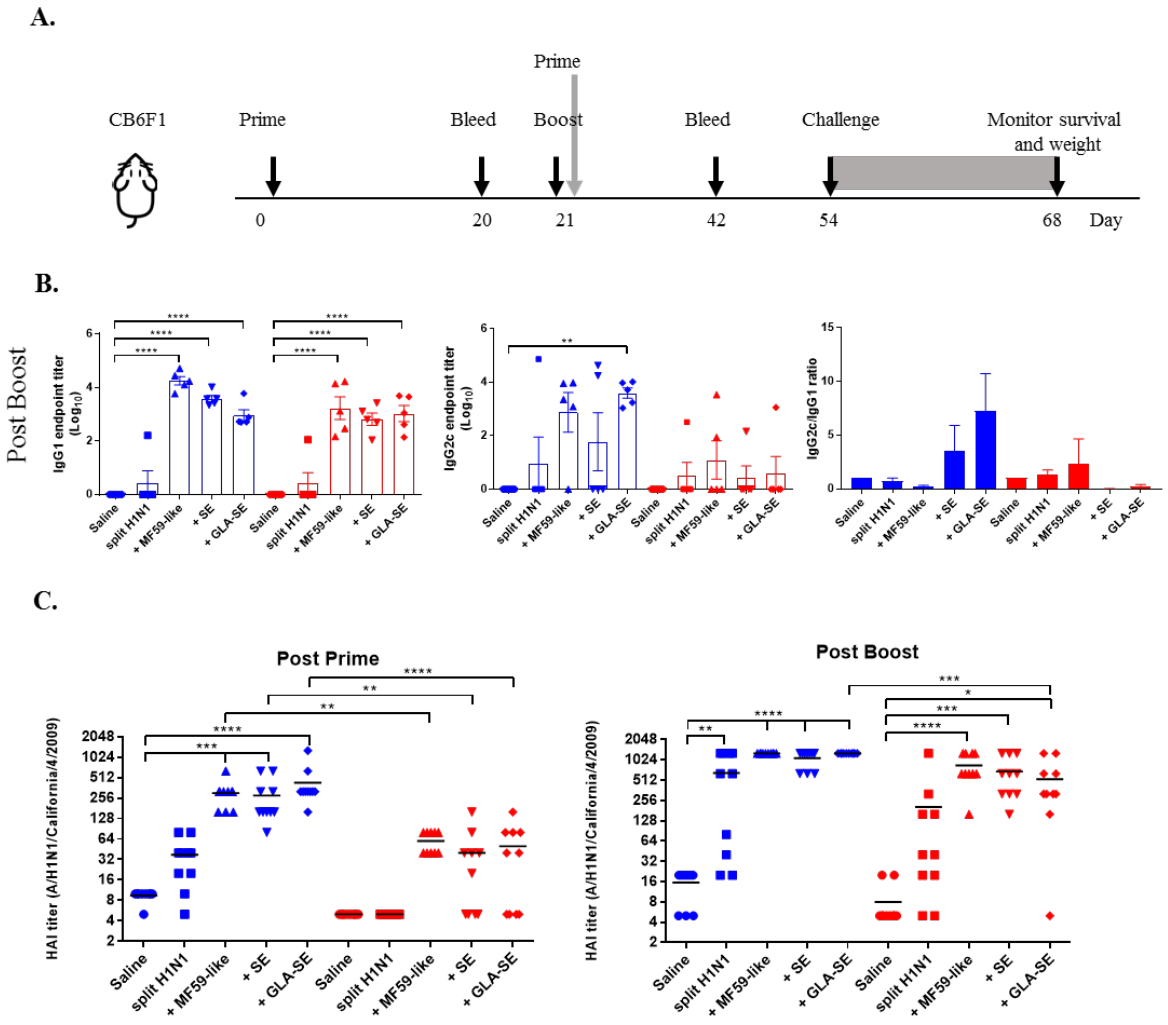

Figure 5.2 Adjuvanted sH1N1 vaccines induce antigen-specific IgG1 and IgG2c antibodies in young mice and HAI titers in young and aged CB6F1 mice. (A) Scheme of immunization procedure: CB6F1 mice were immunized i.m. either once or twice, three weeks apart, and antibody analysis was determined on sera collected three weeks following immunization. All mice were challenged with $100LD_{50}$ A/H1N1/California/4/2009 at day 54 and their physical condition was monitored over 14 days. Data for young mice were color-coded as blue; aged mice were color-coded as red for entire figure. **(B)** Sera from saline, sH1N1, sH1N1+MF59-like, sH1N1+SE and sH1N1+GLA-SE groups were analyzed for H1-specific IgG1 and IgG2c endpoint titers. Results are represented as the mean endpoint titer (log10) ± SEM. ** indicates *p* value <0.01; *** indicates *p* value < 0.001; **** indicates *p* value < 0.0001. **(C)** Sera harvested from mice after a prime (day 20) or boost (day 42) immunization were analyzed for HAI titers. An HAI titer of 5 was assigned to responses below the assay detection limit. *p* values are denoted as follows: * indicates <0.05; ** indicates <0.01; *** indicates < 0.001; **** indicates < 0.0001.

Enhanced body weights and survival in young and aged CB6F1 mice following two immunizations with adjuvanted sH1N1 vaccines

CB6F1 mice were immunized once or twice with 0.01 μg of sH1N1 vaccine either alone or with MF59-like, SE, or GLA-SE adjuvants, and then challenged with $100LD_{50}$ A/H1N1/California/4/2009 (**Figure 5.2 A**). All mice that received a single immunization lost weight after viral challenge, yet we found that young mice immunized with MF59-like, SE and GLA-SE adjuvants could gain weight back by day 5 post infection (**Figure 5.3 A, top left**). Conversely, weight loss continued among aged CB6F1 mice until day 7, and only aged mice that received GLA-SE and SE adjuvants gained back weight over time (**Figure 5.3 A, top right**). Both young and aged mice benefited from two immunizations with adjuvanted sH1N1 vaccines. Young mice given a boost with the adjuvanted vaccines quickly controlled the weight loss at day 3, and aged mice given adjuvanted vaccine only lost approximately 5% of starting weight compared to control animals (**Figure 5.3 A, bottom row**). Aged mice given saline or sH1N1 vaccine alone lost approximately 20% of starting weight at day 6 (**Figure 5.3 A, bottom right**). As shown in Figure 5.3 B, survival in saline and sH1N1 young mice and among all aged animals were severely compromised with one immunization. We observed that most of the young mice (with the exception of the saline group) survived after receiving two immunizations (**Figure 5.3 B, bottom left**). Survival among aged mice given sH1N1 combined with MF59-like, SE and GLA-SE adjuvants was significantly improved with two immunizations (**Figure 5.3 B, bottom right**). Our data suggest that increasing the number of immunizations in aged mice from one to two immunizations could considerably improve clinical outcomes following the early stages of influenza infection. Similar to responses in young and aged mice immunized with adjuvanted sH1N1 vaccines, enhanced survival was observed in both young and aged C57BL/6 mice given

two immunizations with adjuvanted rH1 vaccines (**Figure 5.1 D**). This is particularly interesting based on the low HAI titers observed in aged mice following a boost immunization. The enhanced clinical outcome in aged mice with adjuvanted rH1 vaccine in the absence of HAI titers suggest that a compensatory immune response is contributing to the protective responses seen in aged mice.

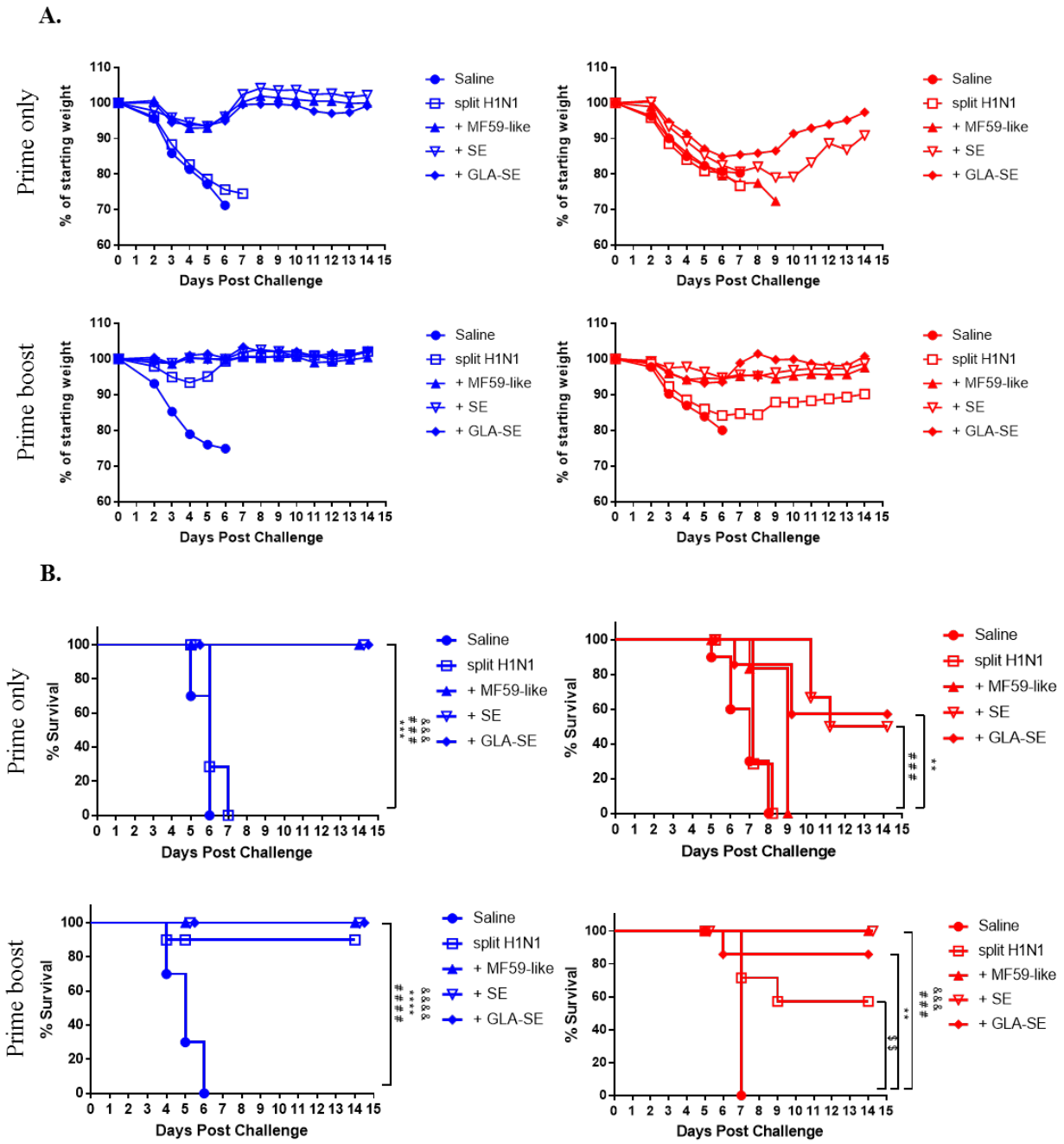

Figure 5.3 Enhanced body weight and survival in young and aged CB6F1 mice with adjuvanted sH1N1 vaccines after boost immunization. Following immunization with adjuvanted and unadjuvanted sH1N1 vaccines (as shown in Figure 5.2A) and challenge with 100 LD_{50} A/H1N1/California/4/2009, **(A)** the body weight and **(B)** survival were monitored every day over the course of 14 days. Young mice were color-coded as blue; aged mice were color-coded as red. *p* values are denoted as follows: ** indicates <0.01; *** indicates < 0.001; **** indicates < 0.0001. $ compares *p* value between saline vs. sH1N1 groups; & compares *p* value between saline vs. MF59-like groups; # compares *p* value between saline vs. SE groups; * compares *p* value between saline vs. GLA-SE groups.

The GLA-SE-based sH1N1 vaccine promotes the generation of cytokine-producing T helper cells, long-lived bone marrow plasma cells and GC B cells in young mice

We next examined the cellular components that may contribute to protective immune responses in young and aged CB6F1 mice. Young and aged mice were immunized twice with adjuvanted sH1N1 vaccines using a slightly modified strategy, denoted in Figure 5.4 A. The immunogenicity of T cell recall responses and germinal center (GC) B cell responses were determined seven days following a boost immunization. Splenocytes from young and aged mice with two immunizations were stimulated with rH1 protein, and cytokine production from antigen-specific $CD4^+$ T cells were determined. We found that young mice that received both MF59-like or GLA-SE adjuvanted vaccines generated antigen-specific $CD4^+$ T cells that produce TNF-α, IL-2 and express CD154. However, only young mice given GLA-SE-adjuvanted vaccine induced IFN-γ-producing $CD4^+$ T cells. From aged mice, we detected a minimal percentage of antigen-specific $CD4^+$ T cells with increased non-specific CD154 levels (representing activated T cells), however some mice were able to produce IL-2 (**Figure 5.4 B**). None of the aged mice induced TNF-α or IFN-γ-producing antigen-specific $CD4^+$ T cells following immunization. These data are consistent with our observation in Figure 5.2 A, where aged mice failed to generate Th1-biased IgG2 antibody responses. Also, similar to previous observations (151), we found that aged mice have an increased percentage of non-specific follicular helper T cells (Tfh, $CD4^+CXCR5^+PD\text{-}1^+$) as compared to young mice (**Figure 5.4 C**). It has been shown that the quality and quantity of neutralizing antibodies is crucial for protective immune responses against viral infection (152). Thus, we examined the induction of GC B cells from spleen and inguinal LNs and long-lived bone marrow plasma cells (BMPCs) in both young and aged mice (**Figure 5.4 D, E**). Interestingly, as shown in Figure 5.4 D, within the spleen, young mice receiving two immunizations with sH1N1 alone had the highest number of GC B cells, whereas aged mice

receiving sH1N1 combined with MF59-like adjuvant and GLA-SE had the highest number of GC B cells (although none of these responses reached statistical significance). The number of $B220^{+}CD95^{+}GL7^{+}$ GC B cells in the inguinal LN from young mice were enhanced after a boost immunization with all of the adjuvanted sH1N1 vaccines tested, although significant responses were observed only with sH1N1+SE (**Figure 5.4 D**). In aged mice, the MF59-like adjuvant induced the highest number of GC B cells in the LN (**Figure 5.4 D**). We also found that young mice that received MF59-like or GLA-SE adjuvanted sH1N1 vaccines generated a significant number of antigen-specific BMPCs (**Figure 5.4 E**). Aged mice that received MF59-like and GLA-SE adjuvanted vaccines showed a similar trend to that seen in young mice, although the responses were not statistically significant (**Figure 5.4 E**).

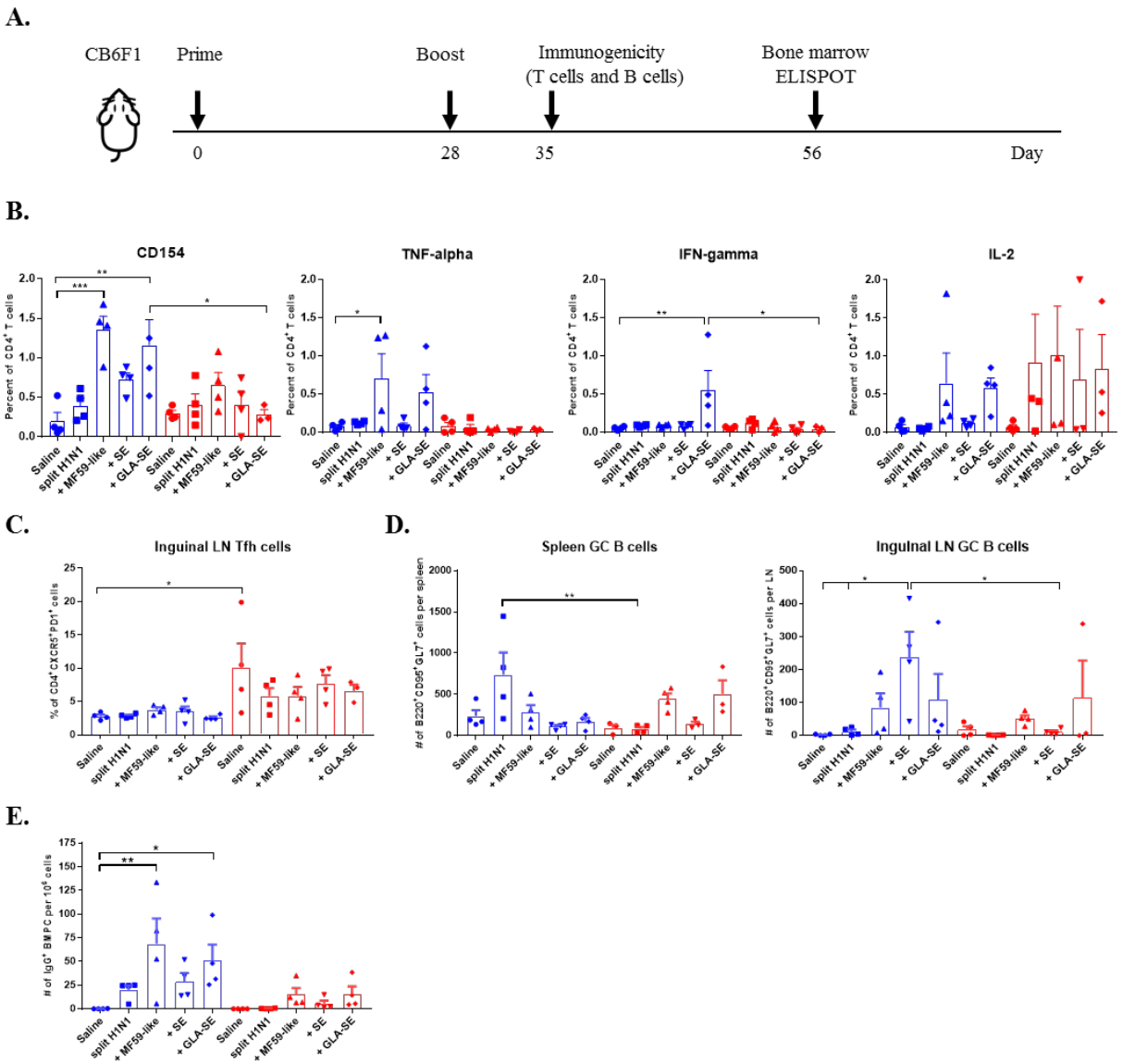

Figure 5.4 MF59-like and GLA-SE-based sH1N1 vaccine promotes the generation of cytokine-producing T helper cells, GC B cells and long-lived bone marrow plasma cells in young CB6F1 mice. (A) Scheme of slightly modified immunization procedure: CB6F1 mice were immunized i.m. twice, four weeks apart and **(B)** the immunogenicity of splenic cytokine-producing $CD4^+$ T cells, **(C)** the percentage of $CD4^+CXCR5^+PD\text{-}1^+$ Tfh cells in inguinal LNs, and **(D)** the number of $B220^+CD95^+GL7^+$ GC B cells in spleen and in inguinal LNs were determined one week after the boost immunization with adjuvanted or unadjuvanted sH1N1 vaccines as indicated **(E)** The number of H1-specific BMPCs were determined four weeks after a boost immunization. Data from young mice were color-coded as blue; Data from aged mice were color-coded as red. * indicates *p* value <0.05; ** indicates *p* value <0.01. Error bars indicate mean ± SEM. GC, germinal center; LN, lymph node; Tfh, follicular T helper cells; BMPC, bone marrow plasma cells. Statistical analysis was performed using one-way ANOVA and Tukey's multiple comparison test except 3E, which used one-way ANOVA and Bonferroni's test.

In vitro adjuvant stimulation of BMDCs and lung cells from aged mice exhibit impaired cytokine-producing ability compared to responses from young mice

Studies have shown that immune responses are reduced in aged animals due to decreased numbers of APCs and stromal cells (153), increased threshold required for TLR signaling (154), reduced B cell repertoire and humoral responses (136), and a phenomenon where immune organs eventually fill with fat or connective tissues (155). Following our observation that the induction of immune responses to sH1N1 vaccines were impaired in aged mice as compared to young mice, we next tested how adjuvants may affect early innate immune responses from both young and aged mice, characterized by *in vitro* cytokine production from BMDCs and lung homogenates. BMDCs, phenotypically and functionally similar to conventional DCs (156), are the surrogate to induction of systemic adaptive immune responses, whereas stimulated lung homogenates illustrate local immune responses. We tested BMDCs and lung homogenates from both young and aged CB6F1 mice in response to various doses of SE and GLA-SE, and found that although BMDCs from aged mice are capable of producing innate inflammatory cytokines upon GLA-SE stimulation, aged cells produced significantly less cytokines compared to those from young animals (**Figure 5.5 A**). Strikingly, we could scarcely detect inflammatory cytokines in the cell supernatants from GLA-SE-stimulated aged lung homogenates, especially for IL-12p40 and IFN-γ (**Figure 5.5 B**). Our data suggest that although immunosenescence in aged mice affects innate immune responses both systemically (BMDCs) and locally (lung homogenates), the specific impairment of local immune responses in aged mice could lead to unfavorable and inefficient pathogen clearance at early stages following infection.

A. BMDCs

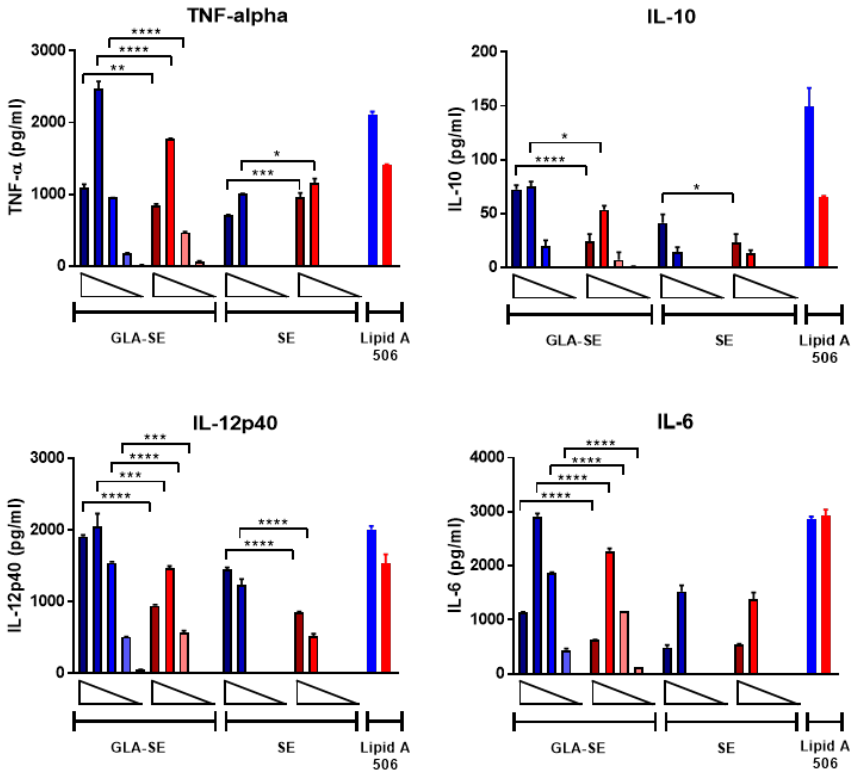

B. Lung homogenates

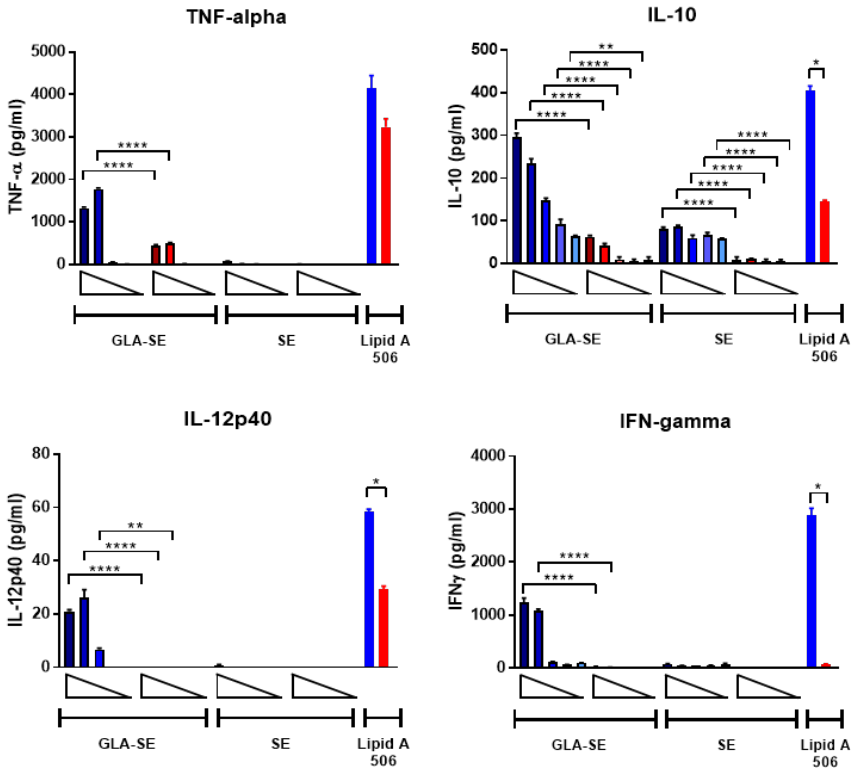

Figure 5.5 BMDCs from aged mice produce lower levels of cytokine upon GLA-SE stimulation and lung homogenates from aged mice have severely impaired cytokine-producing ability. (A) BMDCs and **(B)** lung homogenates from young and aged CB6F1 mice were stimulated with 10-fold dilutions of GLA-SE (2 ng/ml, 20 ng/ml, 200 ng/ml, 2 μg/ml and 20 μg/ml) or SE (0.00008%, 0.0008%, 0.008%, 0.08% and 0.8%) overnight, followed by harvesting the supernatants the next day for cytokine analysis. Open triangles indicate the concentration from highest (left) to the lowest (right). 10 ng/ml Lipid A 506 was used as positive control. Cells from young mice were color-coded as blue; cells from aged mice were color-coded as red. Results are represented as the mean ± SEM. *p* values are denoted as follows: * indicates <0.05; ** indicates <0.01; *** indicates < 0.001; **** indicates < 0.0001. BMDC, bone marrow-derived dendritic cells.

GLA-SE adjuvanted sH1N1 vaccine decreases viral load and prevents prolonged lung inflammation in young CB6F1 mice

Since we observed significant weight change and decrease in survival by day 5 after viral challenge in young and aged mice given either saline or sH1N1 vaccine alone (**Figure 5.3**), we hypothesized that mice immunized with adjuvanted vaccines would be able to control local inflammation in the lung during the early infection phase, preventing subsequent mortality. In order to address this hypothesis, young CB6F1 mice were immunized once with saline, sH1N1, sH1N1+SE or sH1N1+GLA-SE were then challenged with 100 LD_{50} A/H1N1/California/4/2009. Following challenge, viral loads were determined at days 3 or 6 post challenge. Young CB6F1 mice that received GLA-SE adjuvant generated the highest functional neutralizing antibody titers following one immunization as compared to other groups (**Figure 5.6 A**). Consistent with our previous data (**Figure 5.2 C**), mice that received saline or a prime immunization with the sH1N1 vaccine did not generate significant neutralizing antibodies (**Figure 5.6 A**); in addition, we found that the viral loads were 1000-fold higher in saline and sH1N1 groups compared to responses in the sH1N1+GLA-SE group at days 3 and 6 following influenza infection (**Figure 5.6 B**). Interestingly, the sH1N1+SE group had 100-fold higher viral load than the sH1N1+GLA-SE group at day 3, but no differences in virus titer were observed at day 6, suggesting that sH1N1 adjuvanted with GLA-SE is superior to sH1N1 adjuvanted with SE, and animals immunized with sH1N1+GLA-SE were able to clear viral infection earlier after influenza challenge (**Figure 5.6 B**).

Next, we examined the inflammatory cytokines and chemokines in bronchoalveolar lavage fluid (BALF) from young mice at day 3 or 6 after viral challenge. To our surprise, we could not detect any inflammatory cytokines in BALF from mice that received either SE or

GLA-SE adjuvants (**Figure 5.6 C**). IL-6, TNF-α, IFN-γ and IL-12p40 were detected in the BALF from saline and sH1N1 groups at day 3 and 6, indicating that a continuous inflammatory response occurs in the lungs of these mice. Notably, Th2-biased cytokine IL-4, IL-5, and chemokine Eotaxin (data not shown) in the BALF were detected at day 6 from mice that received the sH1N1 vaccine alone. These data corroborate our previous reports that immunization with protein only, or without proper Th1-driving adjuvants, leads to Th2-biased immune responses (157). It has also been reported that alveolar macrophages (AMs) are crucial for lung homeostasis and are the first line cells capable of detecting lung pathogens including bacteria, viruses, in addition to allergens and foreign particles (158). Thus, we examined whether AMs from young mice given a prime immunization were affected after exposure to A/H1N1/California/4/2009 challenge. Interestingly, we found that unvaccinated, young CB6F1 mice (saline group) had dramatically decreased percentages of AMs at day 3 of infection as compared to the other groups. At day 6, both saline and sH1N1 groups had a significantly decreased percentage of AMs as compared to adjuvanted groups, suggesting that AMs are potentially being eliminated by the viral infection (159) (**Figure 5.6 D**). Similarly, a reduction in the percentage of AMs following influenza infection correlate with an increased viral load within the lung. As shown in Figure 5.7, we found that in young mice given one immunization, only mice that received the sH1N1+GLA-SE vaccine maintain AM homeostasis and prevent inflammatory cell infiltration (including eosinophils, neutrophils, inflammatory Mϕs and NK cells) in the lung at both day 3 and 6 post infection. After influenza infection, cells such as AMs that express TLR7 are able to detect single-strand RNA fragments released from viral particles. We found that expression of TLR7 on AMs were relatively consistent among all groups at day 3, however, the TLR7 levels were significantly decreased in saline, sH1N1 and sH1N1+SE groups

by day 6 as compared to sH1N1+GLA-SE group (**Figure 5.6 E**). Overall, our data suggests that the GLA-SE adjuvanted sH1N1 vaccine provides superior protection in young mice by clearing influenza virus early after infection, and through maintenance of AMs and TLR7 expression levels in the early infection phase.

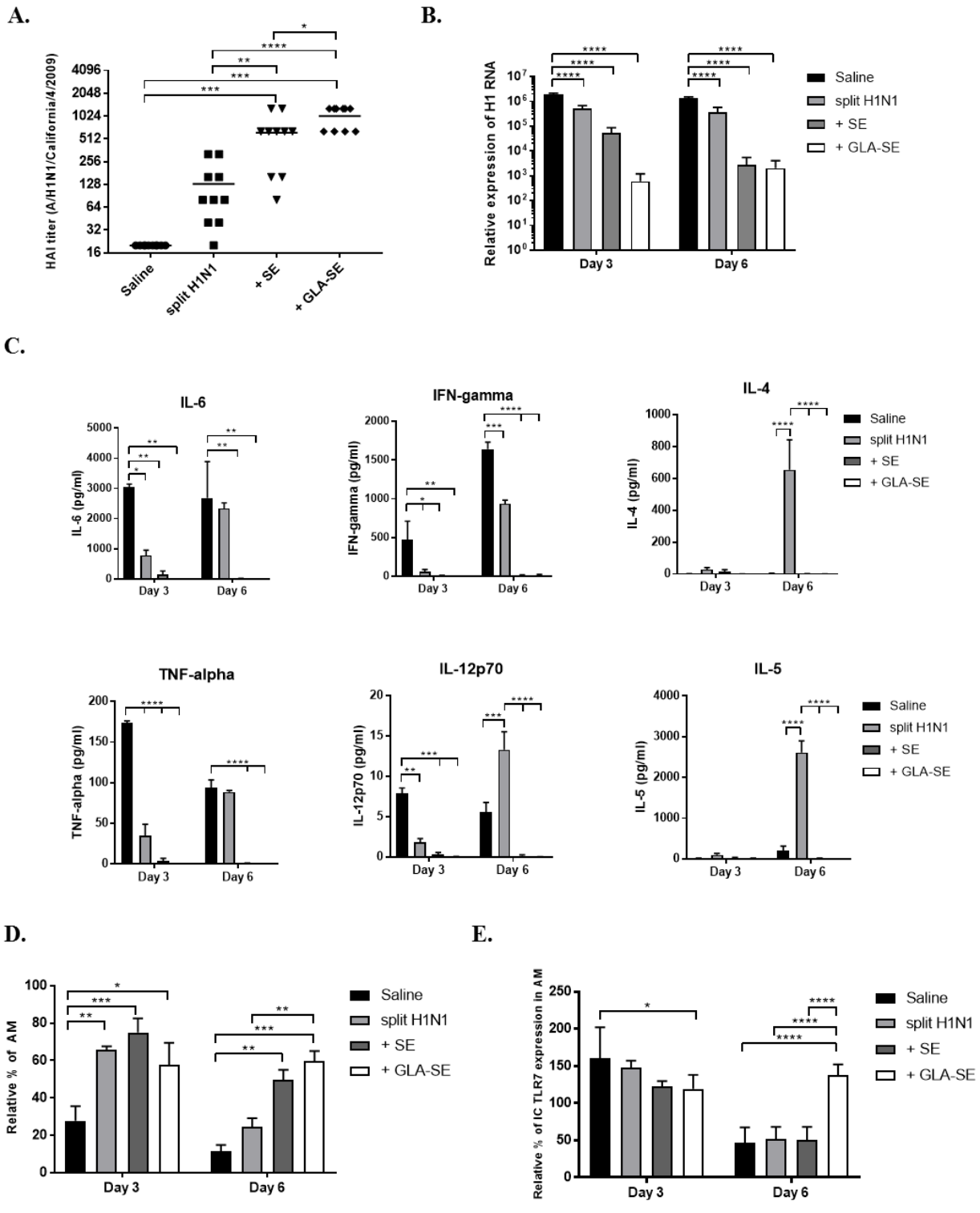

Figure 5.6 GLA-SE adjuvanted sH1N1 decreases viral load and prevents prolonged lung inflammation in young CB6F1 mice. Young CB6F1 mice (age of 6-8 week old) were

immunized once with saline, sH1N1, sH1N1+SE, or sH1N1+GLA-SE, and sera were harvested three weeks after prime. All mice were challenged with $100LD_{50}$ A/H1N1/California/4/2009 at day 28 and BALF and lung homogenates were harvested at day 3 and day 6 post infection. **(A)** HAI titer against A/H1N1/California/4/2009 was determined. **(B)** The relative expression of H1 was determined by real time Q-PCR. The expression of H1 of each sample was normalized to GAPDH (graph is on log10 scale). **(C)** BALF from all infected mice were harvested at day 3 and day 6 post infection, and the levels of IL-6, IFN-γ TNF-α, IL-12p70, IL-4 and IL-5 cytokines were determined by Luminex. **(D)** The percentage of AMs was determined by flow cytometry, and were normalized to uninfected, naïve mice (as 100%). AMs in the lung homogenates were defined as $CD11b^{-}CD11c^{+}Siglec\text{-}F^{+}NK1.1^{-}$ population. **(E)** The intracellular expression of TLR7 by AMs was determined by flow cytometry, and was normalized to uninfected, naïve mice (as 100%). *p* values are denoted as follows: * indicates <0.05; ** indicates <0.01; *** indicates < 0.001; **** indicates < 0.0001. Results are represented as the mean ± SEM. BALF, bronchoalveolar lavage fluid; AM, alveolar macrophages.

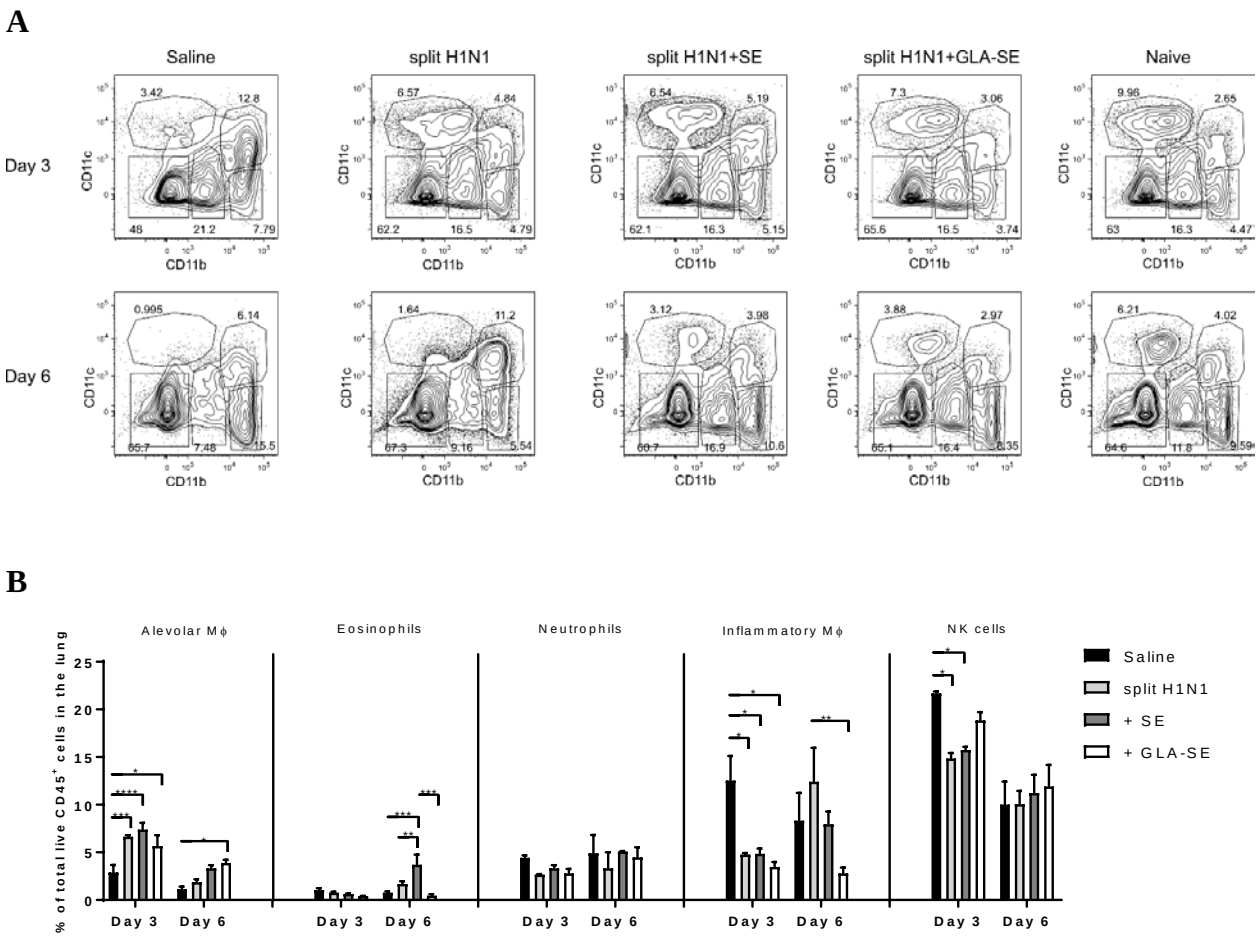

Figure 5.7 Split H1N1 vaccine adjuvanted with GLA-SE maintains AM homeostasis and prevents inflammatory cell infiltration in the lung during the early infection phase. (A) Phenotypic analysis of cell populations in the lungs from young CB6F1 mice. Representative flow plots of cell populations in the lungs of naïve mice (no infection), control mice (saline), or immunized mice at day 3 and day 6 post H1N1 infection. Mice were immunized once with sH1N1, sH1N1+SE, sH1N1+GLA-SE, or were injected with saline, and were challenged 3 weeks later with $100LD_{50}$ A/H1N1/California/4/2009. Cells are pre-gated on singlet, live and $CD45^+$ populations. Alveolar macrophages (Mf) are defined as $CD11b^{lo/-}CD11c^+Siglec\text{-}F^+$ cells; inflammatory Mf are defined as $CD11b^{hi}CD11c^+Siglec\text{-}F^-$ cells; granulocytes including eosinophils and neutrophils are defined as $CD11b^{hi}CD11c^-Siglec\text{-}F^+Ly6G^{mid}$ and $CD11b^{hi}CD11c^-Siglec\text{-}F^-Ly6G^+$, respectively; NK cells are defined as $CD11b^{mid}CD11c^-NK1.1^+$. **(B)** Cellular percentages of alveolar Mf, eosinophils, neutrophils, inflammatory Mf and NK cells in total live $CD45^+$ cells in the lung. Results are represented as the mean ± SEM (n=4 per group). *p* values are denoted as follows: * indicates <0.05; ** indicates <0.01; *** indicates < 0.001; **** indicates < 0.0001.

Discussion

In this study, the influence of different adjuvants on the efficacy of two types of seasonal influenza vaccine: a rH1 protein vaccine, and a sH1N1 vaccine was evaluated. Adjuvants examined include two squalene-based oil-in-water emulsions [a MF59-like adjuvant and SE (a stable emulsion adjuvant)] and a synthetic TLR4 agonist formulated with SE (GLA-SE). In CB6F1 mice, we showed that both the MF59-like adjuvant and GLA-SE plus sH1N1 vaccine contribute to Th1-biased vaccine-specific IgG2 immune responses following a boost immunization, whereas significantly higher IgG2c titers were not induced in aged mice. HAI titers were, however, induced in both young and aged CB6F1 mice after two immunizations. In contrast, in C57BL/6 mice, we observed an increase in vaccine-specific IgG1 and IgG2c responses following a boost immunization with all of the adjuvanted rH1 vaccines tested. However, whereas HAI titers were above the 1:40 threshold with adjuvanted rH1 vaccines in young C57BL/6 mice [HAI titers above a titer of ≥1:40 in humans is associated with a 50% reduction in seasonal influenza infection, and is considered a correlate of protection (52, 160)], HAI titers were not increased in aged mice. Following a boost immunization, aged C57BL/6 and CB6F1 mice induced significant levels of either vaccine-specific IgG2c or HAI titers, respectively, leading to protection against influenza challenge. This observation is of interest as cellular immunity is known to decline with age and compensatory mechanisms induced by adjuvants may aid protection in the elderly. Recently, the induction of IgG2 antibodies have been a focus of interest for protection against infection, including influenza infection. An M2e-specific IgG2c monoclonal antibody was reported to protect mice against influenza infection more effectively than an IgG1 monoclonal due to Fc activation properties (161).

The use of adjuvants as a strategy for enhancing the quality and magnitude of protective antibody responses to influenza vaccines is not a new concept. We have shown previously that the addition of adjuvants such as GLA-SE are able to increase dose-sparing properties and broaden HAI titers against drifted influenza viruses (141). In this manner, applying the GLA-SE adjuvant to influenza vaccine design addresses a noted and significant complication of reduced vaccine-specific antibody responses observed in aged individuals (138). GLA-SE combined with a recombinant H5N1 avian influenza vaccine (rH5)also increases the breadth of the antibody responses and provides protection against a heterosubtypic influenza virus, compared to the vaccine combined with SE (143).

One of the benefits of using GLA-SE as a vaccine adjuvant is the Th1-inducing innate responses that promote protective adaptive Th1-mediated cellular and humoral immunity (141, 157, 162). Characterization of this pure synthetic TLR4 agonist adjuvant in comparison to another TLR4 agonist, monophosphoryl lipid A (MPL) which is derived naturally from the bacterium *Salmonella minnesota*, has been shown following stimulation of DCs from both humans and mice (163). Both agonists were shown to increase DC activation and maturation, and induce proinflammatory cytokines and chemokines (141). In elderly humans, the responses of monocyte-derived DCs stimulated with GLA-SE appear intact (145). Here, we add to this paradigm and demonstrate that BMDCs derived from aged mice respond to GLA-SE stimulation, however cytokine responses are lower than observed following GLA-SE stimulation of young BMDCs.

PBMCs from elderly patients stimulated with GLA-SE and split virus vaccine (SVV) have also been shown to increase the ratio of IFN-γ:IL-10, in addition to granzyme B, further supporting this as a potentially effective candidate adjuvant for use in the elderly (148). In our

study, MF59-like adjuvant was also capable of promoting vaccine-specific $CD4^+$ T cell responses, GC B cells, and induction of long-lived BMPCs, and like the SE adjuvant, was able to induce HAI titers after a boost immunization leading to protection in mice against challenge with H1N1. The history, safety, and efficacy of the MF59 adjuvant has been recently reviewed (146, 164).

One of the most striking observations in our study was the differential cytokine responses to adjuvant in aged versus young lung homogenates. The *in vitro* stimulatory response of GLA-SE on lung homogenates from young mice led to the induction of TNF-α, IL-12p40, IFN-γ, and IL-10, whereas only TNF-α and IL-10 were induced in samples from aged mice. This potential local impairment (within the lung) could have substantial consequences following acute infection with influenza virus and other pulmonary infections.

In order to determine the protective mechanism of action of sH1N1 adjuvanted with GLA-SE within the lungs of young mice, we further characterized the pulmonary responses following H1N1 infection, including assessment of viral load and inflammatory responses. We observed less virus in the lung at day 3 post challenge, in mice immunized once with sH1N1 combined with GLA-SE, and decreased levels of virus at day 6 post challenge in mice immunized with SE compared to saline or sH1N1 vaccine only. The magnitude of the neutralizing HAI titer was also highest in mice given the sH1N1+GLA-SE. Furthermore, a drastic reduction in the inflammatory responses within the lungs of mice immunized with the sH1N1+GLA-SE was observed, compared to the Th2-biased inflammatory responses that were seen in the sH1N1 vaccine alone group. At day 6 of infection, the percentage of AMs was also significantly higher in the sH1N1+GLA-SE group compared to both saline and sH1N1 immunized mice. Interestingly, TLR7 expression within AMs was also significantly higher in the

sH1N1+GLA-SE treated mice compared to mice that were immunized with sH1N1 vaccine only and sH1N1+SE Recently, Wong et al. reported that AMs from aged mice have an intrinsically impaired function to limit lung damage during influenza viral lung infection, and suggested that enhancing the function of AMs may improve outcomes in elderly individuals infected with respiratory viruses (159). It will be of great interest to determine if administration of Th1-inducing vaccines in aged animals can preserve the numbers and functions of AMs during acute phases of infection, and how this might reduce the morbidity and mortality in aged individuals. This significant hypothesis warrants further exploration. We have previously shown, in both mice and non-human primates, that Fluzone® (a trivalent inactivated influenza vaccine) adjuvanted with GLA-SE, increases the magnitude of HAI titers, induces Th1 cellular immune responses, and enhances cross-reactive antibody responses to drifted influenza strains (141). Our current work further addresses additional attributes of GLA-SE-adjuvanted influenza vaccines in the context of increased age.

Finally, the CDC estimates that during the 2015-2016 influenza season the elderly (making up only 15% of the overall US population) accounted for half or more of hospitalizations associated with influenza and 64% of deaths associated with pneumonia and influenza (37). Our data suggests that the staggering burden of morbidity and mortality due to influenza infection in the elderly population may be alleviated by further detailed and mechanistic selection of proper adjuvants to be included in seasonal vaccines.

Chapter 6: Concluding Remarks and Future Directions

Preexisting immunity to influenza has long been known to impact subsequent responses either detrimentally or constructively. However, the way in which different immunological memory components influence responses in humans, despite intense interest, is difficult to isolate and elucidate due to long exposure histories. Therefore, we established and characterized mouse models of preexisting immunity with two vastly different immune outcomes in Chapter 2. We then used depletion and transfer techniques to determine how preexisting immunity, cellular and humoral, to influenza broadly augments responses to drifted influenza virus in Chapter 3. We demonstrated that cross-reactive memory HA-specific $CD4^+$ T cells are crucial to accelerating responses to intra-subtype virus and must be primarily elicited by infection or adjuvanted immunization. Without cognate memory $CD4^+$ T cells, B cell reactivity does not adapt to become specific for the drifted influenza, displaying an OAS phenotype. Importantly, in Chapter 4 we demonstrate with our model that this negative outcome can be reversed by engaging preexisting cognate T cell help, a possible strategy for future vaccine design. This finding, in conjunction with previous literature, suggests that in addition to HA undergoing antigenic drift to evade antibodies, that MHC Class II reactivity may also be drifting and thus detrimentally altering subsequent responses. Further it suggests that initial exposure to influenza is formative in eliciting a memory T cell reactive bank that if utilized in subsequent responses can drive protection.

This knowledge could be applied to update preexisting immunity to be more potent against differing strains or alternatively, employed to prevent adaptation of memory B cells, retaining broader responses, a goal of many universal vaccine candidates. Indeed, application of

this knowledge is currently being pursued primarily by including adjuvants in avian influenza vaccine candidates to strongly elicit $CD4^+$ T cell reactivity (165). Additionally, new influenza vaccine candidates are endeavoring to engineer in universal T cell epitopes into Avian H7 HA (166-168). Undeniably, these techniques of T cell inclusion are challenging, as HA folding is sensitive to modification and structural integrity must be maintained to provide adequate B cell stimulation. Furthermore, in humans with many different MHC Class II haplotypes, finding a suitable T cell epitope poses further challenges (169). Theoretically, if inclusion of a universal T cell epitope did not interfere with the integrity of HA, this could be used with adjuvant prior to any influenza exposure to elicit a foundational responses. These foundational responses could then be exploited to boost out any subsequent responses that contained the universal T cell epitope, eliciting a more robust and specific response toward the antigen of interest. Further work will be required to identify how memory $CD4^+$ T cells and in particular, Tfh cells, are elicited and maintained in non-naïve and naive individuals to improve human vaccination strategies. Some remaining questions include: What TLR pathway is best to target for Tfh induction (170, 171)? Despite accumulation of Tfh cells in immunosenescent mice, as shown in Chapter 5, how do they change over time resulting in a more regulatory phenotype and does this happen in humans(172)? Does adjuvant inclusion result in durable Tfh or transient responses?

This dissertation work yielded valuable new insights into the specific players in the preexisting immune repertoire that contribute to the OAS phenotype and conversely, in enhancement of responses to subsequent drifted influenza exposure. Further comprehensive investigation of these immune contributors have the potential to significantly contribute to novel influenza vaccine design with the intention of promoting increased protection to drifted influenza.

REFERENCES

1. Taubenberger JK, Kash JC. Influenza virus evolution, host adaptation, and pandemic formation. Cell Host Microbe. 2010;7(6):440-51.
2. Palese P. Influenza: old and new threats. Nat Med. 2004;10(12 Suppl):S82-7.
3. Air GM. Sequence relationships among the hemagglutinin genes of 12 subtypes of influenza A virus. Proc Natl Acad Sci U S A. 1981;78(12):7639-43.
4. Ito T, Couceiro JN, Kelm S, Baum LG, Krauss S, Castrucci MR, et al. Molecular basis for the generation in pigs of influenza A viruses with pandemic potential. J Virol. 1998;72(9):7367-73.
5. Matrosovich M, Tuzikov A, Bovin N, Gambaryan A, Klimov A, Castrucci MR, et al. Early alterations of the receptor-binding properties of H1, H2, and H3 avian influenza virus hemagglutinins after their introduction into mammals. J Virol. 2000;74(18):8502-12.
6. Cauldwell AV, Long JS, Moncorgé O, Barclay WS. Viral determinants of influenza A virus host range. J Gen Virol. 2014;95(Pt 6):1193-210.
7. Palese P, Wang TT. Why do influenza virus subtypes die out? A hypothesis. MBio. 2011;2(5).
8. Thompson WW, Weintraub E, Dhankhar P, Cheng PY, Brammer L, Meltzer MI, et al. Estimates of US influenza-associated deaths made using four different methods. Influenza Other Respir Viruses. 2009;3(1):37-49.
9. Clem A, Galwankar S. Seasonal influenza: waiting for the next pandemic. J Glob Infect Dis. 2009;1(1):51-6.
10. Lowen AC, Mubareka S, Steel J, Palese P. Influenza virus transmission is dependent on relative humidity and temperature. PLoS Pathog. 2007;3(10):1470-6.
11. Shaman J, Kohn M. Absolute humidity modulates influenza survival, transmission, and seasonality. Proc Natl Acad Sci U S A. 2009;106(9):3243-8.
12. Carrat F, Flahault A. Influenza vaccine: the challenge of antigenic drift. Vaccine. 2007;25(39-40):6852-62.
13. Dormitzer PR, Galli G, Castellino F, Golding H, Khurana S, Del Giudice G, et al. Influenza vaccine immunology. Immunol Rev. 2011;239(1):167-77.
14. Houser K, Subbarao K. Influenza vaccines: challenges and solutions. Cell Host Microbe. 2015;17(3):295-300.
15. Boni MF. Vaccination and antigenic drift in influenza. Vaccine. 2008;26 Suppl 3:C8-14.
16. Sanjuán R, Nebot MR, Chirico N, Mansky LM, Belshaw R. Viral mutation rates. J Virol. 2010;84(19):9733-48.
17. Hay AJ, Gregory V, Douglas AR, Lin YP. The evolution of human influenza viruses. Philos Trans R Soc Lond B Biol Sci. 2001;356(1416):1861-70.
18. Trifonov V, Khiabanian H, Rabadan R. Geographic dependence, surveillance, and origins of the 2009 influenza A (H1N1) virus. N Engl J Med. 2009;361(2):115-9.
19. Antigenic shift and drift. Nature. 1980;283(5747):524-5.
20. Bouvier NM, Palese P. The biology of influenza viruses. Vaccine. 2008;26 Suppl 4:D49-53.

21. Bautista E, Chotpitayasunondh T, Gao Z, Harper SA, Shaw M, Uyeki TM, et al. Clinical aspects of pandemic 2009 influenza A (H1N1) virus infection. N Engl J Med. 2010;362(18):1708-19.
22. Brydon EW, Morris SJ, Sweet C. Role of apoptosis and cytokines in influenza virus morbidity. FEMS Microbiol Rev. 2005;29(4):837-50.
23. Gao R, Bhatnagar J, Blau DM, Greer P, Rollin DC, Denison AM, et al. Cytokine and chemokine profiles in lung tissues from fatal cases of 2009 pandemic influenza A (H1N1): role of the host immune response in pathogenesis. Am J Pathol. 2013;183(4):1258-68.
24. Lee N, Wong CK, Chan PK, Chan MC, Wong RY, Lun SW, et al. Cytokine response patterns in severe pandemic 2009 H1N1 and seasonal influenza among hospitalized adults. PLoS One. 2011;6(10):e26050.
25. Osterholm MT, Kelley NS, Sommer A, Belongia EA. Efficacy and effectiveness of influenza vaccines: a systematic review and meta-analysis. Lancet Infect Dis. 2012;12(1):36-44.
26. Arriola C, Garg S, Anderson EJ, Ryan PA, George A, Zansky SM, et al. Influenza Vaccination Modifies Disease Severity Among Community-dwelling Adults Hospitalized With Influenza. Clin Infect Dis. 2017;65(8):1289-97.
27. Victora GD, Wilson PC. Germinal center selection and the antibody response to influenza. Cell. 2015;163(3):545-8.
28. Chiu C, Wrammert J, Li GM, McCausland M, Wilson PC, Ahmed R. Cross-reactive humoral responses to influenza and their implications for a universal vaccine. Ann N Y Acad Sci. 2013;1283:13-21.
29. Krammer F, Palese P, Steel J. Advances in universal influenza virus vaccine design and antibody mediated therapies based on conserved regions of the hemagglutinin. Curr Top Microbiol Immunol. 2015;386:301-21.
30. Krammer F, Palese P. Advances in the development of influenza virus vaccines. Nat Rev Drug Discov. 2015;14(3):167-82.
31. Nakaya HI, Wrammert J, Lee EK, Racioppi L, Marie-Kunze S, Haining WN, et al. Systems biology of vaccination for seasonal influenza in humans. Nat Immunol. 2011;12(8):786-95.
32. Wikramaratna PS, Rambaut A. Relationship between haemagglutination inhibition titre and immunity to influenza in ferrets. Vaccine. 2015;33(41):5380-5.
33. Jackson LA, Gaglani MJ, Keyserling HL, Balser J, Bouveret N, Fries L, et al. Safety, efficacy, and immunogenicity of an inactivated influenza vaccine in healthy adults: a randomized, placebo-controlled trial over two influenza seasons. BMC Infect Dis. 2010;10:71.
34. Jackson KJ, Liu Y, Roskin KM, Glanville J, Hoh RA, Seo K, et al. Human responses to influenza vaccination show seroconversion signatures and convergent antibody rearrangements. Cell Host Microbe. 2014;16(1):105-14.
35. Katz JM, Hancock K, Xu X. Serologic assays for influenza surveillance, diagnosis and vaccine evaluation. Expert Rev Anti Infect Ther. 2011;9(6):669-83.
36. Zost SJ, Parkhouse K, Gumina ME, Kim K, Diaz Perez S, Wilson PC, et al. Contemporary H3N2 influenza viruses have a glycosylation site that alters binding of antibodies elicited by egg-adapted vaccine strains. Proc Natl Acad Sci U S A. 2017;114(47):12578-83.
37. Wu NC, Zost SJ, Thompson AJ, Oyen D, Nycholat CM, McBride R, et al. A structural explanation for the low effectiveness of the seasonal influenza H3N2 vaccine. PLoS Pathog. 2017;13(10):e1006682.

38. Cobey S, Gouma S, Parkhouse K, Chambers BS, Ertl HC, Schmader KE, et al. Poor immunogenicity, not vaccine strain egg adaptation, may explain the low H3N2 influenza vaccine effectiveness in 2012-13. Clin Infect Dis. 2018.
39. Linderman SL, Chambers BS, Zost SJ, Parkhouse K, Li Y, Herrmann C, et al. Potential antigenic explanation for atypical H1N1 infections among middle-aged adults during the 2013-2014 influenza season. Proc Natl Acad Sci U S A. 2014;111(44):15798-803.
40. Cobey S, Hensley SE. Immune history and influenza virus susceptibility. Curr Opin Virol. 2017;22:105-11.
41. Hensley SE. Challenges of selecting seasonal influenza vaccine strains for humans with diverse pre-exposure histories. Curr Opin Virol. 2014;8:85-9.
42. Ellebedy AH, Ahmed R. Re-engaging cross-reactive memory B cells: the influenza puzzle. Front Immunol. 2012;3:53.
43. Domínguez A, Godoy P, Torner N. The Effectiveness of Influenza Vaccination in Different Groups. Expert Rev Vaccines. 2016;15(6):751-64.
44. Kucharski AJ, Lessler J, Read JM, Zhu H, Jiang CQ, Guan Y, et al. Estimating the life course of influenza A(H3N2) antibody responses from cross-sectional data. PLoS Biol. 2015;13(3):e1002082.
45. Webster RG. Original antigenic sin in ferrets: the response to sequential infections with influenza viruses. J Immunol. 1966;97(2):177-83.
46. JENSEN KE, DAVENPORT FM, HENNESSY AV, FRANCIS T. Characterization of influenza antibodies by serum absorption. J Exp Med. 1956;104(2):199-209.
47. Fazekas de St Groth, Webster RG. Disquisitions on Original Antigenic Sin. II. Proof in lower creatures. J Exp Med. 1966;124(3):347-61.
48. Lessler J, Riley S, Read JM, Wang S, Zhu H, Smith GJ, et al. Evidence for antigenic seniority in influenza A (H3N2) antibody responses in southern China. PLoS Pathog. 2012;8(7):e1002802.
49. Fonville JM, Wilks SH, James SL, Fox A, Ventresca M, Aban M, et al. Antibody landscapes after influenza virus infection or vaccination. Science. 2014;346(6212):996-1000.
50. Fonville JM, Fraaij PL, de Mutsert G, Wilks SH, van Beek R, Fouchier RA, et al. Antigenic Maps of Influenza A(H3N2) Produced With Human Antisera Obtained After Primary Infection. J Infect Dis. 2016;213(1):31-8.
51. Miller MS, Gardner TJ, Krammer F, Aguado LC, Tortorella D, Basler CF, et al. Neutralizing antibodies against previously encountered influenza virus strains increase over time: a longitudinal analysis. Sci Transl Med. 2013;5(198):198ra07.
52. Potter CW, Oxford JS. Determinants of immunity to influenza infection in man. Br Med Bull. 1979;35(1):69-75.
53. (CDC) CfDCaP. Serum cross-reactive antibody response to a novel influenza A (H1N1) virus after vaccination with seasonal influenza vaccine. MMWR Morb Mortal Wkly Rep. 2009;58(19):521-4.
54. Bournazos S, Ravetch JV. Fcγ receptor pathways during active and passive immunization. Immunol Rev. 2015;268(1):88-103.
55. Maamary J, Wang TT, Tan GS, Palese P, Ravetch JV. Increasing the breadth and potency of response to the seasonal influenza virus vaccine by immune complex immunization. Proc Natl Acad Sci U S A. 2017;114(38):10172-7.

56. DiLillo DJ, Tan GS, Palese P, Ravetch JV. Broadly neutralizing hemagglutinin stalk-specific antibodies require FcγR interactions for protection against influenza virus in vivo. Nat Med. 2014;20(2):143-51.
57. DiPiazza A, Richards KA, Knowlden ZA, Nayak JL, Sant AJ. The Role of CD4 T Cell Memory in Generating Protective Immunity to Novel and Potentially Pandemic Strains of Influenza. Front Immunol. 2016;7:10.
58. Huber VC, Lynch JM, Bucher DJ, Le J, Metzger DW. Fc receptor-mediated phagocytosis makes a significant contribution to clearance of influenza virus infections. J Immunol. 2001;166(12):7381-8.
59. Linderman SL, Hensley SE. Antibodies with 'Original Antigenic Sin' Properties Are Valuable Components of Secondary Immune Responses to Influenza Viruses. PLoS Pathog. 2016;12(8):e1005806.
60. DiLillo DJ, Palese P, Wilson PC, Ravetch JV. Broadly neutralizing anti-influenza antibodies require Fc receptor engagement for in vivo protection. J Clin Invest. 2016;126(2):605-10.
61. Andrews SF, Huang Y, Kaur K, Popova LI, Ho IY, Pauli NT, et al. Immune history profoundly affects broadly protective B cell responses to influenza. Sci Transl Med. 2015;7(316):316ra192.
62. Wrammert J, Smith K, Miller J, Langley WA, Kokko K, Larsen C, et al. Rapid cloning of high-affinity human monoclonal antibodies against influenza virus. Nature. 2008;453(7195):667-71.
63. Tan YC, Blum LK, Kongpachith S, Ju CH, Cai X, Lindstrom TM, et al. High-throughput sequencing of natively paired antibody chains provides evidence for original antigenic sin shaping the antibody response to influenza vaccination. Clin Immunol. 2014;151(1):55-65.
64. Schmidt AG, Do KT, McCarthy KR, Kepler TB, Liao HX, Moody MA, et al. Immunogenic Stimulus for Germline Precursors of Antibodies that Engage the Influenza Hemagglutinin Receptor-Binding Site. Cell Rep. 2015;13(12):2842-50.
65. Kurosaki T, Kometani K, Ise W. Memory B cells. Nat Rev Immunol. 2015;15(3):149-59.
66. Rothaeusler K, Baumgarth N. B-cell fate decisions following influenza virus infection. Eur J Immunol. 2010;40(2):366-77.
67. Kometani K, Nakagawa R, Shinnakasu R, Kaji T, Rybouchkin A, Moriyama S, et al. Repression of the transcription factor Bach2 contributes to predisposition of IgG1 memory B cells toward plasma cell differentiation. Immunity. 2013;39(1):136-47.
68. Aiba Y, Kometani K, Hamadate M, Moriyama S, Sakaue-Sawano A, Tomura M, et al. Preferential localization of IgG memory B cells adjacent to contracted germinal centers. Proc Natl Acad Sci U S A. 2010;107(27):12192-7.
69. Taylor JJ, Jenkins MK, Pape KA. Heterogeneity in the differentiation and function of memory B cells. Trends Immunol. 2012;33(12):590-7.
70. McHeyzer-Williams LJ, Milpied PJ, Okitsu SL, McHeyzer-Williams MG. Class-switched memory B cells remodel BCRs within secondary germinal centers. Nat Immunol. 2015;16(3):296-305.
71. Pape KA, Taylor JJ, Maul RW, Gearhart PJ, Jenkins MK. Different B cell populations mediate early and late memory during an endogenous immune response. Science. 2011;331(6021):1203-7.
72. Zens KD, Farber DL. Memory CD4 T cells in influenza. Curr Top Microbiol Immunol. 2015;386:399-421.

73. Hufford MM, Kim TS, Sun J, Braciale TJ. The effector T cell response to influenza infection. Curr Top Microbiol Immunol. 2015;386:423-55.
74. Swain SL, McKinstry KK, Strutt TM. Expanding roles for CD4^{+} T cells in immunity to viruses. Nat Rev Immunol. 2012;12(2):136-48.
75. De Silva NS, Klein U. Dynamics of B cells in germinal centres. Nat Rev Immunol. 2015;15(3):137-48.
76. Gitlin AD, Shulman Z, Nussenzweig MC. Clonal selection in the germinal centre by regulated proliferation and hypermutation. Nature. 2014;509(7502):637-40.
77. Alam S, Knowlden ZA, Sangster MY, Sant AJ. CD4 T cell help is limiting and selective during the primary B cell response to influenza virus infection. J Virol. 2014;88(1):314-24.
78. Nayak JL, Richards KA, Yang H, Treanor JJ, Sant AJ. Effect of influenza A(H5N1) vaccine prepandemic priming on CD4+ T-cell responses. J Infect Dis. 2015;211(9):1408-17.
79. Alam S, Sant AJ. Infection with seasonal influenza virus elicits CD4 T cells specific for genetically conserved epitopes that can be rapidly mobilized for protective immunity to pandemic H1N1 influenza virus. J Virol. 2011;85(24):13310-21.
80. Alam S, Chan C, Qiu X, Shannon I, White CL, Sant AJ, et al. Selective pre-priming of HA-specific CD4 T cells restores immunological reactivity to HA on heterosubtypic influenza infection. PLoS One. 2017;12(5):e0176407.
81. van der Most RG, Roman FP, Innis B, Hanon E, Vaughn DW, Gillard P, et al. Seeking help: B cells adapting to flu variability. Sci Transl Med. 2014;6(246):246ps8.
82. Nayak JL, Alam S, Sant AJ. Cutting edge: Heterosubtypic influenza infection antagonizes elicitation of immunological reactivity to hemagglutinin. J Immunol. 2013;191(3):1001-5.
83. Marshall NB, Swain SL. Cytotoxic CD4 T cells in antiviral immunity. J Biomed Biotechnol. 2011;2011:954602.
84. Powell TJ, Strutt T, Reome J, Hollenbaugh JA, Roberts AD, Woodland DL, et al. Priming with cold-adapted influenza A does not prevent infection but elicits long-lived protection against supralethal challenge with heterosubtypic virus. J Immunol. 2007;178(2):1030-8.
85. McKinstry KK, Strutt TM, Kuang Y, Brown DM, Sell S, Dutton RW, et al. Memory CD4+ T cells protect against influenza through multiple synergizing mechanisms. J Clin Invest. 2012;122(8):2847-56.
86. Brown DM, Dilzer AM, Meents DL, Swain SL. CD4 T cell-mediated protection from lethal influenza: perforin and antibody-mediated mechanisms give a one-two punch. J Immunol. 2006;177(5):2888-98.
87. Brown DM, Lee S, Garcia-Hernandez MeL, Swain SL. Multifunctional CD4 cells expressing gamma interferon and perforin mediate protection against lethal influenza virus infection. J Virol. 2012;86(12):6792-803.
88. Teijaro JR, Verhoeven D, Page CA, Turner D, Farber DL. Memory CD4 T cells direct protective responses to influenza virus in the lungs through helper-independent mechanisms. J Virol. 2010;84(18):9217-26.
89. Wilkinson TM, Li CK, Chui CS, Huang AK, Perkins M, Liebner JC, et al. Preexisting influenza-specific CD4+ T cells correlate with disease protection against influenza challenge in humans. Nat Med. 2012;18(2):274-80.

90. Tate MD, Deng YM, Jones JE, Anderson GP, Brooks AG, Reading PC. Neutrophils ameliorate lung injury and the development of severe disease during influenza infection. J Immunol. 2009;183(11):7441-50.
91. Tate MD, Pickett DL, van Rooijen N, Brooks AG, Reading PC. Critical role of airway macrophages in modulating disease severity during influenza virus infection of mice. J Virol. 2010;84(15):7569-80.
92. Waffarn EE, Baumgarth N. Protective B cell responses to flu--no fluke! J Immunol. 2011;186(7):3823-9.
93. Chang WL, Coro ES, Rau FC, Xiao Y, Erle DJ, Baumgarth N. Influenza virus infection causes global respiratory tract B cell response modulation via innate immune signals. J Immunol. 2007;178(3):1457-67.
94. Baumgarth N, Herman OC, Jager GC, Brown L, Herzenberg LA. Innate and acquired humoral immunities to influenza virus are mediated by distinct arms of the immune system. Proc Natl Acad Sci U S A. 1999;96(5):2250-5.
95. Nichol KL, Margolis KL, Wouremna J, von Sternberg T. Effectiveness of influenza vaccine in the elderly. Gerontology. 1996;42(5):274-9.
96. Aspinall R, Lang PO. Vaccine responsiveness in the elderly: best practice for the clinic. Expert Rev Vaccines. 2014;13(7):885-94.
97. Robertson CA, DiazGranados CA, Decker MD, Chit A, Mercer M, Greenberg DP. Fluzone® High-Dose Influenza Vaccine. Expert Rev Vaccines. 2016;15(12):1495-505.
98. Faenzi E, Zedda L, Bardelli M, Spensieri F, Borgogni E, Volpini G, et al. One dose of an MF59-adjuvanted pandemic A/H1N1 vaccine recruits pre-existing immune memory and induces the rapid rise of neutralizing antibodies. Vaccine. 2012;30(27):4086-94.
99. Higgins DA, Carlson JR, Van Nest G. MF59 adjuvant enhances the immunogenicity of influenza vaccine in both young and old mice. Vaccine. 1996;14(6):478-84.
100. Domnich A, Arata L, Amicizia D, Puig-Barberà J, Gasparini R, Panatto D. Effectiveness of MF59-adjuvanted seasonal influenza vaccine in the elderly: A systematic review and meta-analysis. Vaccine. 2017;35(4):513-20.
101. Kim JH, Skountzou I, Compans R, Jacob J. Original antigenic sin responses to influenza viruses. J Immunol. 2009;183(5):3294-301.
102. Kim JH, Davis WG, Sambhara S, Jacob J. Strategies to alleviate original antigenic sin responses to influenza viruses. Proc Natl Acad Sci U S A. 2012;109(34):13751-6.
103. Kim JH, Liepkalns J, Reber AJ, Lu X, Music N, Jacob J, et al. Prior infection with influenza virus but not vaccination leaves a long-term immunological imprint that intensifies the protective efficacy of antigenically drifted vaccine strains. Vaccine. 2016;34(4):495-502.
104. Hirst GK. THE QUANTITATIVE DETERMINATION OF INFLUENZA VIRUS AND ANTIBODIES BY MEANS OF RED CELL AGGLUTINATION. J Exp Med. 1942;75(1):49-64.
105. Kim JH, Reber AJ, Kumar A, Ramos P, Sica G, Music N, et al. Non-neutralizing antibodies induced by seasonal influenza vaccine prevent, not exacerbate A(H1N1)pdm09 disease. Sci Rep. 2016;6:37341.
106. La Gruta NL, Turner SJ. T cell mediated immunity to influenza: mechanisms of viral control. Trends Immunol. 2014;35(8):396-402.
107. Nüssing S, Sant S, Koutsakos M, Subbarao K, Nguyen THO, Kedzierska K. Innate and adaptive T cells in influenza disease. Front Med. 2018;12(1):34-47.

108. Olafsdottir TA, Lindqvist M, Nookaew I, Andersen P, Maertzdorf J, Persson J, et al. Comparative Systems Analyses Reveal Molecular Signatures of Clinically tested Vaccine Adjuvants. Sci Rep. 2016;6:39097.
109. Asahi Y, Yoshikawa T, Watanabe I, Iwasaki T, Hasegawa H, Sato Y, et al. Protection against influenza virus infection in polymeric Ig receptor knockout mice immunized intranasally with adjuvant-combined vaccines. J Immunol. 2002;168(6):2930-8.
110. Crowe SR, Miller SC, Brown DM, Adams PS, Dutton RW, Harmsen AG, et al. Uneven distribution of MHC class II epitopes within the influenza virus. Vaccine. 2006;24(4):457-67.
111. Takamura S. Persistence in Temporary Lung Niches: A Survival Strategy of Lung-Resident Memory CD8. Viral Immunol. 2017;30(6):438-50.
112. Crotty S. A brief history of T cell help to B cells. Nat Rev Immunol. 2015;15(3):185-9.
113. Dubois Cauwelaert N, Baldwin SL, Orr MT, Desbien AL, Gage E, Hofmeyer KA, et al. Antigen presentation by B cells guides programing of memory CD4. Eur J Immunol. 2016;46(12):2719-29.
114. Priyamvada L, Cho A, Onlamoon N, Zheng NY, Huang M, Kovalenkov Y, et al. B Cell Responses during Secondary Dengue Virus Infection Are Dominated by Highly Cross-Reactive, Memory-Derived Plasmablasts. J Virol. 2016;90(12):5574-85.
115. Weiskopf D, Sette A. T-cell immunity to infection with dengue virus in humans. Front Immunol. 2014;5:93.
116. Stamper CT, Wilson PC. What Are the Primary Limitations in B-Cell Affinity Maturation, and How Much Affinity Maturation Can We Drive with Vaccination? Is Affinity Maturation a Self-Defeating Process for Eliciting Broad Protection? Cold Spring Harb Perspect Biol. 2017.
117. Clarke SH, Huppi K, Ruezinsky D, Staudt L, Gerhard W, Weigert M. Inter- and intraclonal diversity in the antibody response to influenza hemagglutinin. J Exp Med. 1985;161(4):687-704.
118. McHeyzer-Williams MG, McLean MJ, Lalor PA, Nossal GJ. Antigen-driven B cell differentiation in vivo. J Exp Med. 1993;178(1):295-307.
119. Garside P, Ingulli E, Merica RR, Johnson JG, Noelle RJ, Jenkins MK. Visualization of specific B and T lymphocyte interactions in the lymph node. Science. 1998;281(5373):96-9.
120. Victora GD, Schwickert TA, Fooksman DR, Kamphorst AO, Meyer-Hermann M, Dustin ML, et al. Germinal center dynamics revealed by multiphoton microscopy with a photoactivatable fluorescent reporter. Cell. 2010;143(4):592-605.
121. Taylor JJ, Pape KA, Steach HR, Jenkins MK. Humoral immunity. Apoptosis and antigen affinity limit effector cell differentiation of a single naïve B cell. Science. 2015;347(6223):784-7.
122. Wang Y, Carter RH. CD19 regulates B cell maturation, proliferation, and positive selection in the FDC zone of murine splenic germinal centers. Immunity. 2005;22(6):749-61.
123. Meyer-Hermann ME, Maini PK, Iber D. An analysis of B cell selection mechanisms in germinal centers. Math Med Biol. 2006;23(3):255-77.
124. Krishnamurty AT, Thouvenel CD, Portugal S, Keitany GJ, Kim KS, Holder A, et al. Somatically Hypermutated Plasmodium-Specific IgM(+) Memory B Cells Are Rapid, Plastic, Early Responders upon Malaria Rechallenge. Immunity. 2016;45(2):402-14.
125. Hoffmann E, Krauss S, Perez D, Webby R, Webster RG. Eight-plasmid system for rapid generation of influenza virus vaccines. Vaccine. 2002;20(25-26):3165-70.
126. Lee CW. Reverse genetics of influenza virus. Methods Mol Biol. 2014;1161:37-50.

127. Pleschka S, Jaskunas R, Engelhardt OG, Zürcher T, Palese P, García-Sastre A. A plasmid-based reverse genetics system for influenza A virus. J Virol. 1996;70(6):4188-92.
128. Casares S, Brumeanu TD, Bot A, Bona CA. Protective immunity elicited by vaccination with DNA encoding for a B cell and a T cell epitope of the A/PR/8/34 influenza virus. Viral Immunol. 1997;10(3):129-36.
129. Frosch AE, Odumade OA, Taylor JJ, Ireland K, Ayodo G, Ondigo B, et al. Decrease in Numbers of Naive and Resting B Cells in HIV-Infected Kenyan Adults Leads to a Proportional Increase in Total and. J Immunol. 2017;198(12):4629-38.
130. Thompson WW, Shay DK, Weintraub E, Brammer L, Cox N, Anderson LJ, et al. Mortality associated with influenza and respiratory syncytial virus in the United States. JAMA. 2003;289(2):179-86.
131. Fry AM, Shay DK, Holman RC, Curns AT, Anderson LJ. Trends in hospitalizations for pneumonia among persons aged 65 years or older in the United States, 1988-2002. JAMA. 2005;294(21):2712-9.
132. López-Otín C, Blasco MA, Partridge L, Serrano M, Kroemer G. The hallmarks of aging. Cell. 2013;153(6):1194-217.
133. Renshaw M, Rockwell J, Engleman C, Gewirtz A, Katz J, Sambhara S. Cutting edge: impaired Toll-like receptor expression and function in aging. J Immunol. 2002;169(9):4697-701.
134. Stout-Delgado HW, Yang X, Walker WE, Tesar BM, Goldstein DR. Aging impairs IFN regulatory factor 7 up-regulation in plasmacytoid dendritic cells during TLR9 activation. J Immunol. 2008;181(10):6747-56.
135. Johnson SA, Cambier JC. Ageing, autoimmunity and arthritis: senescence of the B cell compartment - implications for humoral immunity. Arthritis Res Ther. 2004;6(4):131-9.
136. Linton PJ, Dorshkind K. Age-related changes in lymphocyte development and function. Nat Immunol. 2004;5(2):133-9.
137. Tamir A, Eisenbraun MD, Garcia GG, Miller RA. Age-dependent alterations in the assembly of signal transduction complexes at the site of T cell/APC interaction. J Immunol. 2000;165(3):1243-51.
138. Sasaki S, Sullivan M, Narvaez CF, Holmes TH, Furman D, Zheng NY, et al. Limited efficacy of inactivated influenza vaccine in elderly individuals is associated with decreased production of vaccine-specific antibodies. J Clin Invest. 2011;121(8):3109-19.
139. Lefebvre JS, Haynes L. Vaccine strategies to enhance immune responses in the aged. Curr Opin Immunol. 2013;25(4):523-8.
140. Garçon N, Wettendorff M, Van Mechelen M. Role of AS04 in human papillomavirus vaccine: mode of action and clinical profile. Expert Opin Biol Ther. 2011;11(5):667-77.
141. Coler RN, Baldwin SL, Shaverdian N, Bertholet S, Reed SJ, Raman VS, et al. A synthetic adjuvant to enhance and expand immune responses to influenza vaccines. PLoS One. 2010;5(10):e13677.
142. Clegg CH, Roque R, Perrone LA, Rininger JA, Bowen R, Reed SG. GLA-AF, an emulsion-free vaccine adjuvant for pandemic influenza. PLoS One. 2014;9(2):e88979.
143. Clegg CH, Roque R, Van Hoeven N, Perrone L, Baldwin SL, Rininger JA, et al. Adjuvant solution for pandemic influenza vaccine production. Proc Natl Acad Sci U S A. 2012;109(43):17585-90.
144. Treanor JJ, Essink B, Hull S, Reed S, Izikson R, Patriarca P, et al. Evaluation of safety and immunogenicity of recombinant influenza hemagglutinin (H5/Indonesia/05/2005)

formulated with and without a stable oil-in-water emulsion containing glucopyranosyl-lipid A (SE+GLA) adjuvant. Vaccine. 2013;31(48):5760-5.
145. Weinberger B, Joos C, Reed SG, Coler R, Grubeck-Loebenstein B. The stimulatory effect of the TLR4-mediated adjuvant glucopyranosyl lipid A is well preserved in old age. Biogerontology. 2016;17(1):177-87.
146. O'Hagan DT, Ott GS, Nest GV, Rappuoli R, Giudice GD. The history of MF59(®) adjuvant: a phoenix that arose from the ashes. Expert Rev Vaccines. 2013;12(1):13-30.
147. Fox CB, Barnes V L, Evers T, Chesko JD, Vedvick TS, Coler RN, et al. Adjuvanted pandemic influenza vaccine: variation of emulsion components affects stability, antigen structure, and vaccine efficacy. Influenza Other Respir Viruses. 2013;7(5):815-26.
148. Behzad H, Huckriede AL, Haynes L, Gentleman B, Coyle K, Wilschut JC, et al. GLA-SE, a synthetic toll-like receptor 4 agonist, enhances T-cell responses to influenza vaccine in older adults. J Infect Dis. 2012;205(3):466-73.
149. Toellner KM, Luther SA, Sze DM, Choy RK, Taylor DR, MacLennan IC, et al. T helper 1 (Th1) and Th2 characteristics start to develop during T cell priming and are associated with an immediate ability to induce immunoglobulin class switching. J Exp Med. 1998;187(8):1193-204.
150. Wang R, Sheng ZM, Taubenberger JK. Detection of novel (swine origin) H1N1 influenza A virus by quantitative real-time reverse transcription-PCR. J Clin Microbiol. 2009;47(8):2675-7.
151. Lefebvre JS, Masters AR, Hopkins JW, Haynes L. Age-related impairment of humoral response to influenza is associated with changes in antigen specific T follicular helper cell responses. Sci Rep. 2016;6:25051.
152. Amanna IJ, Carlson NE, Slifka MK. Duration of humoral immunity to common viral and vaccine antigens. N Engl J Med. 2007;357(19):1903-15.
153. Boraschi D, Aguado MT, Dutel C, Goronzy J, Louis J, Grubeck-Loebenstein B, et al. The gracefully aging immune system. Sci Transl Med. 2013;5(185):185ps8.
154. Panda A, Qian F, Mohanty S, van Duin D, Newman FK, Zhang L, et al. Age-associated decrease in TLR function in primary human dendritic cells predicts influenza vaccine response. J Immunol. 2010;184(5):2518-27.
155. Aspinall R, Andrew D. Thymic involution in aging. J Clin Immunol. 2000;20(4):250-6.
156. Helft J, Böttcher J, Chakravarty P, Zelenay S, Huotari J, Schraml BU, et al. GM-CSF Mouse Bone Marrow Cultures Comprise a Heterogeneous Population of CD11c(+)MHCII(+) Macrophages and Dendritic Cells. Immunity. 2015;42(6):1197-211.
157. Coler RN, Duthie MS, Hofmeyer KA, Guderian J, Jayashankar L, Vergara J, et al. From mouse to man: safety, immunogenicity and efficacy of a candidate leishmaniasis vaccine LEISH-F3+GLA-SE. Clin Transl Immunology. 2015;4(4):e35.
158. Hussell T, Bell TJ. Alveolar macrophages: plasticity in a tissue-specific context. Nat Rev Immunol. 2014;14(2):81-93.
159. Wong CK, Smith CA, Sakamoto K, Kaminski N, Koff JL, Goldstein DR. Aging Impairs Alveolar Macrophage Phagocytosis and Increases Influenza-Induced Mortality in Mice. J Immunol. 2017;199(3):1060-8.
160. SALK JE, PEARSON HE. Immunization against influenza with observations during an epidemic of influenza A one year after vaccination. Am J Hyg. 1945;42:307-22.
161. Van den Hoecke S, Ehrhardt K, Kolpe A, El Bakkouri K, Deng L, Grootaert H, et al. Hierarchical and Redundant Roles of Activating FcγRs in Protection against Influenza Disease by M2e-Specific IgG1 and IgG2a Antibodies. J Virol. 2017;91(7).

162. Windish HP, Duthie MS, Misquith A, Ireton G, Lucas E, Laurance JD, et al. Protection of mice from Mycobacterium tuberculosis by ID87/GLA-SE, a novel tuberculosis subunit vaccine candidate. Vaccine. 2011;29(44):7842-8.
163. Ismaili J, Rennesson J, Aksoy E, Vekemans J, Vincart B, Amraoui Z, et al. Monophosphoryl lipid A activates both human dendritic cells and T cells. J Immunol. 2002;168(2):926-32.
164. Fox CB, Haensler J. An update on safety and immunogenicity of vaccines containing emulsion-based adjuvants. Expert Rev Vaccines. 2013;12(7):747-58.
165. He F, Leyrer S, Kwang J. Strategies towards universal pandemic influenza vaccines. Expert Rev Vaccines. 2016;15(2):215-25.
166. De Groot AS, McClaine E, Moise L, Martin W. Time for T?: Thoughts about the 2009 novel H1N1 influenza outbreak and the role of T cell epitopes in the next generation of influenza vaccines. Hum Vaccin. 2010;6(2):161-63.
167. De Groot AS, Moise L, Liu R, Gutierrez AH, Terry F, Koita OA, et al. Cross-conservation of T-cell epitopes: now even more relevant to (H7N9) influenza vaccine design. Hum Vaccin Immunother. 2014;10(2):256-62.
168. Liu R, Moise L, Tassone R, Gutierrez AH, Terry FE, Sangare K, et al. H7N9 T-cell epitopes that mimic human sequences are less immunogenic and may induce Treg-mediated tolerance. Hum Vaccin Immunother. 2015;11(9):2241-52.
169. Bui HH, Peters B, Assarsson E, Mbawuike I, Sette A. Ab and T cell epitopes of influenza A virus, knowledge and opportunities. Proc Natl Acad Sci U S A. 2007;104(1):246-51.
170. Martins KAO, Cooper CL, Stronsky SM, Norris SLW, Kwilas SA, Steffens JT, et al. Adjuvant-enhanced CD4 T Cell Responses are Critical to Durable Vaccine Immunity. EBioMedicine. 2016;3:67-78.
171. Ugolini M, Gerhard J, Burkert S, Jensen KJ, Georg P, Ebner F, et al. Recognition of microbial viability via TLR8 drives T. Nat Immunol. 2018;19(4):386-96.
172. Zhang W, Brahmakshatriya V, Swain SL. CD4 T cell defects in the aged: causes, consequences and strategies to circumvent. Exp Gerontol. 2014;54:67-70.